

**A STUDY ON ADVANCED CONTROL FOR AN
INDUSTRIAL SCALE DISTILLATION COLUMN:
MODEL DEVELOPMENT AND CONTROL SIMULATIONS**

By

John Martin Wassick

A DISSERTATION

**Submitted to
Michigan State University
in partial fulfillment of the requirements
for the degree of**

DOCTOR OF PHILOSOPHY

**Department of Electrical Engineering
and Systems Science**

1987

ABSTRACT

A STUDY ON ADVANCED CONTROL FOR AN INDUSTRIAL SCALE DISTILLATION COLUMN: MODEL DEVELOPMENT AND CONTROL SIMULATIONS

By

John Martin Wassick

This thesis describes the research that was performed to investigate the modelling and control of an industrial scale distillation column located at The Dow Chemical Company's Michigan Division. The overall objective of this thesis was to determine if advanced control would be beneficial to the column under study. This objective led to two major themes in the research: 1) develop a dynamic, multivariable model of the column, and 2) propose an alternate model based control scheme and test it through simulation.

The model that is developed is a 2 input, 2 output matrix of discrete time transfer functions. A novel identification procedure is developed which greatly reduces the number of parameters necessary to describe the behavior of multivariable systems with multiple time delays and is based on a new "delayed polynomial matrix" representation of discrete systems. A computer algorithm for the delayed polynomial matrix method is described in a way that makes it suitable for interactive use. A simulated example demonstrates the ability of this new identification method to perform with up to 20% additive noise on the data.

Least squares parameter estimation of the identified model is based on real operating data. It was found that the concentration on the 57th tray exhibited inverse response to changing reflux flow. This was totally unexpected and has not been mentioned in the chemical engineering literature. Discussion of the Linde column model shows that other aspects of the model were very consistent with the experience of the operating personnel.

The alternate control strategy selected is a feedforward version of Internal Model Control, IMC. Two peculiarities of the column required extensions of existing theory on IMC, they are: 1) multirate sampling of the two product concentrations and 2) the inverse response already mentioned. The multirate sampling problem is addressed by a unique implementation of feedforward control. A reduced order controller design technique is developed to handle the non-minimum phase behavior.

The multivariable controller out performs the conventional controllers in load change simulations. Improved disturbance rejection was achieved in both product streams.

To Maria, my loving wife, whose patience and sacrifice made this accomplishment possible.

ACKNOWLEDGMENTS

I am indebted to several individuals for help in preparation of this thesis. I thank Lal Tummala, my thesis advisor, for his guidance and his thoughtful comments on the manuscript. I am also thank the rest of my guidance committee: Robert Barr, Robert Schlueter, Hassan Khalil, Krishnamurthy Jayaraman, and David Yen for their timely suggestions which saved me many hours of frustration. My heartfelt appreciation goes to my wife, Maria, for the time she found in her hectic day to help type the manuscript.

I must express my sincere gratitude to The Dow Chemical Company for its generous financial support and for the use of its process equipment and computer resources. In particular, I thank Ray Murphy and Fred Swinehart for having the enough faith in me to muster the support for such a long project. Finally, I thank my colleague Dave Camp for his encouragement that ensured I finished this project.

TABLE OF CONTENTS

LIST OF TABLES	vii
LIST OF FIGURES	viii
Chapter One, Introduction and Description of Thesis	1
1.1 Introduction	1
1.2 Research Objectives	2
1.3 Outline of the Thesis	4
1.4 Summary	5
Chapter Two, Description of the Process	6
2.1 Fundamentals of Distillation	6
2.2 Distillation Control Fundamentals	9
2.3 Description of the Linde Column	9
2.4 Current Control of the Linde Column	12
2.5 Summary of Chapter Two	12
Chapter Three, Linde Column Modelling	14
3.1 Literature Survey of Distillation Modelling	14
3.2 Current Model Identification Methods	16
3.2.1 Identification Literature	18
3.3 Delayed Polynomial Matrices	19

3.4	Structural Identification	37
3.4.1	Phase 1	38
3.4.2	Phase 2	40
3.5	Computer Implementation	45
3.5.1	Singular Value Decomposition	46
3.5.2	Computer Algorithm	48
3.5.3	Noise Compensation	53
3.5.4	SVD Subroutines	54
3.5.5	Simulation Results	55
3.5.6	Summary of Computer Implementation	64
3.6	Linde Column Model	64
3.6.1	Linde Column Operating Data	65
3.6.2	Least Squares Parameter Estimation	75
3.6.3	Transfer Function Identification	78
3.6.4	Results of Column Modelling	80
3.6.5	Discussion of the Linde Column Model	91
3.7	Summary of Chapter Three	93
Chapter Four, Advanced Control for the Linde Column		95
4.1	Current Control Strategy	95
4.2	Literature Survey on Distillation Control	98
4.3	Model Based Control, SISO	100
4.3.1	Minimum Phase Processes	102
4.3.2	Non-minimum Phase Processes	106
4.4	Model Based Control, MIMO	118
4.4.1	Feedforward Internal Model Control	118
4.4.2	IMC for the Linde Column	124
4.5	Results and Discussion	131
4.6	Summary of Chapter Four	144
Chapter Five, Summary and Recommendations		146
5.1	Summary of Linde Column Modelling	147
5.1.1	Results of Linde Column Modelling	148
5.1.2	Future Research on Distillation Modelling	149
5.2	Summary of Advanced Control for the Linde Column	150
5.2.1	Results of Advanced Control Simulations	153

5.2.2 Future Control Research	154
5.3 Future Research Opportunities	156
APPENDIX	161
LIST OF REFERENCES	163

LIST OF TABLES

Table 4-1 IMC Transfer Functions

135

LIST OF FIGURES

Figure 2-1	Major components of the distillation process	7
Figure 2-2	Linde Column instrumentation	11
Figure 3-1	2 input, 2 output system with time delays	34
Figure 3-2	Model order estimation with different amounts of additive noise	56
Figure 3-3	Input delay test for y_1 with 0% noise	58
Figure 3-4	Input delay test for y_1 with 10% noise	59
Figure 3-5	Input delay test for y_1 with 20% noise	60
Figure 3-6	Input delay test for y_2 with 0% noise	61
Figure 3-7	Input delay test for y_2 with 10% noise	62
Figure 3-8	Input delay test for y_2 with 20% noise	63
Figure 3-9	Inputs and outputs of the Linde Column	66
Figure 3-10	Recorded reflux flow (data set 1)	67
Figure 3-11	Recorded concentration on the 57th tray (data set 1)	67
Figure 3-12	Recorded bottoms concentration (data set 1)	68
Figure 3-13	Recorded reboiler steam pressure (data set 1)	68
Figure 3-14	Recorded reboiler steam pressure (data set 2)	70

Figure 3-15	Recorded bottoms concentration (data set 2)	70
Figure 3-16	Recorded reflux flow (data set 2)	71
Figure 3-17	Recorded concentration on the 57th tray (data set 2)	71
Figure 3-18	Recorded reflux flow (data set 3)	72
Figure 3-19	Recorded reboiler steam pressure (data set 3)	72
Figure 3-20	Recorded concentration on the 57th tray (data set 3)	73
Figure 3-21	Recorded bottoms concentration (data set 3)	73
Figure 3-22	Results of the delayed polynomial matrix test for $G_{11}(z)$	81
Figure 3-23	Mean square residuals for G_{11} with a time delay of 5	82
Figure 3-24	Auto-correlation of residuals of 4th order model with a delay of 5 for G_{11}	82
Figure 3-25	Response of estimated G_{11} to the re- corded reflux flow of data set 1	84
Figure 3-26	A portion of the recorded 57th tray concentration from data set 1	84
Figure 3-27	Order test for G_{12}	85
Figure 3-28	Mean square residuals for G_{12} with a time delay of zero	85
Figure 3-29	Auto-correlation of residuals of a 3rd order model with a delay of 1 for $G_{21}(z)$	87
Figure 3-30	Response of the estimated G_{21} to a portion of the recorded reflux flow of data set 1	88
Figure 3-31	A portion of the recorded bottoms concentration from data set 1	88

Figure 3-32	Response of estimated G_{22} to a portion of the recorded steam pressure from data set 2	90
Figure 3-33	A portion of the recorded bottoms concentration from data set 2	90
Figure 4-1	Basic Internal Model Control structure	101
Figure 4-2	Filtered Internal Model Control structure	101
Figure 4-3	Response of $G_{11}(z)$ to a step load disturbance	110
Figure 4-4	Response of $G_{11}(z)$ to a step load disturbance, IMC control with $G_c(z) = 1/G_{11}(1)$ and no filtering	112
Figure 4-5	Response of $G_{11}(z)$ to a step load disturbance, PI control	117
Figure 4-6	Response of $G_{11}(z)$ to a step load disturbance, IMC control	117
Figure 4-7	Brosilow's feedforward Internal Model Control structure	119
Figure 4-8	Revised feedforward Internal Model Control structure	120
Figure 4-9	Simplified Decoupling with Revised Feedforward IMC	126
Figure 4-10	Simplified Decoupling with Brosilow's feedforward IMC	128
Figure 4-11	Critical Decoupling with Revised Feedforward IMC	132
Figure 4-12	Critical Decoupling with Brosilow's feedforward IMC	133
Figure 4-13	Response of the 57th tray concentration to a step load disturbance	136
Figure 4-14	Response of the 57th tray concentration to a step load disturbance in the bottoms concentration	137

Figure 4-15	Response of bottoms concentration to a step load disturbance on the 57th tray	138
Figure 4-16	Response of bottoms concentration to a step load disturbance	139
Figure 4-17	Response of simply decoupled IMC (Brosilow's version) to a step load disturbance	141
Figure 4-18	Response of critically decoupled IMC (Brosilow's version) to a step load disturbance	143
Figure 4-19	Stable images of unstable zeros	108

CHAPTER ONE

INTRODUCTION AND DESCRIPTION OF THE THESIS

1.1 Introduction

The research presented in this thesis has been motivated by the technology gap that exists between "advanced control theory" and industrial practice. The vast majority of literature on advanced process control has concentrated on the derivation of various techniques and the mathematical advantages and disadvantages of these techniques. A survey of the literature will show that the few papers addressing the application of advanced control achieve their results through lab scale equipment or computer simulation. Very few papers investigate the application of advanced control to full scale processes. In the last few years several noted authors in the field have cited a need for application oriented research [1]. This thesis addresses this problem.

In this thesis we will consider: lack of well defined process models, non-uniform sampling, robustness of controllers, and the economic incentive or disincentive for using advanced control strategies. The specific application of this research is an industrial scale distillation column at Dow Chemical Company's Michigan Division. This type of process operation was selected because distillation is one of the most important unit operations in the petrochemical industry. Also, distillation columns are one of the largest energy consumers in a chemical plant and improved control has been shown

to be effective in reducing energy costs. For the column of this study, reducing the energy consumption by one percent would result in a cost savings of \$30,000 in one year alone. Improved control could also be used to increase the product quality of the column. Estimates predict that a one percent reduction in the overheads product impurity would produce a savings of \$25,000 per year. Production supervision easily agreed to support this research given these potential savings and the admission by operating personnel that the current control showed deficiencies. In addition, such research could develop solutions to some of the practical problems involved in implementing advanced control theory while solving the specific control problem presented by the application. Also, a channel of communication between industry and academia would be fostered by application oriented research. This thesis describes such research.

1.2 Research Objectives

The overall objective of this research was to determine if advanced control would be beneficial to a commercially successful industrial scale distillation column. In other words, what potential does advanced control have to improve control. Typically energy savings and greater product quality of a distillation column are realized through improved regulation of the two product streams. Usually these streams are dynamically coupled so that action taken to correct one will also affect the other. This situation lends itself to a multivariable control strategy which requires a multi-input multi-output model of the column.

From this perspective, the major goals of this research are:

1. Develop a column model (the major task of this research).
2. Propose an advanced control scheme based on considerations of the model and practical issues such as robustness of the control and how well plant personnel would understand and therefore accept a new control approach.
3. Test the proposed control scheme through simulation and compare to conventional control.

The relatively straight forward approach outlined above was complicated by problems that are not frequently discussed in the literature. Due to the multiple stages of a distillation column, time delay, often called deadtime, is an important parameter of the model. The model constructed for the column is a matrix of linear discrete time transfer functions. Model order estimation and time delay estimation needed to be performed simultaneously. Also, the column could only be studied as it produced a salable product, therefore meaningful data for model building was not easily obtained. In addition, the measurement of one of process variables had a fixed sampling rate while all others were virtually continuously measured. This produced a multirate sampling problem. Finally, part of the column exhibited unexpected non-minimum phase behavior which led to a novel approach to the controller design. The original contributions of this research contain solutions to these problems.

1.3 Outline of the Thesis

The remainder of this thesis is divided into four chapters. In Chapter Two, the basics operation and control of a distillation column is introduced. A physical description of the Dow column and its control system is also provided.

Chapter Three is concerned with the problem of identification and parameter estimation of the model of the Dow column. A survey of the literature regarding distillation column modelling is given. In this chapter the problem of time delay plus model order estimation is defined. Singular value decomposition is described and a method for estimating time delay and model order is then developed which uses this mathematical tool. Simulated data is used to show the ability of this method. Real operating data of the column is presented next and the method is applied to it. Other model order estimating techniques are used to confirm the model order. Then parameter estimation is performed. The resulting model is then discussed in the light of a prior knowledge of the column.

Chapter Four deals with the design of an advanced control strategy for the column using the model of Chapter Three. First the control implications of the model are discussed. Next a survey of the literature on distillation column control is presented. Then Internal Model Control is introduced and a multirate feed forward version is developed for the column. Also, a reduced order controller is presented to handle the non-minimum phase dynamics in the column. Simulations of the column under the standard proportional / integral control and IMC

are described and the results presented. Implications of the simulation results are discussed while considering the practical matter of running the column for production.

Chapter Five presents a summary of the results of the research described in the previous chapters. Conclusions are drawn and recommendations are made for future research.

1.4 Summary

The results of this thesis have been disseminated throughout The Dow Chemical Company before the publication of this thesis. It has been presented to a body of managers representing Dow's global operations and to a conference of researchers and engineers working on advanced process control from Dow's global manufacturing sites. Follow up research has already begun at Dow Canada's Sarnia Ontario plant to further understand the implications of the inverse response and its control in their Linde type column. In addition, the technique developed for the design of IMC for non-minimum phase processes has been adopted in the design of a temperature controller for an extruder at Dow's Michigan Division. The interest shown in this research and the additional research it has spawned is a true measure of the success this work is as an applied thesis.

CHAPTER TWO
DESCRIPTION OF THE PROCESS

The purpose of this chapter is to describe the fundamentals of the distillation process and how they relate to control. Also provided is a description of the physical make-up of the Linde Column and its current control system.

2.1 Fundamentals of Distillation

The purpose of a distillation column is to separate the chemical components of a feed stream into more or less pure product streams. The separation is based on the well known fact that pure liquids exhibit different volatilities (tendency to vaporize). Thus, heat applied to a mixture of substances will generate a vapor which is rich in the more volatile substances and leave a liquid which is more rich in the less volatile substances. If the vapor is condensed the remaining liquids represent the purified products of the distillation process.

Typically a distillation column consists of a cylindrical vessel containing a number of equally spaced trays inside, Figure 2-1. A weir mounted on each tray maintains the liquid level on the tray. Liquid overflowing the weir travels through a downcomer to the tray below. The trays are equipped with a means to allow vapor to flow from below and mix with the liquid on the tray. The bottom of the distillation column is connected to a heating unit called a reboiler, which provides the

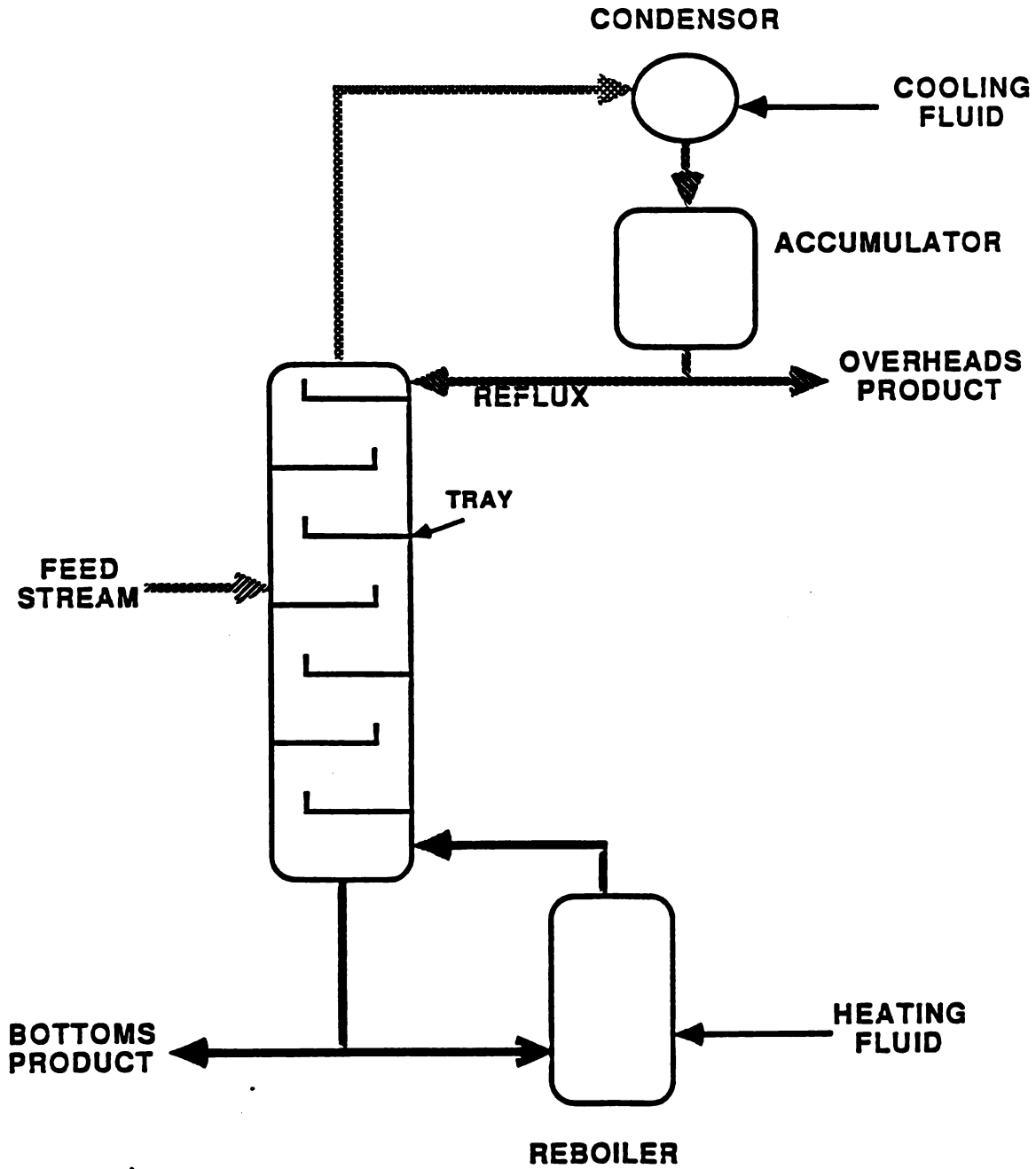


Figure 2-1 Major components of the distillation process

energy to create a vapor flow up the column. A portion of the liquid at the bottom not vaporized is removed from the column and is known as the bottoms product. The top of the distillation column is connected to a cooling device called a condenser, which condenses the vapors leaving the column. A portion of the condensed vapors, called reflux, is generally returned to the column to flow from top to bottom. What remains of the condensed vapors is drawn off the column and is called the overheads product or distillate. The feed stream of the column is usually introduced near the middle of the column.

The operation of a distillation column is a series of heat and mass transfer operations occurring on each tray. Consider the simplest separation of a binary liquid mixture. Feed entering the column flows down from tray to tray to the bottom. As it flows down it is contacted by the vapor rising up. This contact initiates a heat and mass transfer which results in the vaporization of the more volatile, lighter, component in the liquid and condensation of the less volatile, heavier, component in the vapor. So as the feed travels down the column it becomes more and more concentrated in the less volatile component of the feed. The vapor becomes more and more concentrated in the more volatile substance as it rises up the column. Above the feed tray the reflux returned at the top of the column serves to mix with the rising vapor. Each end of the column represents the extremes in concentration for both components, the top for the lighter component, the bottom for the heavier component.

2.2 Distillation Control Fundamentals

The variables used to control the concentrations of the product streams are usually the reflux flow and the vapor flow (through the amount of energy added to the reboiler). By far the most common control strategy used in industry is to manipulate the heat added to the reboiler to control the bottoms product concentration and adjust the reflux flow to control the overheads product concentration. Simply put, if the concentration of the lighter component in the bottom is too high heat is added to boil it off, and if the concentration of the heavier component is too high in the distillate more is returned as reflux to be distilled again. This simple single input, single output strategy has limitations since vapor used to control the bottom of the column must reach the top of the column and has affects there. In the same way, reflux used to control the top of the column must flow to the bottom and have an affect there. Consideration of the column as a two input, two output system can improve the control, which is part of this research.

2.3 Description of the Linde Column

The subject of this research was a distillation column located in Dow Chemical Company's Michigan Division which is 12 feet in diameter and 90 feet tall. The column performs a binary separation of styrene and ethylbenzene. The distillation unit is equipped with 70 Linde type trays giving rise to its name, "Linde Column". Liquid is drawn off the bottom of the column and pumped through a vertical reboiler using steam

as a heating medium. Vapor drawn off the top of the column is totally condensed in six air cooled condensers. The feed flow is introduced around the 45 tray.

A Dow designed process control computer manages the process through direct digital control, therefore the process is fully equipped with electronic instrumentation. Feed flow rate and reflux flow rate are measured by orifice type flow meters. Steam pressure in the reboiler is measured by an electronic pressure transmitter. Feed temperature is measured by resistance temperature bulb. The concentration of styrene on the 57th tray, which is used to control the concentration in the overhead product, is measured by an online refractive index analyzer. The concentration of ethylbenzene in the bottom product is measured by samples taken in the reboiler loop and analyzed by a gas chromatograph. The gas chromatograph sampling rate is fixed at 8 minutes. All other measurements are continuous. Figure 2-2 illustrates the total instrumentation of the Linde column.

Operating data was logged on a PDP11/44 digital computer which communicated with the Dow process control computer. The data was then read to a flexible magnetic disk and transported to Michigan State University where it was read into a PDP11/04 computer and transmitted to the College of Engineering's Prime Computer. The bulk of the analysis was performed on the Prime Computer. The data was also transmitted from the PDP11/44 through a local area network to a VAX 11/785 for further analysis.

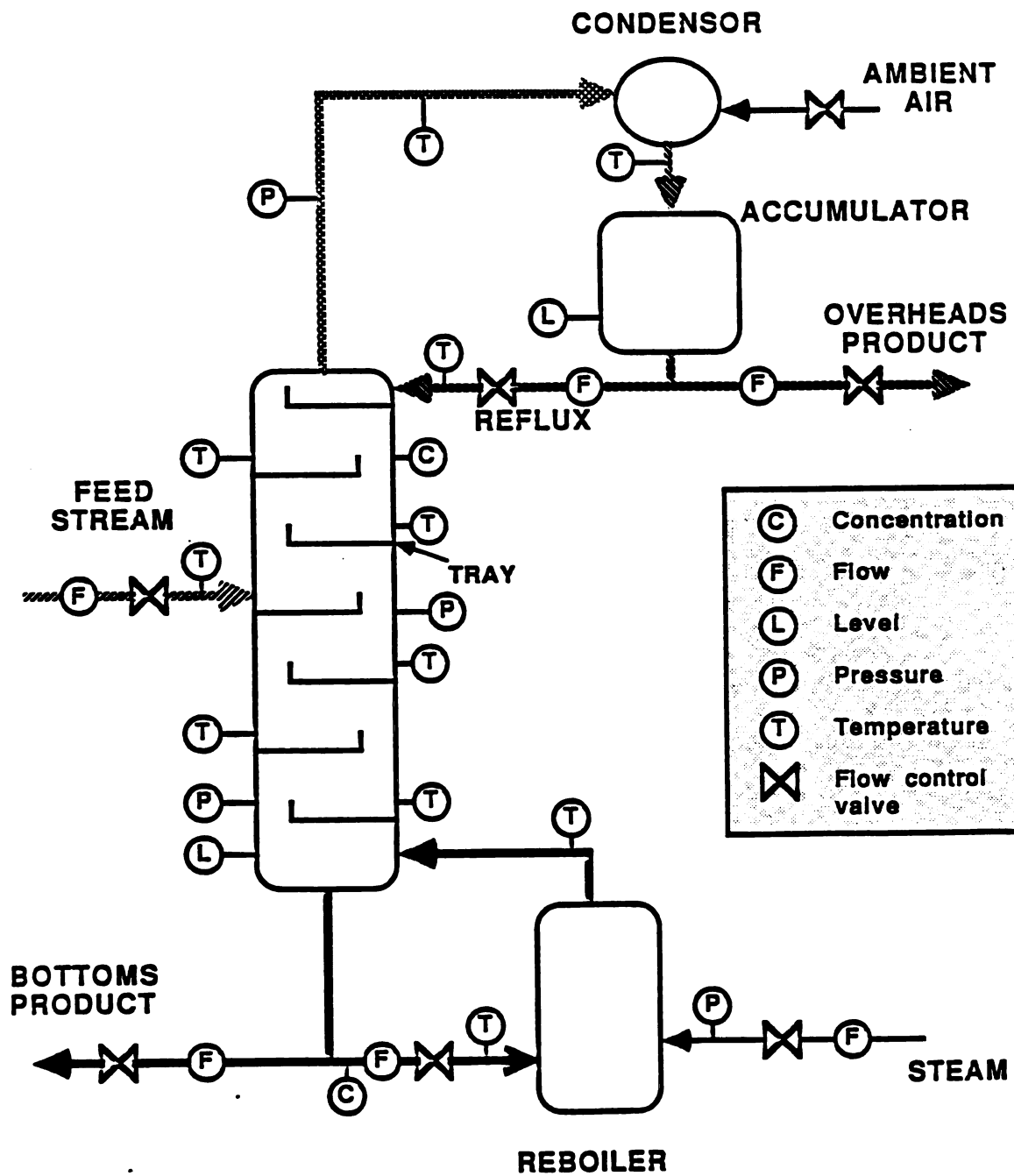


Figure 2-2 Linde Column instrumentation

2.4 Current Control of the Linde Column

The current control strategy to maintain product quality is based on digital Proportional-Integral controllers. The bottom composition is regulated by changing steam flow to the reboiler through a cascade control scheme. To maintain bottoms composition, the set point of a slave steam pressure controller is adjusted. This slave controller in turn regulates the flow of steam to the reboiler through a pneumatically operated control valve.

The top product is also controlled by a cascading of control loops. The overhead composition is maintained by regulating the concentration on the 57th tray by indirectly manipulating reflux flow through changes in overhead product draw off. Changes in overhead product flow are transformed into reflux flow changes through the overhead accumulator which is level controlled by reflux flow. Although these controllers are slightly more complex than the conventional control scheme already described, the Linde Column controls still use steam to control the bottom product and reflux to control the top product.

2.5 Summary of Chapter Two

This chapter has shown distillation to be a complex chemical process. Even so, the generally applied control scheme of industry is simple independent PI controllers applied to each product stream. In the case of the Linde column, much more complex schemes can be applied

due to the full complement of electronic instrumentation coupled with direct digital control. This situation offers good opportunities for the application of more advanced control strategies.

CHAPTER THREE

LINDE COLUMN MODELLING

The purpose of this chapter is to develop a dynamic model of the Linde Column. The model is a 2 input, 2 output matrix of discrete time transfer functions. A survey of the literature on distillation column modelling is given first. Then as a preliminary, the problem of determining the structure and order of a multi-input, multi-output model is addressed in the general sense. A new solution is presented. It is then used on real data from the Linde Column. Parameters of the model are determined by least squares estimation. Finally the identified model is discussed in light of the operating experience of the column.

3.1 Literature Survey of Distillation Column Modelling

Distillation columns have been popular subjects of identification in the literature. Industrial columns as well as pilot scale columns have been considered. As in this research, several authors have derived discrete time models of distillation columns using operating data. However the research in this thesis differs significantly from each.

For example, Williams [3] modeled a six plate pilot scale column using step and Pseudo Random Binary Signal (PRBS) inputs. He only considered the dynamics between reflux flow and top product composition

and did not consider the steam flow to the reboiler as an input as was done in this research.

Krishnamoorthy and Edgar [4] used pulse testing to model a pilot scale column as a two input two output system. They used least squares estimation and employed several methods to determine model order. Their main concern was to properly prefilter the sampled data before estimating the model order. Time delay was estimated by shifting the data and then correlating the input output data and by finding the time lag which minimized the resulting estimation error. They concluded that prefiltering resulted in consistent estimation of model order by the different techniques, but failed to report the models they derived.

Foulard and Bornard [5] report on both steady state and dynamic modelling of pilot scale and industrial distillation columns. Different estimating techniques were used to develop low order dynamic models with no time delay. Correct model order was determined by finding the order that minimized the estimation error. Unlike this research, only single input single output relationships were considered. Main conclusions were that the type of input signal greatly affects the results of the modelling procedure and that there exists a significant problem in obtaining good experimental data from an industrial column.

A full scale column is modelled by Gauthier and Landau [6]. The input applied to the column is two uncorrelated PRBS signals added to the set points of the overhead and bottom temperature control loops,

rather than perturbing the inputs to the column as was done for this research. A two input two output model was identified using a method similar to that used in this research but time delay was not considered. The instrumental variable method of estimating as well as Landau's output error estimator were used to fit the model to the experimental data.

Gustavsson [7] surveys other applications of discrete time modelling to industrial scale distillation columns. The applications of his survey that are the most similar to the present research are still deficient in some area. Most did not evaluate any control strategy that the derived model might have suggested. Some applications did not model the column under study as a two input two output system. Other applications considered tray temperatures rather than product compositions as outputs. All authors did find modelling of an industrial scale column a problem that is compounded by the lack of control the experimenter has on the column as a whole.

3.2 Current Model Identification Methods

A prerequisite to the estimation of parameters of a dynamic model of a process is the knowledge or at least an estimate of the model structure and order. In some sense the identification of model structure and order is a much more difficult task than the estimation of parameters. In practice, the model structure and order are determined partly through the existing knowledge of the process and partly through

a combination of statistical tests. The original tests of model order were based on statistical evaluations of estimated models. Although these tests are reliable, they require large amounts of computing because all competing models must be estimated in order to apply the tests. In recent years several techniques to estimate model order prior to parameter estimation have been presented in the literature. A very recent comparison of the most popular techniques is given by Freeman [15]. The obvious advantage of these tests is that they significantly reduce the computational burden of model development by eliminating the need to estimate all competing models.

The aim here is to extend an existing multivariable technique to include explicit consideration of an important structural parameter of discrete linear models, namely time delay. The importance of time delay in a model used for control is illustrated by the numerous techniques that exist to compensate for it. In terms of modelling chemical processes, time delay occurs very often because of actual transport delays that exist in the process and because it is an effective means to approximate higher order dynamics. Therefore any effective modelling procedure must consider time delay.

Numerical robustness is another important attribute of an identification procedure. This is because the computations of any algorithm will be performed on a digital computer which has finite accuracy limits. This is also addressed in this thesis.

3.2.1 Identification Literature

There are several statistical tests of the estimated model that have seen wide spread use. Astrom [16] suggested using the statistical F-test on models of increasing order. Tests based on the sum of residuals squared or the sum of the reconstruction error are also popular, see Gustavsson [17]. Akaike [18,19] has suggested two tests that combine the variance of the residuals with the number of parameters into a single measure. Tests based on the auto-correlations of the residuals are also widely used. Although these tests can only be applied after a model has been estimated, they are still useful in validating the model structure which is selected by methods applied to the data prior to parameter estimation.

Tests applied prior to parameter estimation are based on determining the linear dependence between input and output data. Lee [20] was the first to exploit this relationship by testing the singularity of the product moment matrix. Woodside [21] then extended this idea by developing three measures testing the singularity of the product moment matrix. Wellstead [22] modified this idea by basing a test on an instrumental product moment matrix and also included a procedure to estimate time delay in a single input single output model.

The existing multivariable techniques for model identification, suggested by Budin [24] and Guidorzi [25], do not explicitly estimate the time delay of the model. Instead they estimate a model order which is large enough to include the time delay. This results in a model

with many parameters which have values identically equal to zero. In principle these methods rely on the parameter estimation scheme to detect the magnitude of time delay by the number of parameters with estimated values close to zero. In practice this methodology can break down when applied to noisy data. A more reliable means to estimate time delay would result if the zero valued parameters could be identified prior to parameter estimation and then confirmed by other statistical tests applied to the estimated model.

3.3 Delayed Polynomial Matrices

A method to identify multi-input, multi-output models with time delay prior to parameter estimation is developed as follows. First a theorem is proven which relates a system's state space realization with input delays to a canonical input - output realization. Next the results of the theorem are used to develop a method which estimates model order and time delay in multivariable systems. Then singular value decomposition is introduced as a means to detect near singularity of matrices and it is then used as a measure to determine model order and time delays in multivariable systems. Simulated data is then used to demonstrate the ability of the method. Finally the method is applied to real data from the Linde column.

Theorem 3.1

Let a completely observable discrete time system with input delays be described by the following state space equations

$$\mathbf{x}(k+1) = \mathbf{A}\mathbf{x}(k) + \mathbf{B}_1\mathbf{u}(k-d_1) + \mathbf{B}_2\mathbf{u}(k-d_2) + \dots + \mathbf{B}_s\mathbf{u}(k-d_s) \quad (3.1)$$

$$\mathbf{y}(k) = \mathbf{C}\mathbf{x}(k) \quad (3.2)$$

$$0 < d_1 < d_2 < \dots < d_s, \quad s \in I$$

where $\mathbf{x} \in \mathbb{R}^n$, $\mathbf{u} \in \mathbb{R}^r$, and $\mathbf{y} \in \mathbb{R}^m$.

Then there exists an equivalent input-output description of the system with the following form

$$\mathbf{P}(z)\mathbf{y}(k) = \mathbf{Q}_1\mathbf{u}(k-d_1) + \mathbf{Q}_2\mathbf{u}(k-d_2) + \dots + \mathbf{Q}_s\mathbf{u}(k-d_s) \quad (3.3)$$

where $\mathbf{P}(z)$ and $\mathbf{Q}_\alpha(z)$, $\alpha = 1, 2, \dots, s$, are polynomial matrices whose entries satisfy the following relations

$$\deg\{p_{ii}(z)\} > \deg\{p_{ij}(z)\}, \quad j > i \quad (3.4a)$$

$$\deg\{p_{ii}(z)\} \geq \deg\{p_{ij}(z)\}, \quad j < i \quad (3.4b)$$

$$\deg\{p_{ii}(z)\} > \deg\{p_{ji}(z)\}, \quad j \neq i \quad (3.4c)$$

$$\deg\{p_{ii}(z)\} > \deg\{q_{\alpha, ij}(z)\} \quad (3.4d)$$

The degree of each of the polynomials is directly related to the structure of A and C .

Proof:

First consider C as a matrix of row vectors

$$C = \begin{bmatrix} C_1^T \\ C_2^T \\ \vdots \\ C_m^T \end{bmatrix} \quad (3.5)$$

Now the observability matrix may be constructed as

$$O = [C^T, A^T C^T, A^{T^2} C^T, \dots, A^{T^{(n-1)}} C^T] \quad (3.6)$$

And the columns of O searched for linearly independent columns in the following order

$$C_1, C_2, \dots, C_m, A^T C_1, A^T C_2, \dots, A^T C_m, A^{T^2} C_1, A^{T^2} C_2, \dots \quad (3.7)$$

It is well known that a equivalence transformation matrix T may be constructed by arranging the independent columns in the following way

$$T = [C_1, A^T C_1, \dots, A^{T(\nu_1-1)} C_1, C_2, \dots, A^{T(\nu_m-1)} C_m] \quad (3.8)$$

Application of the transformation matrix T produces a new system of equations

$$w(k+1) = A^* w(k) + B_1^* u(k-d_1) + B_2^* u(k-d_2) + \dots + B_s^* u(k-d_s) \quad (3.9)$$

$$y(k) = C^* w(k) \quad (3.10)$$

where $w = Tx$. The form of the matrix T imposes a special structure on the matrices A^* and C^* ,

$$A^* = TAT^{-1} = (A_{ij}^*), \text{ where } i, j = 1, 2, \dots, m \text{ and}$$

$$A_{ii}^* = \begin{bmatrix} 0 & & & & \\ 0 & & & & \\ \vdots & & & & \\ 0 & & & & \\ a_{ii,1} & a_{ii,2} & \dots & a_{ii,\nu_i} & \end{bmatrix} \quad (\nu_i \times \nu_i) \quad (3.11)$$

$$A_{ij}^* = \begin{bmatrix} 0 & 0 & 0 & 0 & \dots & \dots & \dots & \dots & 0 & 0 \\ 0 & & & & & & & & & \\ \vdots & & & & & & & & & \\ 0 & & & & & & & & & \\ a_{ij,1} & a_{ij,2} & \dots & a_{ij,\nu_{ij}} & 0 & \dots & 0 & & & \end{bmatrix} \quad (\nu_i \times \nu_j) \quad (3.12)$$

$$C^* = CT^{-1} = \begin{bmatrix} 1 & 0 & 0 & \dots & \dots & \dots & 0 \\ 0 & 0 & \dots & 1 & 0 & 0 & \dots & \dots & 0 \\ \vdots & \vdots \\ 0 & 0 & \dots & 0 & 0 & \dots & 0 & 1 & 0 & 0 \dots 0 \end{bmatrix} \quad (3.13)$$

$\uparrow \qquad \qquad \qquad \uparrow \qquad \qquad \qquad \uparrow$
 $1 \qquad \qquad (\nu_1+1) \dots (\nu_1+\dots+\nu_{m-1}+1)$

We see that C^* is composed of row vectors which have only one non-zero entry (equal to unity). The position of this non-zero entry is shown for the first, the second and the m th row. Meanwhile B_α^* , $\alpha = 1, 2, \dots, s$, has the generic form

$$B_\alpha^* = \begin{bmatrix} b_{\alpha,1l}^* & \dots & b_{\alpha,1r}^* \\ \vdots & & \vdots \\ b_{\alpha,nl}^* & \dots & b_{\alpha,nr}^* \end{bmatrix} = \begin{bmatrix} b_{\alpha,1}^{*T} \\ \vdots \\ b_{\alpha,n}^{*T} \end{bmatrix} \quad (3.14)$$

It is apparent from the structure of A^* that the original system has been decomposed into m interconnected subsystems. Because of the complete observability of the system it follows that $\nu_1 + \nu_2 \dots + \nu_m = n$. In fact, the integers ν_i define the structure of A^* and C^* and are invariant with respect to changes in state space coordinates, hence the name "Kronecker invariants".

Consider now the vector $w(k)$. For conciseness of notation define $i;k = \nu_1 + \dots + \nu_i + k$. Now $w(k)$ may be expressed as

$$\begin{aligned}
 \mathbf{w}(k) &= \begin{bmatrix} w_1(k) \\ w_2(k) \\ \vdots \\ w_{\nu_1}(k) \\ w_{\nu_1+1}(k) \\ \vdots \\ w_{\nu_1+\nu_2}(k) \\ w_{\nu_1+\nu_2+1}(k) \\ \vdots \\ w_n(k) \end{bmatrix} = \begin{bmatrix} w_{0;1}(k) \\ w_{0;2}(k) \\ \vdots \\ w_{1;0}(k) \\ w_{1;1}(k) \\ \vdots \\ w_{2;0}(k) \\ w_{2;1}(k) \\ \vdots \\ w_n(k) \end{bmatrix}
 \end{aligned}$$

Using equations (3.9) and (3.10), the following equations may be written for the i th subsystem

$$w_{i-1;1}(k) = y_i(k)$$

$$w_{i-1;2}(k) = zy_i(k) - \sum_{\alpha=1}^s b_{\alpha,i-1;1}^{*T} u(k-d_\alpha)$$

$$\begin{aligned}
w_{i-1;3}(k) &= z^2 y_i(k) - z \sum_{\alpha=1}^s b_{\alpha, i-1;1}^{*T} u(k-d_\alpha) \\
&\quad - \sum_{\alpha=1}^s b_{\alpha, i-1;2}^{*T} u(k-d_\alpha) \\
&\quad \cdot \\
&\quad \cdot \\
&\quad \cdot
\end{aligned}$$

$$\begin{aligned}
w_{i;0}(k) &= z^{\nu_i-1} y_i(k) - \\
&\quad z^{\nu_i-2} \sum_{\alpha=1}^s b_{\alpha, i-1;1}^{*T} u(k-d_\alpha) - \dots \\
&\quad - \sum_{\alpha=1}^s b_{\alpha, i; -1}^{*T} u(k-d_\alpha) \quad (3.15)
\end{aligned}$$

where $y_i(k)$ is the i th component of the vector $\mathbf{y}(k)$. Comparable equations for each of the m subsystems can be written in a compact form as

$$\mathbf{w}(k) = \mathbf{V}(z)\mathbf{y}(k) - \sum_{\alpha=1}^s \mathbf{W}_\alpha \mathbf{G}(z) \mathbf{u}(k-d_\alpha) \quad (3.16)$$

where

$$V(z) = \begin{bmatrix} 1 & \dots & \dots & 0 \\ z & & & 0 \\ \vdots & \nu_{i-1} & & 1 \\ z & & & z \\ 0 & & & \vdots \\ 0 & 0 & \dots & 0 & z^{\nu_{m-1}} \end{bmatrix} \quad (3.17)$$

$$W_{\alpha} = \begin{bmatrix} 0 & 0 & \dots & 0 & 0 & 0 \\ b_{\alpha,1}^{*T} & 0 & 0 & \dots & 0 & 0 \\ \vdots & \cdot & & & & \\ b_{\alpha,\nu_1-1}^{*T} & \dots & b_{\alpha,1}^{*T} & 0 & 0 \\ \cdot & & & & & \\ \cdot & & & & & \\ \cdot & & & & & \\ 0 & 0 & \dots & 0 & 0 & 0 \\ b_{\alpha,n-\nu_m+1}^{*T} & 0 & \dots & 0 & 0 & 0 \\ \vdots & \cdot & & & & \\ b_{\alpha,n-1}^{*T} & \dots & b_{\alpha,n-\nu_m+1}^{*T} & 0 & & \end{bmatrix} \quad (3.18)$$

[n x r(\nu_M - 1)]

$$G(z) = \begin{bmatrix} I \\ zI \\ \vdots \\ z^{\nu_M-1} I \\ z^{\nu_M-1} I \end{bmatrix} \quad (3.19)$$

[r(\nu_M - 1) x r]

$$\nu_M = \max_i \{\nu_i\}$$

Substitution of (3.16) into (3.9) produces the input-output equation

$$(zI - A^*)V(z)y(k) = \sum_{\alpha=1}^s [(zI - A^*)W_{\alpha}G(z) + B_{\alpha}^*]u(k-d_{\alpha}) \quad (3.20)$$

Of the n equations in (3.20) only m are significant, namely the ν_1 th, the $(\nu_1 + \nu_2)$ th, ..., n th. These m significant equations can be expressed as

$$P(z)y(k) = \sum_{\alpha=1}^s Q_{\alpha}(z)u(k-d_{\alpha}) \quad (3.21)$$

where

$$P(z) = \begin{bmatrix} p_{11}(z) & \dots & p_{1m}(z) \\ \vdots & & \vdots \\ p_{m1}(z) & \dots & p_{mm}(z) \end{bmatrix} \quad (3.22)$$

$$Q_{\alpha}(z) = \begin{bmatrix} q_{\alpha,11}(z) & \dots & q_{\alpha,1r}(z) \\ \vdots & & \vdots \\ q_{\alpha,m1}(z) & \dots & q_{\alpha,mr}(z) \end{bmatrix} \quad (3.23)$$

The polynomials of $P(z)$ can be written directly from (3.20)

$$p_{ii}(z) = z^{\nu_i} - a_{ii,\nu_i} z^{\nu_i-1} - \dots - a_{ii,2} z - a_{ii,1} \quad (3.24)$$

$$p_{ij}(z) = - a_{ij,\nu_{ij}} z^{\nu_{ij}-1} - \dots - a_{ij,2} z - a_{ij,1} \quad (3.25)$$

Straight forward computations lead to the following forms of the polynomials of the $Q_{\alpha}(z)$

$$q_{\alpha,ij}(z) = \beta_{\alpha,i;0,j} z^{\nu_i-1} + \dots + \beta_{\alpha,i-1;1,j} \quad (3.26)$$

Here the coefficients $\beta_{\alpha,ij}$ are obtained from the matrices

$$\bar{B}_{\alpha}^* = MB_{\alpha}^* = \begin{bmatrix} \beta_{\alpha,11} \cdots \beta_{\alpha,1r} \\ \vdots \\ \beta_{\alpha,n1} \cdots \beta_{\alpha,nr} \end{bmatrix} \quad (3.27)$$

where the matrix M is given by

$$M = \begin{bmatrix} -a_{11,2} \cdots -a_{11,\nu_1} \cdot 1 & \cdots & a_{1m,2} \cdots -a_{1m,\nu_{1m}} \cdot 1 \\ -a_{11,3} \quad -a_{11,4} \cdots & \cdots & a_{1m,3} \quad -a_{1m,4} \cdots \\ \vdots & \cdots & \vdots \\ -a_{11,\nu_1} \quad 1 & \cdots & a_{1m,\nu_{1m}} \quad 1 \\ 1 & \cdots & 1 \\ \vdots & \vdots & \vdots \\ \vdots & \vdots & \vdots \\ -a_{m1,2} \cdots -a_{m1,\nu_m} \cdot 1 & \cdots & a_{mm,2} \cdots -a_{mm,\nu_m} \cdot 1 \\ -a_{m1,3} \quad -a_{m1,4} \cdots & \cdots & a_{mm,3} \quad -a_{mm,4} \cdots \\ \vdots & \cdots & \vdots \\ -a_{m1,\nu_m} \quad 1 & \cdots & a_{mm,\nu_m} \quad 1 \\ 0 & \cdots & 1 \end{bmatrix} \quad (3.28)$$

Due to the structure of the matrix A^* the following relations hold for the polynomials of $P(z)$ and the $Q_{\alpha}(z)$:

$$\deg(p_{ii}(z)) > \deg(p_{ij}(z)), \quad j > i \quad (3.29)$$

$$\deg(p_{ii}(z)) \geq \deg(p_{ij}(z)), \quad j < i \quad (3.30)$$

$$\deg(p_{ii}(z)) > \deg(p_{ji}(z)), \quad j \neq i \quad (3.31)$$

$$\deg(p_{ii}(z)) > \deg(q_{\alpha, ij}(z)) \quad (3.32)$$

The validity of the theorem has thus been established.

The input-output description of (3.21) may be modified in a way that is appropriate for the identification of the system from input and output data. This modification is introduced by way of the following lemma.

Lemma 3.1

The representation of (3.21) can be equivalently stated by a composite input-output equation, the so called polynomial matrices

$$P^c(z)y(k) - Q^c(z)u(k) \quad (3.33)$$

where $P^c(z)$ and $Q^c(z)$ are matrices of polynomials whose entries satisfy the relations of (3.29) - (3.32).

Proof:

Multiplication of (3.21) by $z^{\frac{d}{s}}$ produces

$$z^{d_s} P(z) y(k) = z^{d_s - d_1} Q_1(z) u(k) + z^{d_s - d_2} Q_2(z) u(k) + \dots$$

$$\dots + Q_s(z) u(k) \quad (3.34)$$

By making the assignments

$$P^c(z) = z^{d_s} P(z) \quad (3.35)$$

$$\Theta^c(z) = z^{d_s - d_1} Q_1(z) + z^{d_s - d_2} Q_2(z) + \dots + Q_s(z) \quad (3.36)$$

equation (3.33) results.

Now since the degree of each element of $P^c(z)$ is just the degree of the corresponding element of $P(z)$ increased by d_s , equations (3.29) - (3.31) hold. The degree of any element of $\Theta^c(z)$ can be at most equal to the degree of the corresponding element of $Q_1(z)$ increased by $d_s - d_1$, so equation (3.32) holds. The lemma has thus been proven.

The polynomial matrix description of (3.33) was first introduced by Guidorzi [25]. The development found in [25] inspired its extension to systems with input time delay found in this thesis.

REMARK 3.1

Often the identification of a model of a linear multivariable system with multiple input delays is made from input and output data. It is natural to consider an input-output description like that of (3.21) or (3.33) coupled with the relations of (3.29) - (3.32). However these two forms make inefficient use in the number of parameters. This can best be seen by considering an arbitrary 2 input, 2 output system with 2 input delays.

$$\begin{bmatrix} p_{11}(z) & p_{12}(z) \\ p_{21}(z) & p_{22}(z) \end{bmatrix} \begin{bmatrix} y_1(k) \\ y_2(k) \end{bmatrix} = \begin{bmatrix} q_{1,11}(z) & q_{1,12}(z) \\ q_{1,21}(z) & q_{1,22}(z) \end{bmatrix} \begin{bmatrix} u_1(k-d_1) \\ u_2(k-d_1) \end{bmatrix} + \\ \begin{bmatrix} q_{2,11}(z) & q_{2,12}(z) \\ q_{2,21}(z) & q_{2,22}(z) \end{bmatrix} \begin{bmatrix} u_1(k-d_2) \\ u_2(k-d_2) \end{bmatrix}$$

Neglecting for the moment $q_{1,12}(z)$ and $q_{2,12}(z)$ the first equation represented by (3.33) would be

$$\begin{aligned} & (z^{\nu_1+d_2} - a_{11,\nu_1} z^{\nu_1+d_2-1} - \dots - a_{11,1} z^{d_2} - 0z^{d_2-1} - \dots - 0)y_1(k) + \\ & (z^{\nu_{12}+d_2} - a_{12,\nu_1} z^{\nu_{12}+d_2-1} - \dots - a_{12,1} z^{d_2} - 0z^{d_2-1} - \dots - 0)y_2(k) = \\ & (0z^{\nu_1+d_2-1} + \dots + 0z^{\nu_1+d_2-d_1+1} + \beta_{1,\nu_1} z^{\nu_1+d_2-d_1} + \dots + \beta_{2,11})u_1(k) \end{aligned}$$

A more compacted form for writing this equation would be

$$\begin{aligned}
& (z^{\nu_1+d_2-d_1} - \dots - a_{11,1} z^{d_2-d_1} - 0z^{d_2-d_1-1} - \dots - 0)y_1(k) + \\
& (z^{\nu_2+d_2-d_1} - \dots - a_{12,1} z^{d_2-d_1} - 0z^{d_2-d_1-1} - \dots - 0)y_2(k) - \\
& (\beta_{1,\nu_1} z^{\nu_1+d_2-d_1} + \dots + \beta_{2,11}) z^{-d_1} u_1(k)
\end{aligned}$$

where the d_1 trailing coefficients of $p_{11}(z)$ and $p_{12}(z)$ and the d_1 leading coefficients of $q_{11}(z)$ have been taken care of by the delay term z^{-d_1} . Of course this same reasoning can be applied to $u_2(k)$ and its relation to $y_1(k)$ as well.

This more compact representation can be applied to each input/output pair of a multivariable system with an arbitrary number of inputs and outputs. Although the arguments made above only show the existence of delay terms of magnitude equal to d_1 , in general a search can be made to construct a delay term for each entry of $Q(z)$ which is at least d_1 . This produces the following delayed polynomial matrix description which generally has a smaller number of parameters than (3.33), or (3.21)

$$P^*(z)y(k) = Q^*(z)u(k) \quad (3.37)$$

where $P^*(z)$ has the same form as in (3.33) and $Q^*(z)$ is a matrix of dimension $m \times r$ of polynomials whose entries have the form

$$q_{ij}^*(z) = z^{-d_{ij}} \sum_{\alpha=1}^{\gamma_{ij}} b_{ij,\alpha} z^{-\alpha} \quad (3.38)$$

Equation (3.37) represents an input-output description which can have a fewer number of parameters for multiple input, multiple output systems with time delay than the classical transfer matrix description or the polynomial matrix form of (3.33). This is especially true for systems which have common modes in the outputs.

In the next section a procedure will be developed which will estimate the order of the polynomial entries and delay terms of (3.37) from input / output data. The following numerical example will illustrate the usefulness of such a representation.

EXAMPLE 3.1

Consider the 2 input, 2 output system shown in Figure 3-1. A state space equation that describes this system is

$$\mathbf{x}(k+1) = \begin{bmatrix} .8 & 0 & 0 & 0 & 0 \\ 0 & .6 & 0 & 0 & 0 \\ 1 & 0 & 0 & 0 & 0 \\ 0 & 1 & 2 & 0 & 0 \\ 0 & 0 & 0 & 0 & .3 \end{bmatrix} \mathbf{x}(k) + \begin{bmatrix} 1 & 0 \\ 0 & 1 \\ 0 & 0 \\ 0 & 0 \\ 0 & 0 \end{bmatrix} \mathbf{u}(k-1) + \begin{bmatrix} 0 & 0 \\ 0 & 0 \\ 0 & 0 \\ 0 & 0 \\ 0 & 1 \end{bmatrix} \mathbf{u}(k-2)$$

$$\mathbf{y}(k) = \begin{bmatrix} 0 & 1 & 1 & 0 & 0 \\ 0 & 0 & 0 & 1 & 1 \end{bmatrix} \mathbf{x}(k)$$

The observability matrix of this system is

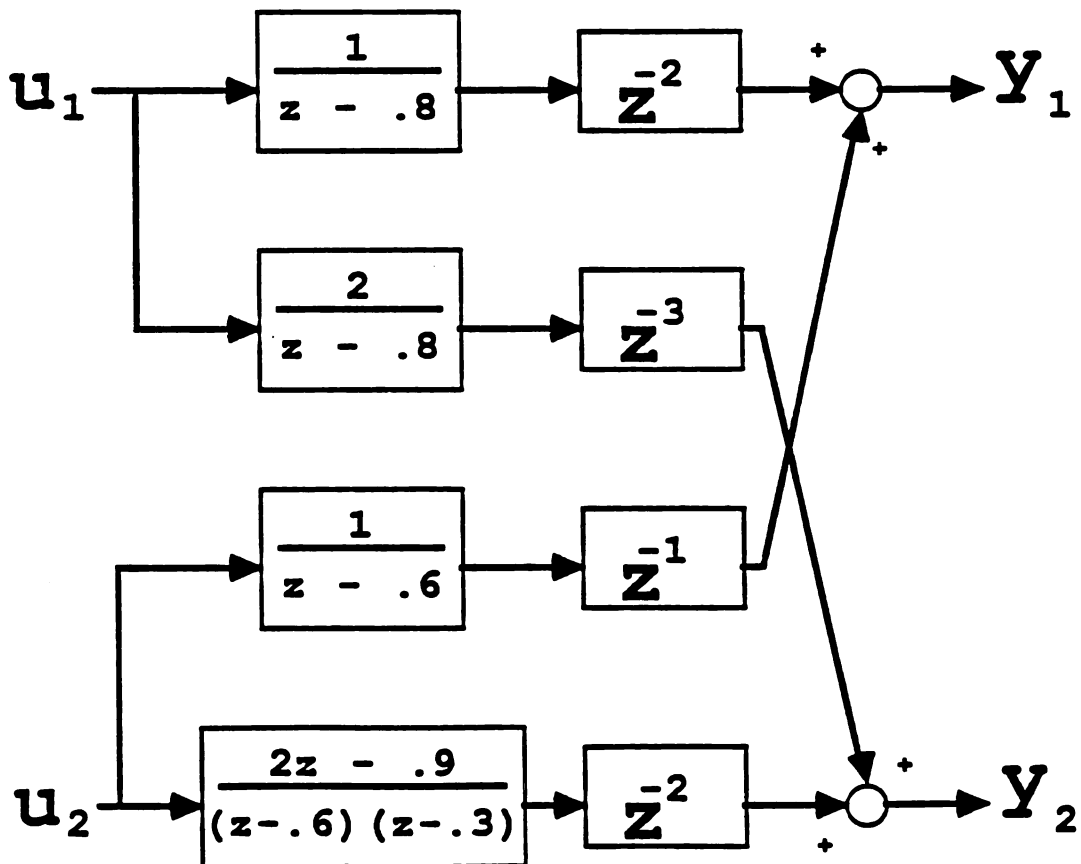


**Figure 3-1 2 input, 2 output system
with time delays**

$$0 = \begin{bmatrix} 0 & 0 & 1 & 0 & .8 & 2 \\ 1 & 0 & .6 & 1 & .36 & .6 \\ 1 & 0 & 0 & 2 & 0 & 0 & \dots \\ 0 & 1 & 0 & 0 & 0 & 0 \\ 0 & 1 & 0 & .3 & 0 & .09 \end{bmatrix}$$

Looking first for the vectors of 0 associated with y_1 produces the following transformation matrix

$$T = \begin{bmatrix} 0 & 1 & 1 & 0 & 0 \\ 1 & .6 & 0 & 0 & 0 \\ .8 & .36 & 0 & 0 & 0 \\ 0 & 0 & 0 & 1 & 1 \\ 0 & 1 & 2 & 0 & .3 \end{bmatrix}$$

Here $\nu_1 = 3$ and $\nu_2 = 2$. Application of T via equations (3.11) and (3.13) gives

$$A^* = TAT^{-1} = \begin{bmatrix} 0 & 1 & 0 & 0 & 0 \\ 0 & 0 & 1 & 0 & 0 \\ 0 & -.48 & 1.4 & 0 & 0 \\ 0 & 0 & 0 & 0 & 1 \\ 0 & 1 & 2 & 0 & .3 \end{bmatrix}$$

$$B_2^* = TB_2 = \begin{bmatrix} 0 & 1 \\ 1 & .6 \\ .8 & .36 \\ 0 & 0 \\ 0 & 1 \end{bmatrix} \quad B_2^* = TB_2 = \begin{bmatrix} 0 & 0 \\ 0 & 0 \\ 0 & 0 \\ 0 & 1 \\ 0 & .3 \end{bmatrix}$$

The matrix M is therefore given as

$$M = \begin{bmatrix} .48 & -1.4 & 1 & 0 & 0 \\ -1.4 & 1 & 0 & 0 & 0 \\ 1 & 0 & 0 & 0 & 0 \\ 0 & -2.5 & 0 & -.3 & 1 \\ -2.5 & 0 & 0 & 1 & 0 \end{bmatrix}$$

which produces

$$\bar{B}_1^* = MB_1^* = \begin{bmatrix} -.6 & 0 \\ 1 & -.8 \\ 0 & 1 \\ -2.5 & -.5 \\ 0 & -2.5 \end{bmatrix} \quad \bar{B}_2^* = MB_2 = \begin{bmatrix} 0 & 0 \\ 0 & 0 \\ 0 & 0 \\ 0 & 0 \\ 0 & 1 \end{bmatrix}$$

The equivalent input-output description of (3.21) is therefore

$$\begin{bmatrix} z^3 - 1.4z^2 + .48z + 0 & 0 \\ -2.5z^2 + 0z - .6 & z^2 - .3z + 0 \end{bmatrix} \begin{bmatrix} y_1(k) \\ y_2(k) \end{bmatrix} = \\ \begin{bmatrix} z - .6 & z^2 - .8z \\ 0z - 2.5 & -2.5z - .5 \end{bmatrix} \begin{bmatrix} u_1(k-1) \\ u_2(k-1) \end{bmatrix} + \begin{bmatrix} 0 & 0 \\ 0 & z \end{bmatrix} \begin{bmatrix} u_1(k-2) \\ u_2(k-2) \end{bmatrix}$$

The number of parameters of this representation is 22. The polynomial matrix description of (3.33) is given by

$$\begin{bmatrix} z^4 - 1.4z^3 + .48z^2 + 0z + 0 & 0 \\ -2.5z^3 + 0z^2 - .6z + 0 & z^3 - .3z^2 + 0z + 0 \end{bmatrix} \begin{bmatrix} y_1(k) \\ y_2(k) \end{bmatrix} = \\ \begin{bmatrix} 0z^3 + 0z^2 + z - .6 & 0z^3 + z^2 - .8z + 0 \\ 0z^2 + 0z - 2.5 & 0z^2 - 2.5z + .5 \end{bmatrix} \begin{bmatrix} u_1(k) \\ u_2(k) \end{bmatrix}$$

The number of the parameters for this representation is 26.

As a contrast the delayed polynomial matrix representation of (3.37) is

$$\begin{bmatrix} z^2 - 1.4z + .48 & 0 \\ -2.5z^2 + 0z - .6 & z^2 - .3z + 0 \end{bmatrix} \begin{bmatrix} y_1(k) \\ y_2(k) \end{bmatrix} = \\ \begin{bmatrix} (z - .6)z^{-2} & (z - .8)z^{-1} \\ (0z - 2.5)z^{-1} & (-2.5z + .5)z^{-1} \end{bmatrix} \begin{bmatrix} u_1(k) \\ u_2(k) \end{bmatrix}$$

Here the number of the parameters is 16.

Example 3.1 demonstrates how representation of a system by delayed polynomial matrices reduces the number of parameters necessary to describe the system behavior. This can lead to more consistent parameter estimation when noisy input-output data is used to fit the parameter values. A method which identifies an delayed polynomial matrix model of a system from input-output data prior to parameter estimation is described next.

3.4 Structural Identification

In this section a method will be described which deduces the structure of the delayed polynomial representation of a discrete system from input and output observations. The term structure relates to the order of the polynomial entries of the matrices $P^*(z)$ and $Q^*(z)$ and to the magnitude of the delay terms of the entries of $Q^*(z)$ found in

equation (3.37). The method that follows can be applied prior to parameter estimation and is suitable for interactive computer use. The method is a two phase procedure:

PHASE 1 Estimate the polynomial matrix representation, equation (3.33)

PHASE 2 Estimate the delay of each input to each output to form the delayed polynomial matrix model, equation (3.37)

3.4.1 Phase 1

In order to identify the polynomial matrix model of a system the Kronicker invariants, ν_{ij} , must be estimated. The structural identification will be performed by exploiting the linear dependence relations imposed by (3.33) and the structural relations imposed by (3.29) thru (3.32).

Consider first the i -th row of (3.33). It may be rewritten as

$$y_i^{(k+\nu_i)} = \sum_{j=1}^r \sum_{l=1}^{\nu_{ij}} a_{ij,l} y_j^{(k+l-1)} +$$

$$\sum_{j=1}^m \sum_{l=1}^{\nu_i} \beta_{(\nu_1 + \dots + \nu_{i-1} + 1), j} u_j^{(k+1-l)} \quad (3.39)$$

where $\nu_i = \nu_{ii}$.

Consider now the vectors of observations given as

$$\eta_i(k) = [y_i(k), y_i(k+1), \dots, y_i(k+N-1)]^T \quad (3.40)$$

$$\kappa_j(k) = [u_j(k), u_j(k+1), \dots, u_j(k+N-1)]^T \quad (3.41)$$

Because of (3.39) the following is true

$$\eta_i^{(k+\nu_i)} = \sum_{j=1}^r \sum_{l=1}^{\nu_{ij}} a_{ij, l} \eta_j^{(k+1-l)} + \sum_{j=1}^m \sum_{l=1}^{\nu_i} \beta_{i-1; l, j} \kappa_j^{(k+1-l)} \quad (3.42)$$

Equation (3.42) suggests the following selection plan to determine each ν_{ij} :

1. Select the observation vectors in the following order

$$\eta_1(k), \eta_2(k), \dots, \eta_r(k), \kappa_1(k), \dots, \kappa_m(k), \eta_1(k+1), \eta_2(k+1), \dots, \\ \eta_r(k+1), \kappa_1(k+1), \dots, \kappa_m(k+1), \eta_1(k+2), \dots$$

(3.43)

2. Retain a vector if and only if it is linearly independent from the previously selected vectors.
3. When a dependent vector $\eta_i(k+\nu_i)$ is found it is no longer necessary to test the vectors $\eta_i(k+\nu_i+j)$, $j > 0$, since they will also be linearly dependent. At this time, note the selected sequence of vectors.
4. Continue until a dependent vector has been found for each output y_i . The Kronecker indices, ν_{ij} , have now been identified.

3.4.2 Phase 2

The structure of the delayed polynomial matrix representation can be deduced from input / output data by using the polynomial matrix form as a starting point. To see this consider the i th row of equation (3.37). It may be rewritten as

$$y_i(k+\nu_i^*) = \sum_{j=1}^r \sum_{l=1}^{\nu_{ij}^*} a_{ij,l}^* y_j(k+1-l) + \sum_{j=1}^m \sum_{l=1}^{\gamma_{ij}^*} b_{ij,l}^* u_j(k+1-l-\tau_{ij}) \quad (3.44)$$

One can remove the time delay in the inputs by equivalently representing the system in prediction form

$$y_i(k+\nu_i^*+\xi_{\max,i}) = \sum_{j=1}^r \sum_{l=1}^{\nu_{ij}^*} a_{ij,l}^* y_j(k+1-l+\xi_{\max,i}) + \sum_{j=1}^m \sum_{l=1}^{\gamma_{ij}^*} b_{ij,l}^* u_j(k+1-l+\xi_{\max,i}-\tau_{ij}) \quad (3.45)$$

where $\xi_{\max,i} = \max(\xi_{ij})$, $\xi_{ij} = \tau_{ij} + \gamma_{ij}$. Furthermore, this system can be equivalently represented by

$$y(k+\nu_i) = \sum_{j=1}^r (a_{ij,\nu_{ij}} z^{\nu_{ij}-1} + \dots + a_{ij,1} z^{\xi_{\max,i}+0} z^{\xi_{\max,i}-1} + \dots + 0) y_j(k) + \sum_{j=1}^m (0 z^{\nu_i-1} + \dots + b_{ij,\gamma_{ij}} z^{\nu_i-\tau_{ij}-1} + \dots + b_{ij,1} z^{\nu_i-\xi_{ij}+0} z^{\nu_i-\xi_{ij}-1} + \dots + 0) u_j(k) \quad (3.46)$$

Where $\nu_i = \nu_i^* + \xi_{\max,i}$ and $\nu_{ij} = \nu_{ij}^* + \xi_{\max,i}$.

This last equation is the same as the i th row of the polynomial matrix form of equation (3.33).

Equations (3.44) - (3.46) suggest that the delayed polynomial matrix representation may be deduced from the normal polynomial matrix representation by identifying the zero valued parameters of (3.46). The following steps accomplish this identification.

STEP 1. Set $\tau_{\max,i} = 0$, for $i = 1, 2, \dots, r$.

Set $\rho_{\max,i} = 0$, for $i = 1, 2, \dots, r$.

STEP 2. Select any output y_i and start with the collection of vectors which produced the linearly dependent vector $\eta_i(k+\nu_i)$. Select any output u_j and remove groups of vectors from the collection in the following order

$$\begin{aligned} &\eta_1(k), \dots, \eta_r(k), \kappa_j(k+\nu_i-1); \\ &\eta_1(k+1), \dots, \eta_r(k+1), \kappa_j(k+\nu_i-2); \\ &\dots \quad (3.47) \end{aligned}$$

STEP 3. Continue to remove vectors until it is found that $\eta_i(k+\nu_i)$ is no longer linearly dependent on the remaining vectors. If the removal

of $\kappa_j(k+\nu_i-d_j)$ eliminates the linear dependence of $\eta_i(k+\nu_i)$ then set

$$\tau_{ij} = d_j - 1 \text{ and } \tau_{\max,i} = \max(\tau_{\max,i}, \tau_{ij})$$

STEP 4. Repeat step 3 for all other inputs u_1 by removing vectors from the collection in the following order

$$\begin{aligned} & \kappa_1(k+\nu_i-1); \\ & \kappa_1(k+\nu_i-2); \dots; \\ & \dots \\ & \kappa_1(k+\nu_i-\tau_{\max,i}); \\ & \eta_1(k+\tau_{\max,i}^1), \dots, \eta_r(k+\tau_{\max,i}^1), \kappa_1(k+\nu_i-\tau_{\max,i}^1); \\ & \eta_1(k+\tau_{\max,i}^2), \dots, \eta_r(k+\tau_{\max,i}^2), \kappa_1(k+\nu_i-\tau_{\max,i}^2); \\ & \dots \quad (3.48) \end{aligned}$$

STEP 5. Having determined $\tau_{\max,i}$, now select any input u_j and remove groups of vectors from the remaining collection using the following order

$$\begin{aligned} & \kappa_j(k); \\ & \kappa_j(k+1); \\ & \dots \\ & \kappa_j(k+\tau_{\max,i}); \\ & \eta_1(k+\tau_{\max,i}^1), \dots, \eta_r(k+\tau_{\max,i}^1), \kappa_1(k+\tau_{\max,i}^1); \end{aligned}$$

$$\eta_1(k+r_{\max,i}+2), \dots, \eta_r(k+r_{\max,i}+2), \kappa_1(k+r_{\max,i}+2);$$

..... (3.49)

STEP 6. Continue to remove vectors until it is found that $\eta_i(k+\nu_i)$ is no longer linearly dependent on the remainder. If the removal of $\kappa_j(k+\rho_j)$ eliminates the linear dependence of $\eta_i(k+\nu_i)$ then set $\gamma_{ij} = \nu_i - \tau_{ij} - \rho_{ij} + 1$ and $\rho_{\max,i} = \max(\rho_{\max,i}, \rho_j)$.

STEP 7. Continue steps 5 and 6 for all other u_1 by removing groups of vectors in the following order

$$\begin{aligned} & \kappa_1(k); \\ & \kappa_1(k+1); \\ & \dots \\ & \kappa_1(k+r_{\max,i}+\rho_{\max,i}-1); \\ & \eta_1(k+r_{\max,i}+\rho_{\max,i}), \dots, \\ & \eta_r(k+r_{\max,i}+\rho_{\max,i}), \kappa_1(k+r_{\max,i}+\rho_{\max,i}); \\ & \dots \end{aligned} \quad (3.50)$$

until all γ_{ij} are identified. Set $\nu_i^* = \nu_i - \tau_{\max,i} - \rho_{\max,i} + 1$.

STEP 8. Go to step 2 and repeat for any previously unselected output.

For the above selection plan to work two conditions on the input must be met. First the length of the observation vectors must be large enough to accomodate (3.42) so

$$N \geq \sum_{i=1}^r \nu_i + r\nu_{\max}, \quad \nu_{\max} = \max(\nu_i)$$

Also the vectors of input observations must be linearly independent. This is the same thing as requiring that the input to the system be persistently exciting.

3.5 Computer Implementation

The success of the selection plan discussed above rests on accurately testing for the linear dependence among the observation vectors. This problem, which is the same as determining the rank of a matrix composed of the observation vectors, is well understood mathematically but as a practical problem it remains a challenge. In the present context the challenge lies in performing the mathematical calculations on a finite precision machine using noisy input and output observations of a dynamic system. As it shall be seen the errors introduced by the computer are handled by a stable numerical algorithm, singular value decomposition. While the noisy data is handled by proper filtering techniques.

There exists several mathematically equivalent techniques to determine the rank of a matrix. Unfortunately, different approaches lead to computational methods which can give different results when implemented on a digital computer. Several reasons exist for these discrepancies. First the computations must be performed in bounded arithmetic, bounded by finite precision and finite range. So computations are executed with truncation errors and must lie within the range of the computing machine. Furthermore, the mathematical problem posed is an inexact representation of the underlying physical system. In other words the linear relationship assumed among the observations is only an approximation to the usually true nonlinear nature of the process which produced them. For these reasons the best that we can hope for is a numerically stable algorithm which quantifies the closeness to singularity of a matrix composed of the set of considered vectors.

3.5.1 Singular Value Decomposition

Singular value decomposition, SVD, is generally acknowledged as the most reliable method for determining rank numerically [26]. As a mathematical tool it has been around since the late nineteenth century. Golub and Reinsch [27] developed an efficient numerical algorithm for computing the SVD in 1970. SVD has seen some use in the control literature since the middle 1970's. However it was overlooked by past authors of techniques to estimate model order by testing the linear dependence of the observations. In fact, the reason SVD was used in

this research is because of the poor performance that was experienced when the competing methods of rank determination, namely determinant calculation and eigen value calculation, were first tried. It is likely that the application reported here will soon be one of the many uses of SVD in the control field.

Singular value decomposition for real matrices can be defined in the following way. Let A be a real matrix of dimensions $n \times m$ with rank r , where $n \geq m \geq r$. Then there exists matrix, U , matrix, V , and matrix, S , such that

$$A = USV^T \quad (3.51)$$

$$S = \begin{bmatrix} s_1 & 0 & 0 & 0 & 0 \\ 0 & \cdot & \cdot & \cdot & 0 \\ 0 & 0 & 0 & 0 & s_m \end{bmatrix} \quad (3.52)$$

The numbers s_1, \dots, s_m are called the singular values of A and by convention $s_1 \geq s_2 \geq \dots \geq s_m$.

The well conditioned nature of the singular values is illustrated by the following property. If $A + F$ has singular values ζ_1, \dots, ζ_m , then $|s_i - \zeta_i| \leq \|F\| - \zeta_i$. Thus, singular values are well conditioned with respect to perturbations in a matrix of noisy input / output data.

Ideally, if $r < m$ then, $s_1 \geq s_2 \geq \dots \geq s_r$ and $s_{r+1} = \dots = s_m = 0$. So the number of non-zero singular values gives the rank of the matrix.

However, s_1 is clearly sensitive to scale so a better dimensionless quantity is s_r / s_1 , which is sometimes called a condition number of the matrix. Calculation of the condition number of a matrix of observation vectors is useful when the values of the inputs and outputs differ greatly in magnitude.

Even by using singular value decomposition one would be ill advised to operate directly on the matrix constructed from the observation vectors of equations (3.43), (3.47)-(3.50) because of its large dimensions. A more efficient algorithm based on the principle that $\text{rank}(\mathbf{A}) = \text{rank}(\mathbf{A}^T \mathbf{A})$ follows.

3.5.2 Computer Algorithm

Some notation must be explained before the computer algorithm to determine the delayed polynomial matrix representation is presented. Consider a single input, single output system and let a matrix of observation vectors be designated as

$$\Omega(\mu_1:\partial_1, \mu_2:\partial_2) = [\eta(k+\partial_1), \eta(k+\partial_1+1), \dots, \eta(k+\mu_1), \\ \kappa(k+\partial_2), \kappa(k+\partial_2+1), \dots, \kappa(k+\mu_2)] \quad (3.53)$$

Now let

$$\Lambda(\mu_1:\partial_1, \mu_2:\partial_2) = \Omega^T(\mu_1:\partial_1, \mu_2:\partial_2)\Omega(\mu_1:\partial_1, \mu_2:\partial_2) \quad (3.54)$$

Therefore a matrix of observation vectors from a system with m inputs and r outputs would be designated as

$$\begin{aligned} \Omega(\mu_1:\partial_1, \dots, \mu_r:\partial_r, \dots, \mu_{r+m}:\partial_{r+m}) = & [\eta_1(k+\partial_1), \dots, \eta_1(k+\mu_1), \eta_2(k+\partial_2), \\ & \dots, \eta_r(k+\mu_r), \kappa_1(k+\partial_{r+1}), \dots, \kappa_m(k+\mu_{r+m})] \end{aligned} \quad (3.55)$$

and

$$\begin{aligned} \Lambda(\mu_1:\partial_1, \dots, \mu_{r+m}:\partial_{r+m}) = \\ \Omega^T(\mu_1:\partial_1, \dots, \mu_{r+m}:\partial_{r+m})\Omega(\mu_1:\partial_1, \dots, \mu_{r+m}:\partial_{r+m}) \end{aligned} \quad (3.56)$$

The two phase method for the identification of delayed polynomial matrices may now be implemented by the following steps on a digital computer:

3.5.2.1 Phase 1

STEP 1. Construct the sequence of increasing dimension matrices

$$\begin{aligned} \Lambda(1:0, 0:0, \dots, 0:0), \Lambda(1:0, 1:0, \dots, 0:0), \dots, \Lambda(1:0, 1:0, \dots, 1:0) \Lambda(2:0, 1:0, \dots, \\ \dots, 1:0), \Lambda(2:0, 2:0, \dots, 1:0), \dots, \Lambda(2:0, 2:0, \dots, 2:0) \Lambda(3:0, 2:0, \dots, 2), \dots \end{aligned} \quad (3.57)$$

STEP 2. Test for the singularity of each matrix by calculating its smallest singular value or its condition number. When a singular matrix is found there will be a large drop in the evolution of the smallest singular value or the condition numbers.

STEP 3. When a singular matrix is encountered, say $\wedge(\mu_1:0, \dots, \nu_i:0, \dots, \mu_{r+m}:0)$, ν_i has been identified. Let $\mu_i = \nu_i - 1$ and remain constant. It also follows that $\nu_{ij} = \mu_j$.

STEP 4. Continue to increase the other indices in the same manner until all observability indices ν_i are found, noting the structure of the \wedge matrix associated with each ν_i .

3.5.2.2 Phase 2

STEP 1. Set $r_{\max,i} = 0$, $i = 1, 2, \dots, r$.

Set $\rho_{\max,i} = 0$, $i = 1, 2, \dots, r$.

STEP 2. Select any output y_i and start with the singular matrix $\wedge(\nu_{i1}:0, \dots, \nu_i:0, \dots, \nu_{ir}:0, \nu_i-1:0, \dots, \nu_i-1:0)$ which identified its ν_i . Select any input u_j and construct the sequence of decreasing dimension matrices

$$\begin{array}{cccccc}
 1 & i & r & r+1 & r+j & r+m \\
 \downarrow & \downarrow & \downarrow & \downarrow & \downarrow & \downarrow \\
 \wedge(\nu_{i1}:1, \dots, \nu_i:1, \dots, \nu_{ir}:1, \nu_i:0, \dots, \nu_i^{-2}:0, \dots, \nu_i:0), \\
 \wedge(\nu_{i1}:2, \dots, \nu_i:2, \dots, \nu_{ir}:2, \nu_i:0, \dots, \nu_i^{-3}:0, \dots, \nu_i:0), \\
 \wedge(\nu_{i1}:3, \dots, \nu_i:3, \dots, \nu_{ir}:3, \nu_i:0, \dots, \nu_i^{-4}:0, \dots, \nu_i:0), \\
 \dots\dots
 \end{array} \tag{3.58}$$

STEP 3. Test for the non-singularity of each matrix by calculating its smallest singular value or its condition number. When a non-singular matrix is found, say $\wedge(\nu_{i1}:d_j, \dots, \nu_i:d_j, \dots, \nu_{ir}:d_j, \nu_i:0, \dots, \nu_i^{-1-d_j}:0, \dots, \nu_i:0), d_j:0, \dots, \nu_i:0)$, there will be a large change in the evolution of the smallest singular value or its condition number. Set $r_{ij} = d_j - 1$ and $r_{\max,i} = \max\{r_{\max,i}, r_{ij}\}$.

STEP 4. Repeat steps 2 and 3 for all other inputs, u_1 , using the sequence of decreasing dimension matrices

$$\begin{array}{cccccc}
 1 & r & r+1 & r+j & r+m \\
 \downarrow & \downarrow & \downarrow & \downarrow & \downarrow \\
 \wedge(\nu_{i1}:r_{\max,i}, \dots, \nu_{ir}:r_{\max,i}, \nu_i:0, \dots, \nu_i^{-2}:0, \dots, \nu_i:0), \\
 \wedge(\nu_{i1}:r_{\max,i}, \dots, \nu_{ir}:r_{\max,i}, \nu_i:0, \dots, \nu_i^{-3}:0, \dots, \nu_i:0), \\
 \dots\dots \\
 \wedge(\nu_{i1}:r_{\max,i}, \dots, \nu_{ir}:r_{\max,i}, \nu_i:0, \dots, \nu_i^{-r_{\max,i}}:0, \dots, \nu_i:0), \\
 \wedge(\nu_{i1}:r_{\max,i}+1, \dots, \nu_{ir}:r_{\max,i}+1, \nu_i:0, \dots, \nu_i^{-r_{\max,i}+1}:0, \dots, \nu_i:0), \\
 \dots\dots
 \end{array} \tag{3.59}$$

STEP 5. Having determined $\tau_{\max, i}$, now select any input u_j and construct the following sequence of decreasing dimension matrices

$$\begin{array}{cccc}
 1 & r & r+1 & r+j \\
 \downarrow & \downarrow & \downarrow & \downarrow \\
 \wedge(\nu_{i1}:\tau_{\max, i}, \dots, \nu_{ir}:\tau_{\max, i}, \nu_{i-\tau_{i1}}:0, \dots, \nu_{i-\tau_{ij}}:1, \dots \\
 & & & \dots, \nu_{i-\tau_{ir}}:0) \\
 \wedge(\nu_{i1}:\tau_{\max, i}, \dots, \nu_{ir}:\tau_{\max, i}, \nu_{i-\tau_{i1}}:0, \dots, \nu_{i-\tau_{ij}}:2, \dots \\
 & & & \dots, \nu_{i-\tau_{ir}}:0) \\
 \wedge(\nu_{i1}:\tau_{\max, i}, \dots, \nu_{ir}:\tau_{\max, i}, \nu_{i-\tau_{i1}}:0, \dots, \nu_{i-\tau_{ij}}:3, \dots \\
 & & & \dots, \nu_{i-\tau_{ir}}:0) \\
 \dots\dots\dots \\
 \wedge(\nu_{i1}:\tau_{\max, i}, \dots, \nu_{ir}:\tau_{\max, i}, \nu_{i-\tau_{i1}}:0, \dots, \nu_{i-\tau_{ij}}:\tau_{\max, i}, \dots \\
 & & & \dots, \nu_{i-\tau_{ir}}:0) \\
 \wedge(\nu_{i1}:\tau_{\max, i}+1, \dots, \nu_{ir}:\tau_{\max, i}+1, \nu_{i-\tau_{i1}}:0, \dots, \nu_{i-\tau_{ij}}:\tau_{\max, i}+1 \\
 & & & \dots, \nu_{i-\tau_{ir}}:0) \\
 \dots\dots\dots & & & (3.60)
 \end{array}$$

STEP 6. Continue until a non-singular matrix is encountered, say

$\wedge(\dots, \nu_{i-\tau_{ij}}:\rho_j, \dots)$. Then set $\gamma_{ij} = \tau_{ij} - \rho_{ij} + 1$.

STEP 7. Continue steps 5 and 6 until all γ_{ij} are identified. Set ν_{ij}^*
 $= \nu_{ij} - \tau_{\max,i} - \rho_{\max,i} + 1$.

STEP 8. Go to step 2 and repeat for any previously unselected output.

3.5.3 Noise Compensation

The above algorithm must be modified when the observation vectors are constructed from noisy measurements. This is due to the fact that because of the random noise, the matrices Ω and Λ are always near full rank. This tends to reduce the significant changes in the evolution of the condition numbers making detection of singularity difficult.

One way to handle noisy observations is to prefilter the data before applying the identification algorithm. To do this, each data set for a particular input or output could be passed through a digital filter whose cut-off frequency is such that it passes only the power in the true signal. A second order Butterworth type would be adequate. The cut-off frequency of each of the filters could be determined by inspecting the power spectrum of each signal. In general, the dynamics of the process are much slower than the noise of its measurements so that a cut-off frequency is easily determined.

If the covariance of the noise on each observation is known then the algorithm can be performed using a compensated Λ matrix as described in

[25]. This method of noise compensation is much simpler than prefiltering since it just involves subtracting the noise covariance matrix from the Λ matrix constructed from the noisy observations. For an uncorrelated noise structure the covariance matrix reduces to a diagonal matrix whose diagonal elements are the variance of the noise on each measurement. An estimate of the noise variances is easily determined by holding all inputs to the process constant and monitoring the deviations of the signals from their steady state values.

3.5.4 SVD Subroutines

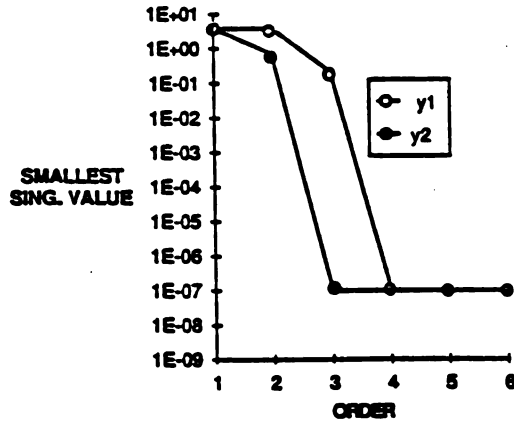
There exists several reliable programs written to perform singular value decomposition which may be used in the procedure just described. The subroutine libraries EISPACK [28] and LINPACK [29] contain fortran callable subroutines to perform singular value decomposition. The Linear Algebraic Systems interpreter contains a function which performs the decomposition. For the research of this thesis an interactive computer subroutine was written utilizing the EISPACK routine SVD. This subroutine steps the user through the algorithm just described and reports the singular values at each step. Only 40 lines of fortran code were necessary for the subroutine.

3.5.5 Simulation Results

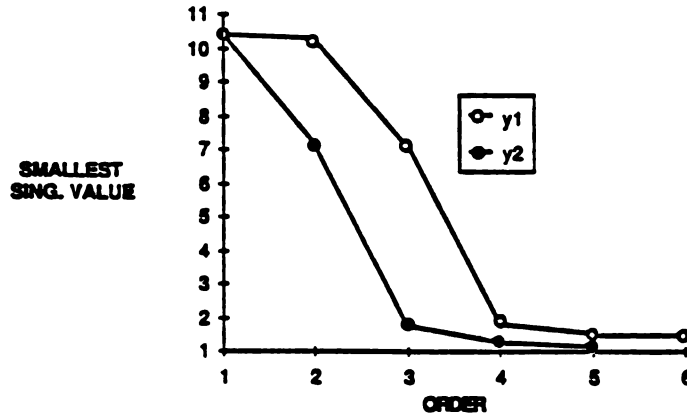
As a means of demonstrating the ability of the proposed algorithm under various conditions, consider again example 3.1. Simulated data was obtained for this system by driving it with two pseudo random binary sequences of 127 samples which were kept uncorrelated by delaying one by half its length. A noise free data set of 500 samples was used to determine the variance of both the outputs. Additive zero mean Gaussian noise was added to the outputs. The ratio of the noise standard deviation to the signal standard deviation was taken to be the noise to signal ratio. Experimental results were obtained for noise to signal ratios of 0%, 10% and 20%. The unfiltered data of length 450 samples was used in all experiments in order to show the degrading effect of noise and yet the ability of the method to perform in spite of it. The test used for all cases was the evolution of the smallest singular value because the magnitude of input and output were comparable.

Results of the identification of the two Kronecker indices for the polynomial matrix model are illustrated in Figure 3-2. Clearly the correct values are obtained for the noise free case. In the results for the case of 10% additive noise it is apparent the significant change in the evolution of the smallest singular value is very much decreased but the correct values for ν_1 and ν_2 are still obtained. Again for 20% noise level, there is a decrease in the significant drop of the evolution of the smallest singular value but the value of the indices can still be identified. Also note that in addition to looking for a

0% NOISE ORDER TEST



10% NOISE ORDER TEST



20% NOISE ORDER TEST

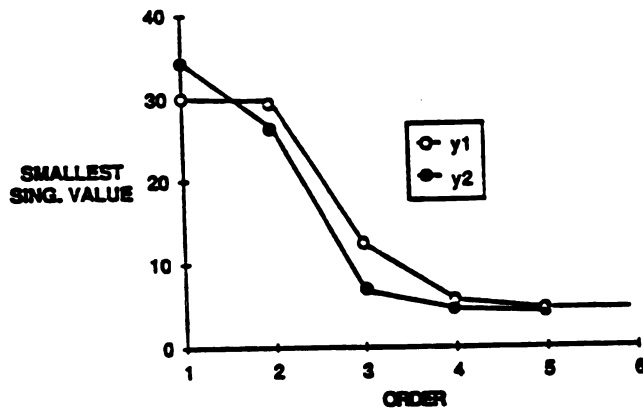


FIGURE 3-2 MODEL ORDER ESTIMATION WITH DIFFERENT AMOUNTS OF ADDITIVE NOISE.

significant change in the evolution of the smallest singular value one can look for the point at which the rate of change is small.

Figures 3-3 thru 3-8 report the value of the smallest singular value as the observation vectors are removed from the matrix which identified the Kronecker index for each output. For the noise free case in Figures 3-3 and 3-6, the values of time delay are very evident due to the enormous change in the smallest singular value. The same is true for the determination of ρ_{ij} .

The tests for the 10% noise case are illustrated in Figures 3-4 and 3-7. The change in the singular values is very much reduced but the true values of time delay and ρ_{ij} are obtained.

The 20% noise level case is shown in Figures 3-5 and 3-8. In this case the delay of u_1 to y_2 is not detected due to the lack of a significant rise in the singular value. The delay from u_2 to y_1 is also questionable. However, correct values for ρ_{ij} are still obtained. These results clearly demonstrate how additive noise prevents the singularity of the Λ matrix.

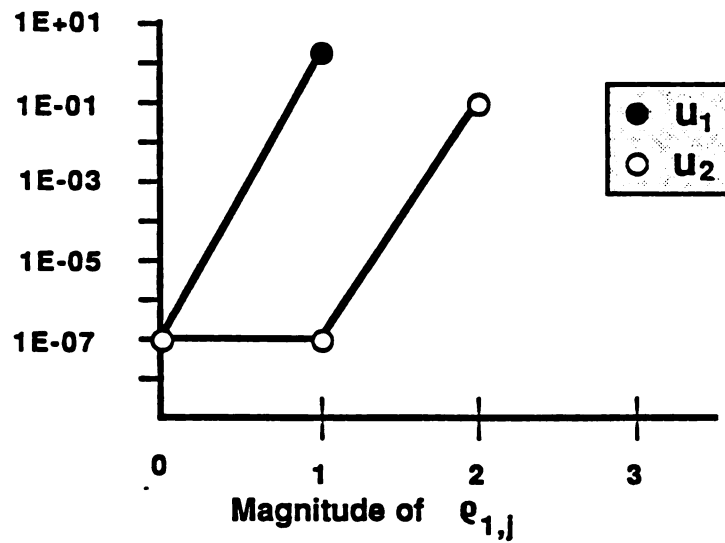
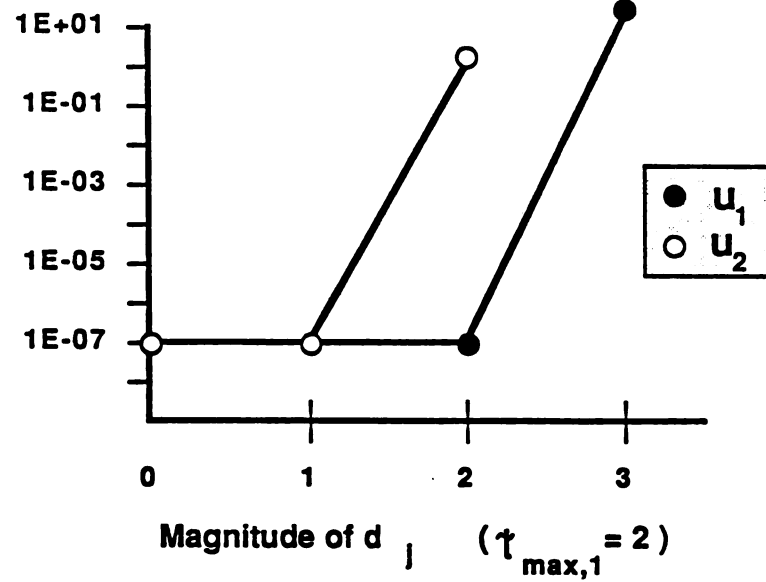


Figure 3-3 Input delay test for y_1 with 0% noise

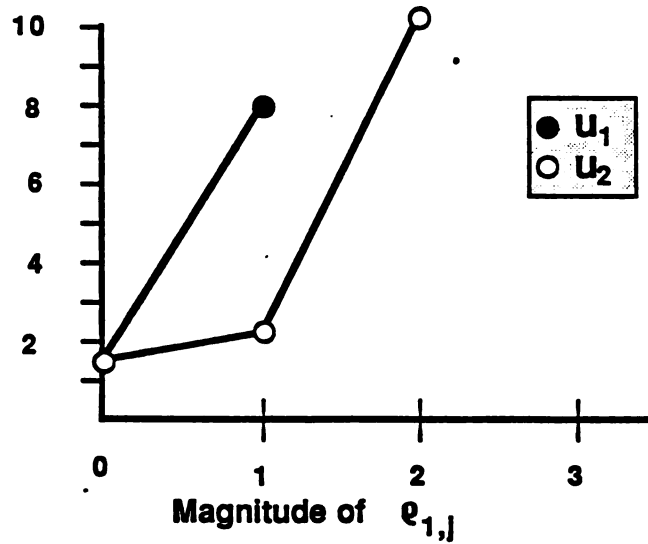
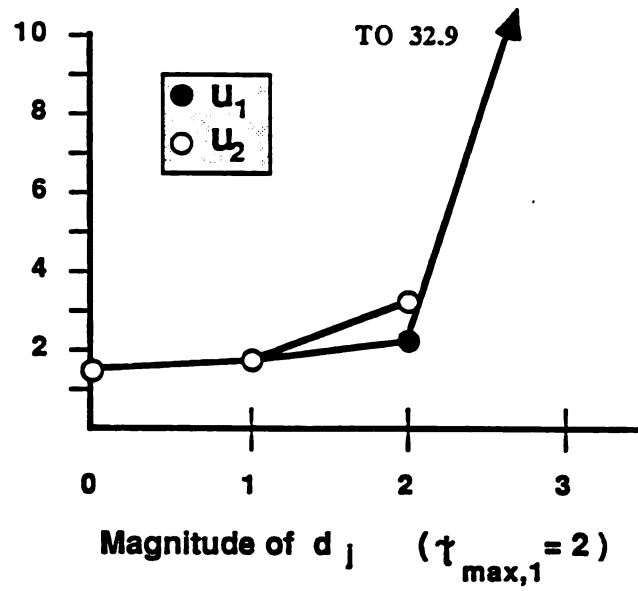


Figure 3-4 Input delay test for y with 10% noise

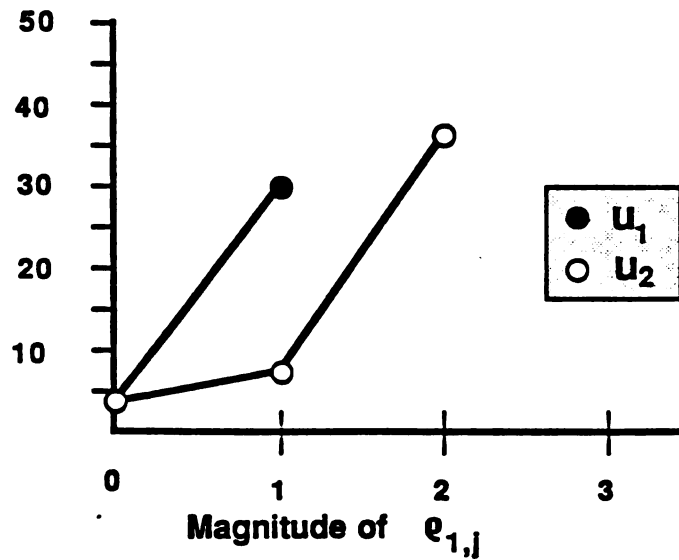
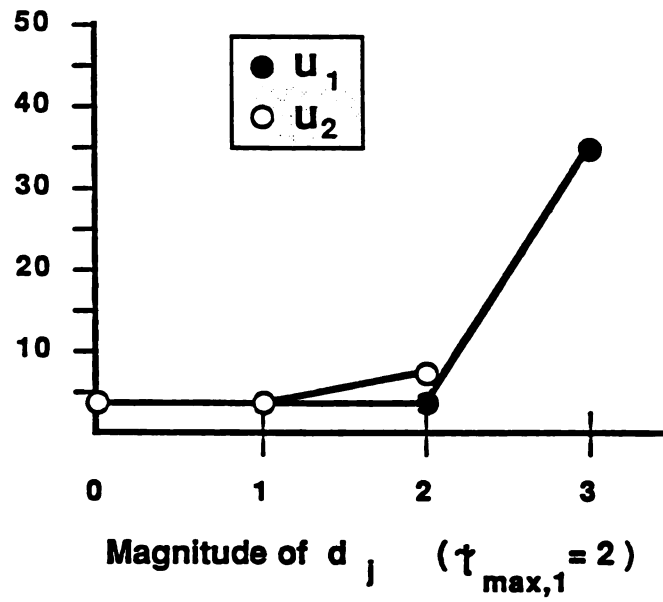


Figure 3-5 Input delay test for y_1 with 20% noise

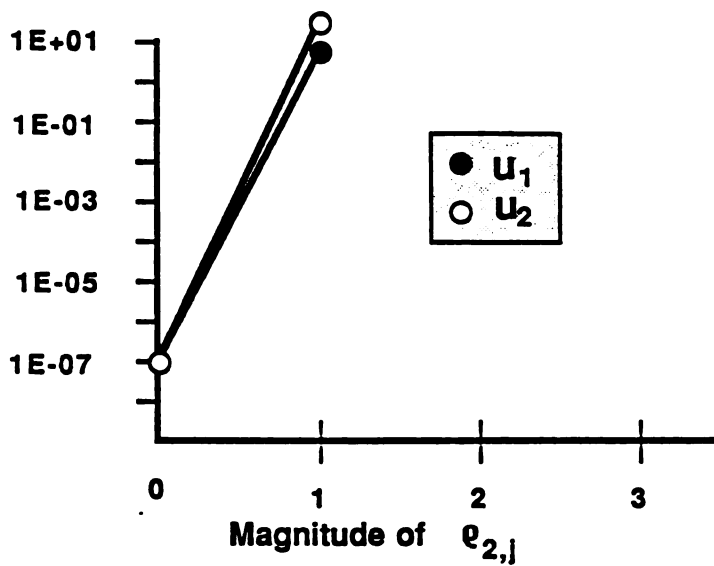
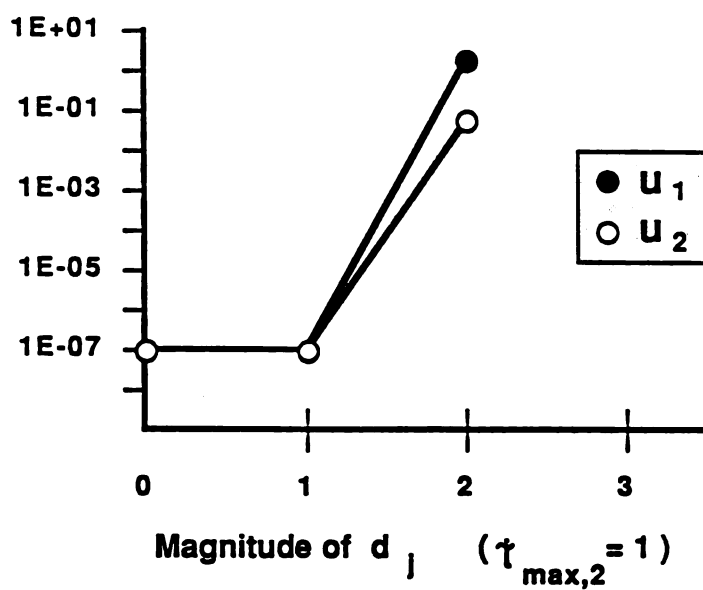


Figure 3-6 Input delay test for y_2 with 0% noise

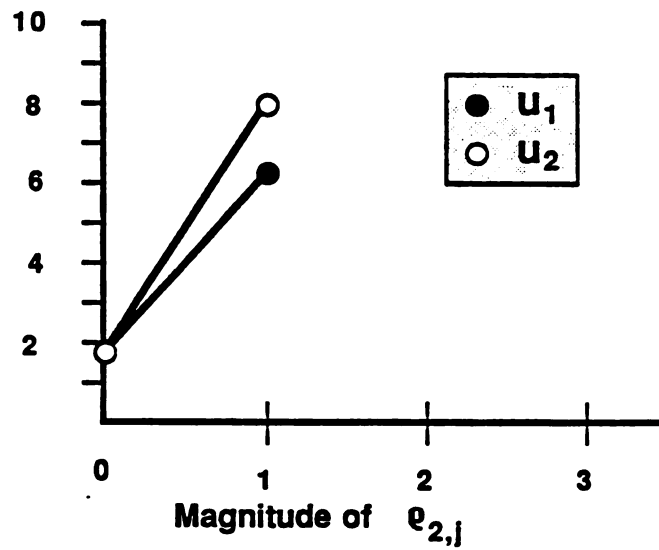
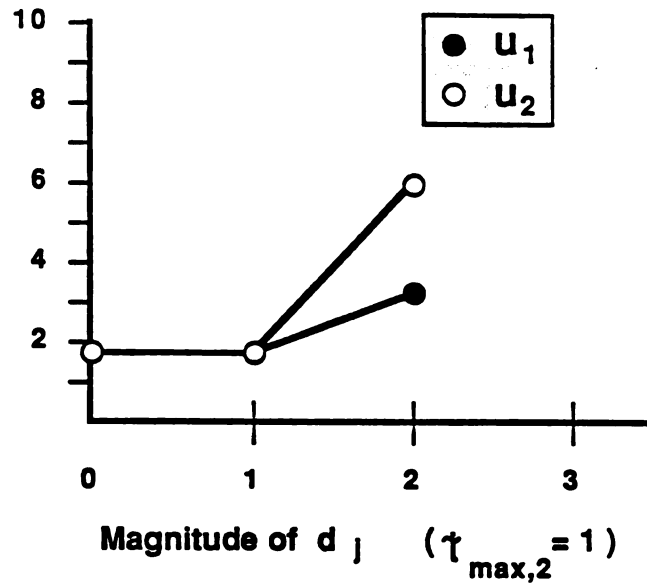


Figure 3-7 Input delay test for y_2 with 10% noise

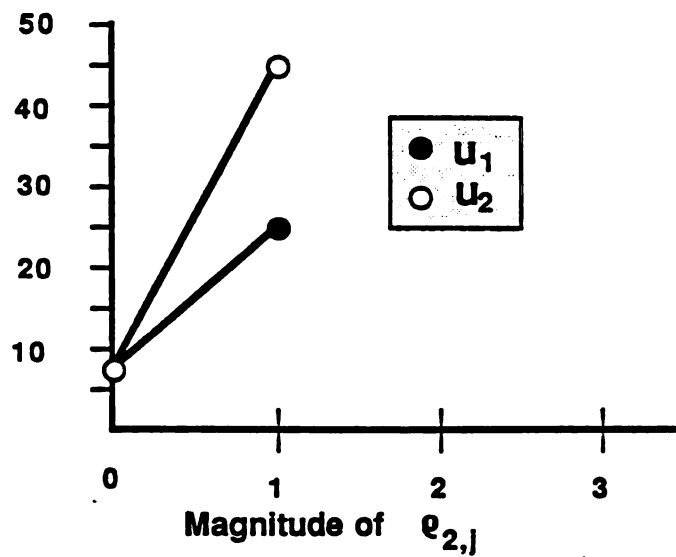
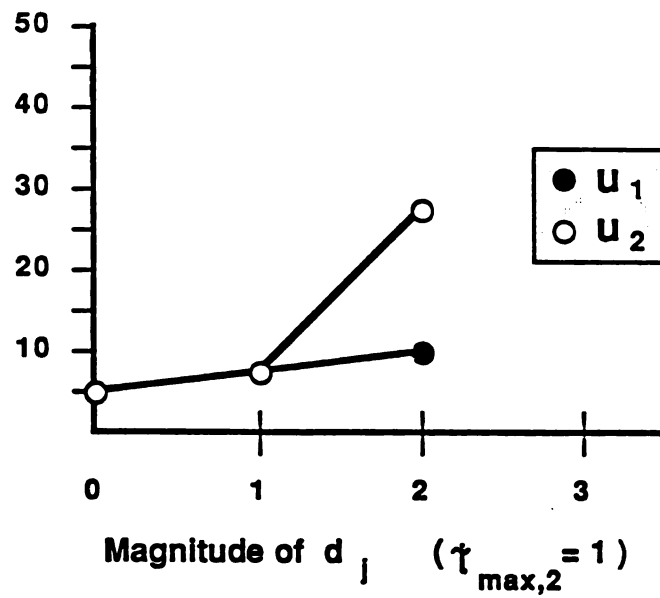


Figure 3-8 Input delay test for y_2 with 20% noise

3.5.6 Summary of Computer Implementation

We see that the delayed polynomial matrix method that has been presented represents a unified approach to the structural identification of multivariable systems even in the presence of relatively high noise. The identified structure is directly linked to a minimal canonical state space representation of the system. For systems with time delay in the inputs, it reduces the number of parameters that need to be estimated below that of previously reported methods of identification. Furthermore, the approach is methodical and very little programming is required to generate a interactive computer aided design tool using this approach. In the next section we will see how this method compares to conventional methods of model identification on real data from the Linde Column.

3.6 Linde Column Model

This section describes the research that produced a dynamic model of the Linde column. The data used for this work and the constraints it imposes on the derived model are first described. Then least squares estimation is explained. This is followed by a description of various tests of model order. Results of model identification and parameter estimation are then presented. Finally, the derived model is discussed with respect to previous knowledge of the column.

3.6.1 Operating Data

In order to fully understand the model developed for the Linde column, it is necessary to review the data used for estimation. For this research it was necessary to use normal operating records of the variables that make up the inputs and outputs shown in Figure 3-9. This allowed for non-interrupted production. When data is collected under these circumstances, the experimenter must be concerned with the quality of information available from the data. The question is whether there is enough transient behavior contained in the data for good model estimation. This can be especially critical when the inputs to the system in question are the result of feedback control as is the case with the Linde Column. As a result, data from the Linde Column was collected (at a sampling rate of one minute) periodically over the course of several months. Each data set was reviewed for transient behavior and only those that showed true excursions from steady state above the signal noise were used for model estimation.

For instance, Data Set 1 contains a series of pulses in the reflux flow, figure 3-10. These pulses are not the result induced by feedback control, but probably occurred because of a sticky valve. The effects of these pulses in the composition on the 57th tray, Figure 3-11, and in the bottoms composition, Figure 3-12, are very pronounced. During this same period the steam pressure on the reboiler remained constant. The noisy recording of the steam pressure is shown in Figure 3-13.

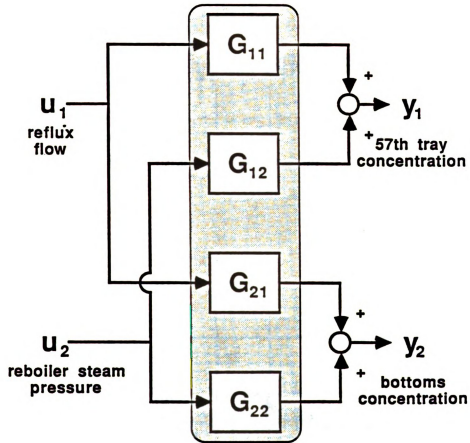


Figure 3-9 Inputs and outputs of the Linde Column

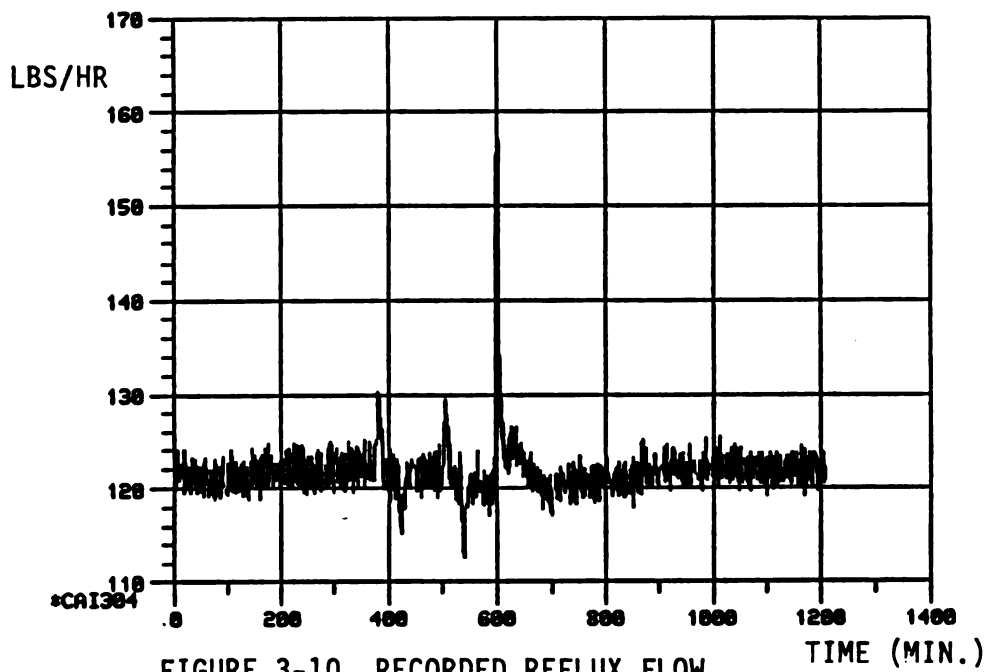


FIGURE 3-10 RECORDED REFLUX FLOW
(DATA SET 1)

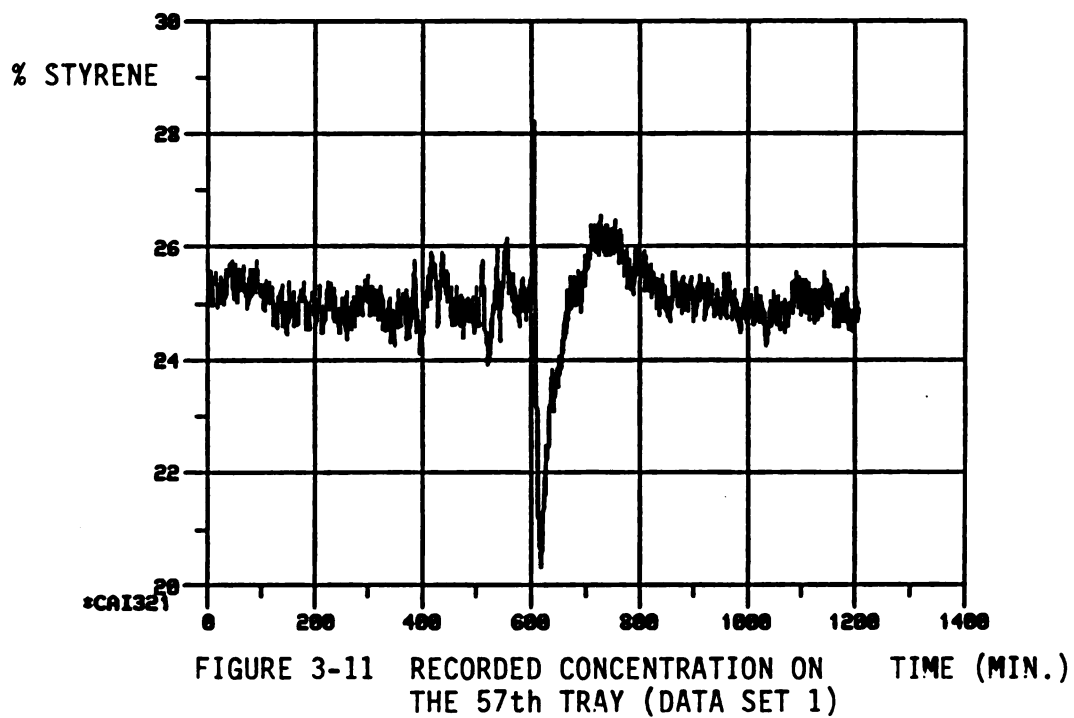


FIGURE 3-11 RECORDED CONCENTRATION ON
THE 57th TRAY (DATA SET 1)

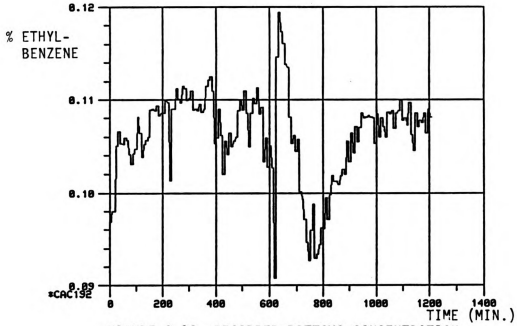


FIGURE 3-12 RECORDED BOTTOMS CONCENTRATION
(DATA SET 1)

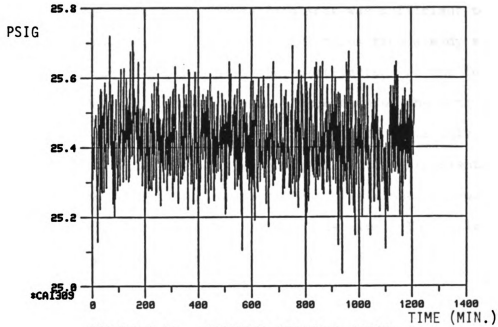


FIGURE 3-13 RECORDED REBOILER STEAM
PRESSURE (DATA SET 1)

In Data Set 2 the changes in steam pressure occurred due to manual control of the pressure controller set point as depicted in Figure 3-14. The response of the column to these changes was the classical step responses in the bottoms concentration shown in Figure 3-15. The reflux flow during this time period shows a slight drift and several small pulses, Figure 3-16. The response of the concentration on the 57th tray is shown in Figure 3-17.

Finally in Data Set 3 a series of pulses occurred in the reflux flow, figure 3-18, while the steam pressure of the reboiler was constant, Figure 3-19. The response of the concentration on the 57th tray, Figure 3-20, is similar to that of Figure 3-11. The response at the bottom of the column is shown in Figure 3-21.

Although the inputs in these data sets was sufficient to produce responses in the outputs with large deviations from steady state, the characteristics of the data still put restrictions on the form of the model that could be estimated. A close inspection of the data will show that when the column was most excited from steady state only one input was the cause. Because of this the polynomial matrix representation of equation (1) could not be estimated directly since it requires both inputs to be sufficiently exciting at the same time. The logical choice in this case is a matrix of transfer functions of the form

$$\begin{bmatrix} y_1(z) \\ y_2(z) \end{bmatrix} = \begin{bmatrix} G_{11}(z) & G_{12}(z) \\ G_{21}(z) & G_{22}(z) \end{bmatrix} \begin{bmatrix} u_1(z) \\ u_2(z) \end{bmatrix} \quad (3.61)$$

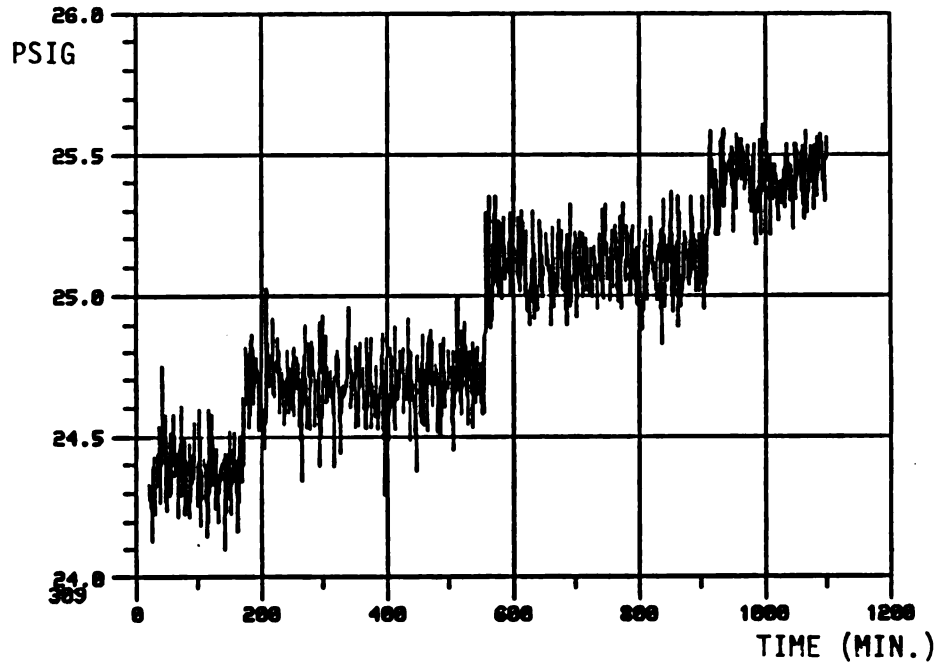


FIGURE 3-14 RECORDED REBOILER STEAM PRESSURE (DATA SET 2)

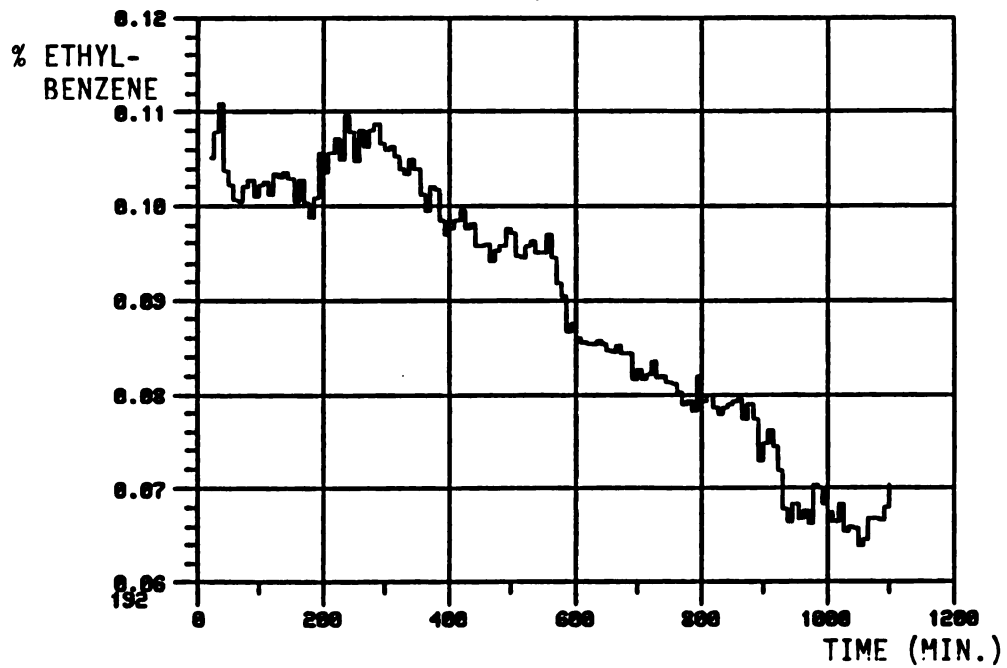


FIGURE 3-15 RECORDED BOTTOMS CONCENTRATION (DATA SET 2)

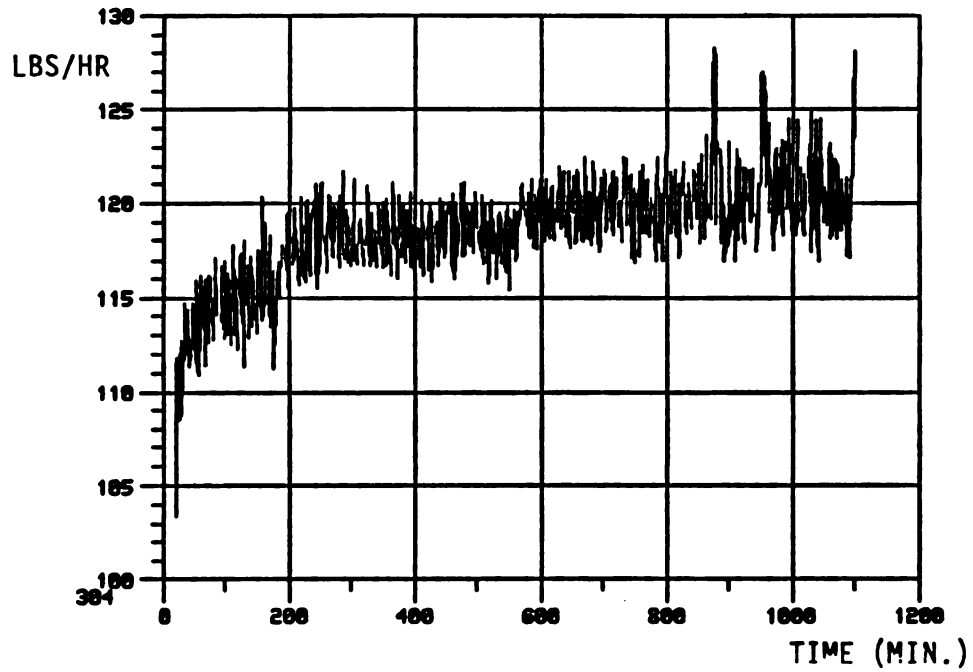


FIGURE 3-16 RECORDED REFLUX FLOW
(DATA SET 2)

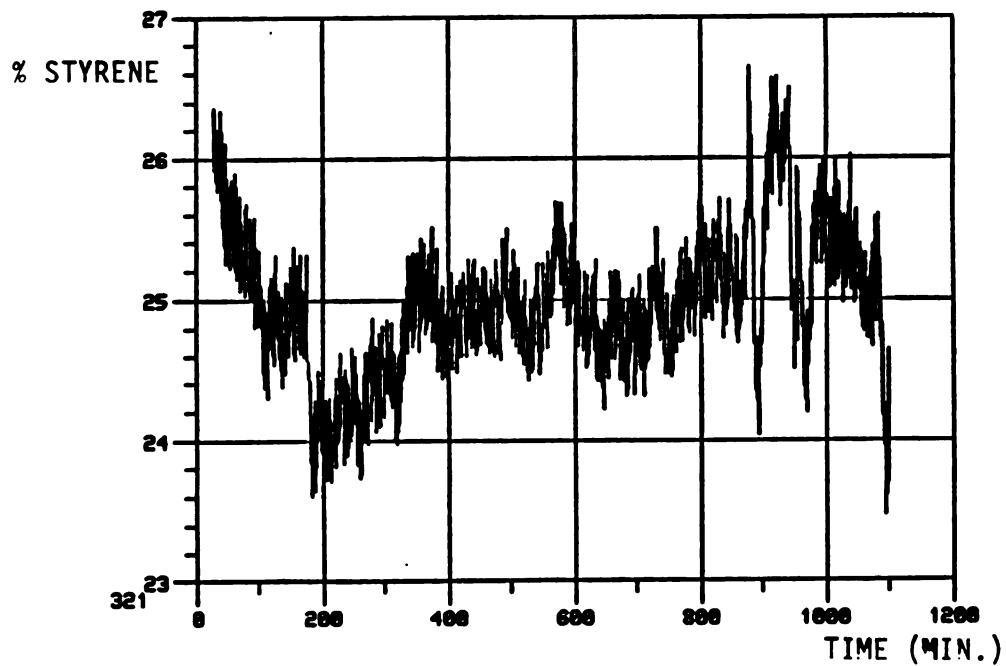


FIGURE 3-17 RECORDED CONCENTRATION
ON THE 57th TRAY
(DATA SET 2)

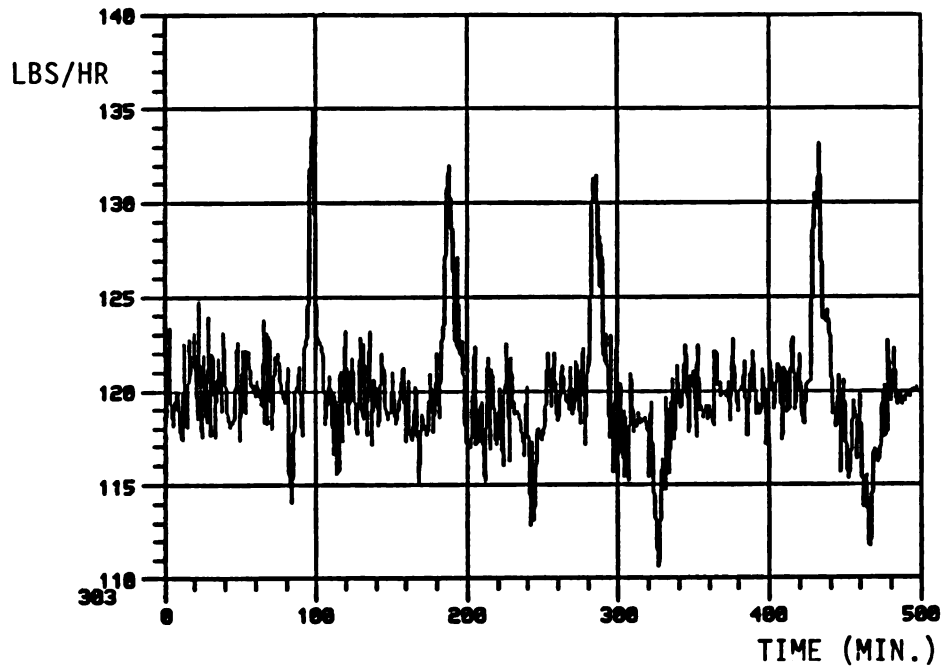


FIGURE 3-18 RECORDED REFLUX FLOW
(DATA SET 3)

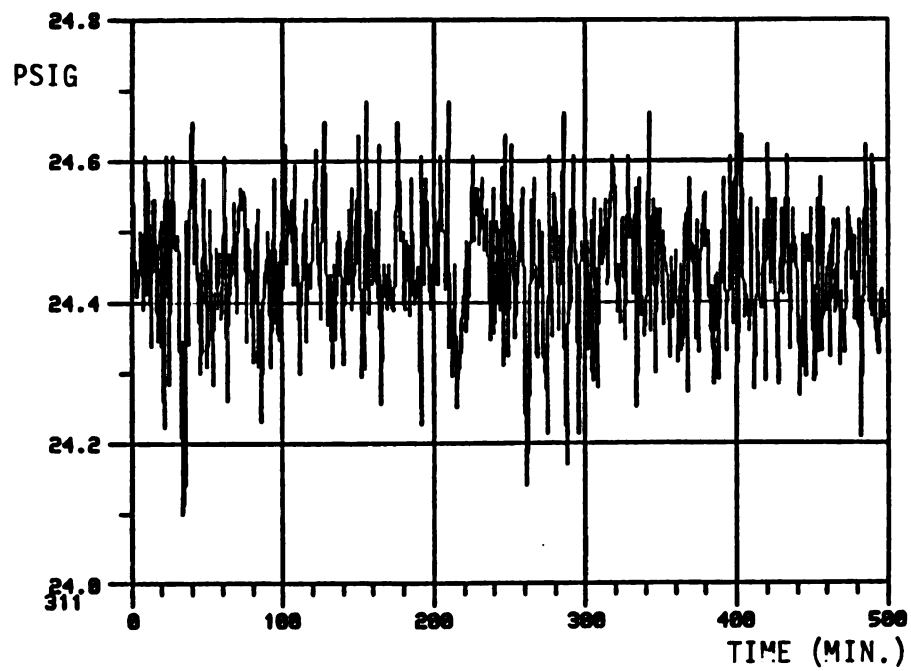


FIGURE 3-19 RECORDED REBOILER
STEAM PRESSURE
(DATA SET 3)

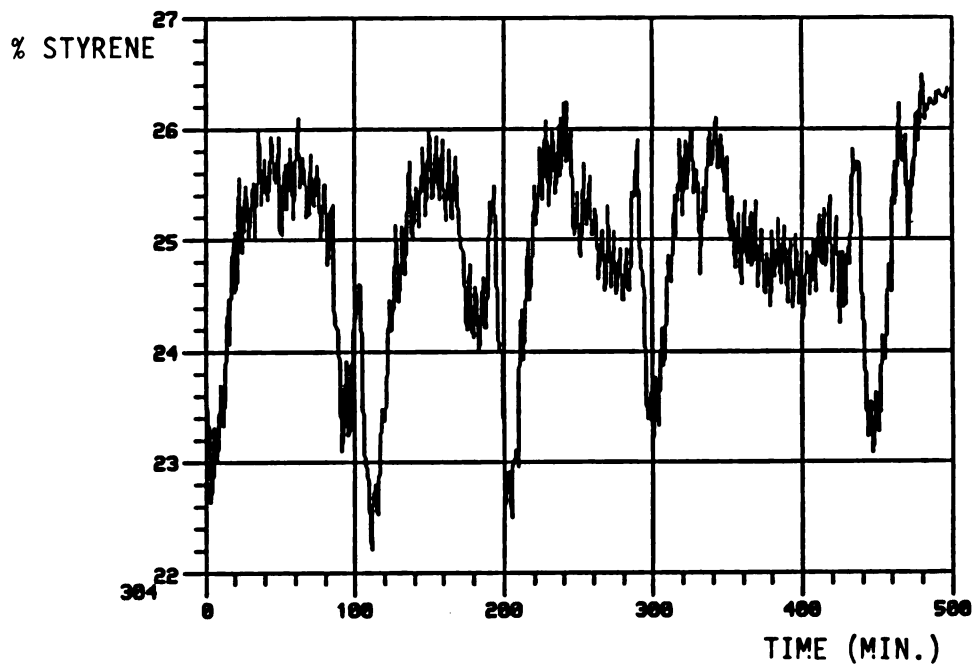


FIGURE 3-20 RECORDED CONCENTRATION
ON THE 57th TRAY
(DATA SET 3)

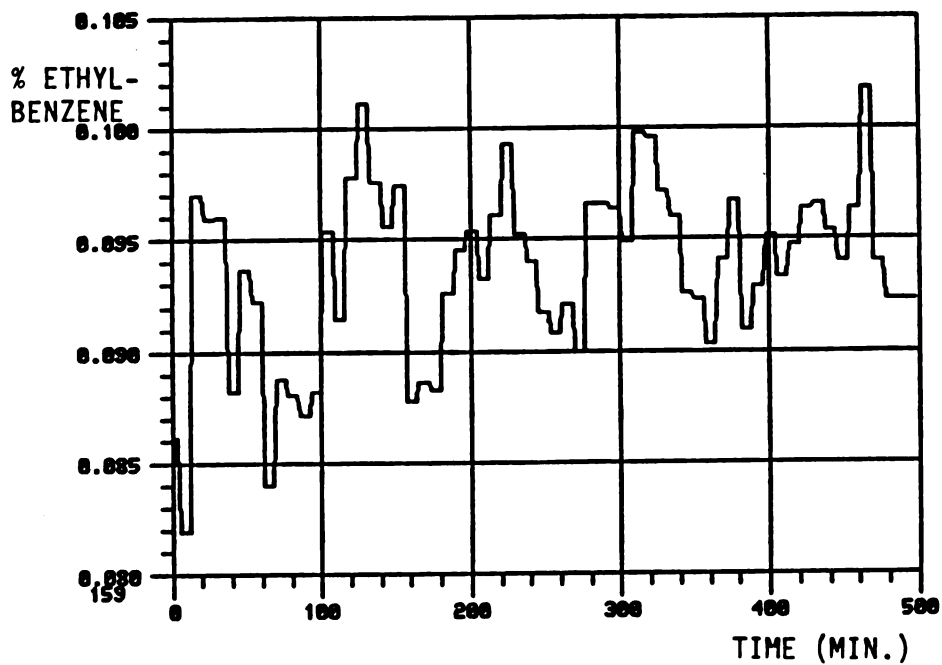


FIGURE 3-21 RECORDED BOTTOMS
CONCENTRATION (DATA SET 3)

Here $u_1(k)$ is the deviation from steady state of the reflux flow into the column and $u_2(k)$ is the deviation from steady state of the steam pressure on the reboiler. Likewise, $y_1(k)$ is the deviation from steady state of the concentration on the 57th tray and $y_2(k)$ is the deviation from steady state of the concentration in the bottoms product. In general each individual transfer function has the form

$$G(z) = \frac{z^{-r} \sum_{\alpha=1}^n b_{\alpha} z^{-\alpha}}{1 + \sum_{\alpha=1}^r a_{\alpha} z^{-\alpha}} \quad (3.62)$$

Another restrictive characteristic of the data is the longer sampling rate of the bottoms concentration. The 8 minute sample and hold function is apparent in the recordings of the bottoms concentration. This led to $G_{21}(z)$ and $G_{22}(z)$ having sample rates of 8 minutes while $G_{11}(z)$ and $G_{12}(z)$ had sample rates of 1 minute.

A final characteristic of the data that restricted the model was the type of inputs. The type of input excitation developed by the reboiler steam pressure was that of a step change. With such an input transfer functions $G_{12}(z)$ and $G_{22}(z)$ must be modified as

$$G(z) = \frac{b_0 z^{-\tau-1}}{1 + \sum_{\alpha=1}^n a_{\alpha} z^{-\alpha}} \quad (3.63)$$

where $b_0 = b_1 + b_1 + \dots + b_n$. To see this, consider (3.62) rewritten as a difference equation

$$y(z) = -\sum_{\alpha=1}^n a_{\alpha} y(k-\alpha) + \sum_{\alpha=1}^n b_{\alpha} u(k-\alpha-\tau) \quad (3.64)$$

Now in the case of a step input $u(k) = c$ for $k > 0$. So at any time k ,

$$y(z) = -\sum_{\alpha=1}^n a_{\alpha} y(k-\alpha) + \sum_{\alpha=1}^n b_{\alpha} c \quad (3.65)$$

Obviously in (3.65) the parameters b_1, \dots, b_n appear as a sum and separation of them is impossible for a constant input.

3.6.2 Least Squares Parameter Estimation

Having established the form of the model the parameter estimation problem may now be stated. The generic transfer function of (3.62) may be rewritten as

$$y(k) = -a_1 y(k-1) - \dots - a_n y(k-n) + b_1 u(k-1-\tau) + \dots \\ \dots + b_n u(k-n-\tau) + \epsilon(k) \quad (3.66)$$

where $\epsilon(k)$ accounts for model error and measurement noise. This can be rewritten more concisely as

$$y(k) = \phi^T(k)\theta + \epsilon(k) \quad (3.67)$$

where $\theta = [-a_1, \dots, -a_n, \dots, b_1, \dots, b_n]^T$ and $\phi = [y(k-1), y(k-2), \dots, y(k-n), u(k-1-\tau), \dots, u(k-n-\tau)]^T$.

Now given the model of (3.67) determine the parameters a_i and b_i that minimize the least squares criterion

$$J_n(\hat{\theta}) = \sum_{k=n}^N \epsilon^2(k; \hat{\theta}) \quad (3.68)$$

over the data $\{y(k), u(k), k = 1, 2, \dots, N\}$.

The least squares estimate of the parameter vector, $\hat{\theta}$, may be found by processing the data in batch form or by proceeding through the data sequentially. The least squares solution for processing the data as a whole has the form

$$\hat{\theta} = [\Phi^T \Phi]^{-1} \Phi^T Y \quad (3.69)$$

where

$$\begin{aligned}\Phi &= [\phi(n), \phi(n+1), \dots, \phi(N)]^T \\ Y &= [y(n), y(n+1), \dots, y(N)]^T\end{aligned}\quad (3.70)$$

For large data sets it may be simpler to process the data a sample at a time thus avoiding having to deal with a large Φ matrix. The recursive least squares algorithm performs such a task. The least squares estimate of θ may be computed iteratively from the following equations

$$\hat{\theta}(k) = \hat{\theta}(k-1) + K(k)[y(k) - \phi^T(k)\hat{\theta}(k-1)] \quad (3.71)$$

where $K(k)$ is the time varying gain matrix computed as

$$K(k) = \frac{P(k-1)\phi(k)}{1 + \phi^T(k)P(k-1)\phi(k)} \quad (3.72)$$

Matrix $P(k)$ is computed recursively from

$$P(k) = P(k-1) - \frac{P(k-1)\phi(k)\phi^T(k)P(k-1)}{1 + \phi^T(k)P(k-1)\phi(k)} \quad (3.73)$$

The recursive equations (3.71) through (3.73) require starting values for $P(0)$ and $\hat{\theta}(0)$. For large data sets the values can simply be $P(0) = \mu I$, where μ is large, and $\hat{\theta}(0) = [0, \dots, 0]^T$.

3.6.3 Transfer Function Identification

The model order n and the time delay τ of each of the four transfer functions in (3.61) were determined by a combination of methods. Where appropriate, the delayed polynomial matrix method presented in the previous section was applied for the single input single output case. Next, models of increasing order and varying time delay were estimated and the mean square residuals, $J_n(\hat{\theta})$, of each was computed. The value of the mean square residuals should decrease as the order of the models is increased toward $n + \tau$. Ideally, when the correct time delay is chosen and the order increased above the true order, the magnitude of the mean square residuals should remain relatively constant. Likewise when the value of the time delay is changed from the true value there should be a corresponding increase in $J_n(\hat{\theta})$.

A statistical method was used to see if the mean square residuals changed significantly for an increase in model order, say from $n = n_1$ to $n = n_2$. This so called F-test assumes that the residuals are Gaussian and that $J_{n_2}(\hat{\theta})$ and $J_{n_1}(\hat{\theta}) - J_{n_2}(\hat{\theta})$ are statistically independent and are Chi-square distributed with $(N - 2n_2)$ and $(2n_2 - 2n_1)$ degrees of

freedom respectively. To test the null hypothesis that n_1 is the true model order, the test statistic

$$t = \frac{J_{n_1} - J_{n_2}}{J_{n_2}} \frac{N - 2n_2}{2(n_2 - n_1)} \quad (3.74)$$

was computed. The statistic t has an $F((2n_2 - 2n_1), (N - 2n_2))$ distribution under the null hypothesis. After a risk level was defined a corresponding t^* was taken from a table of the F distribution. The null hypothesis was rejected for $t > t^*$.

As a final check the sample auto-correlation function of the residuals

$$R_\epsilon(\tau) = \frac{1}{N} \sum_{k=n+1}^{n+N} \epsilon(k)\epsilon(k+\tau) \quad (3.75)$$

$$\tau = 0, 1, 2, \dots$$

was computed for the selected model. Assuming the errors in (3.67) are white, and the correct model is chosen, the residuals should also be white. When this is the case the values of the lags in the sample auto-correlation should all be nearly zero except for the zero lag ($\tau = 0$).

3.6.4 Results of Column Modelling

It was found that nearly all the model order tests for transfer function $G_{11}(z)$ agreed. The results of the delayed polynomial matrix model order test described in the previous section are shown in Figure 3-22. Part a of Figure 3-22 shows the Kronecker index to most likely be 9. Part b indicates that the time delay to be 5. These estimates are supported by the magnitude of the mean square residuals shown in Figure 3-23. It is clear that for a time delay of 5 there is little reduction in the model error for order larger than 4 but a large increase in error for order less than 4. Likewise the value of $J_n(\hat{\theta})$ for order 4 and varying delays were:

delay 4	17.2
delay 5	14.0
delay 6	16.0

indicating that a time delay of 5 is the most appropriate.

Using the F-test with a 10% risk factor the values of t^* are:

$n_2 - n_1$	t^*
1	2.30
2	1.94
3	1.77
4	1.67

For $n_1 = 6$ with a delay of 5 the following values of t resulted:

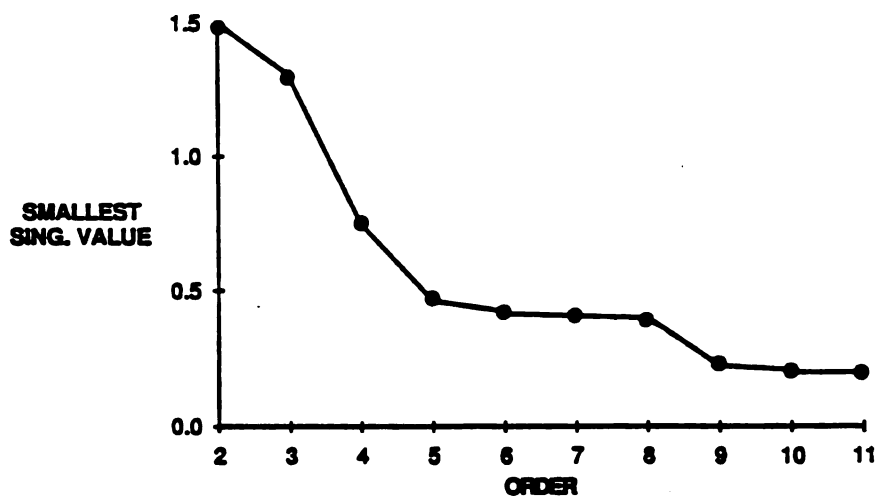
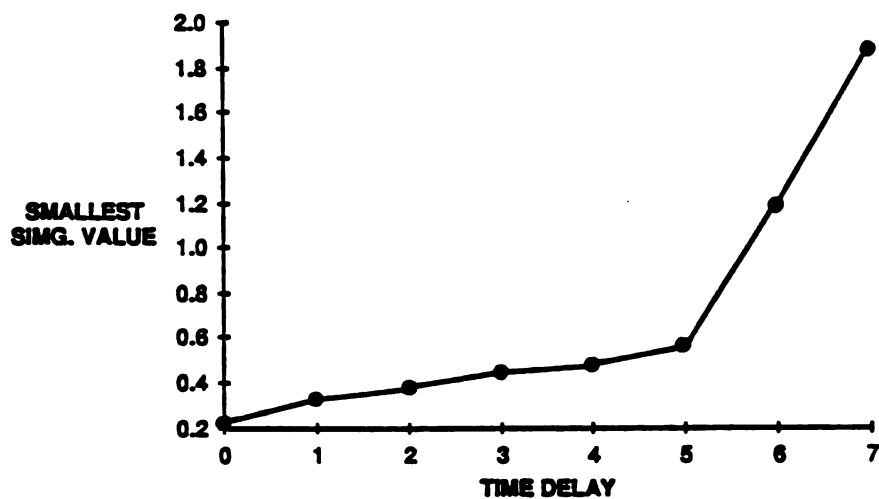
G(11) ORDER TEST**G(11) TIME DELAY TEST**

FIGURE 3-22 RESULTS OF THE DELAYED POLYNOMIAL MATRIX TEST FOR $G_{11}(z)$.

G(11) M. S. RESIDUALS

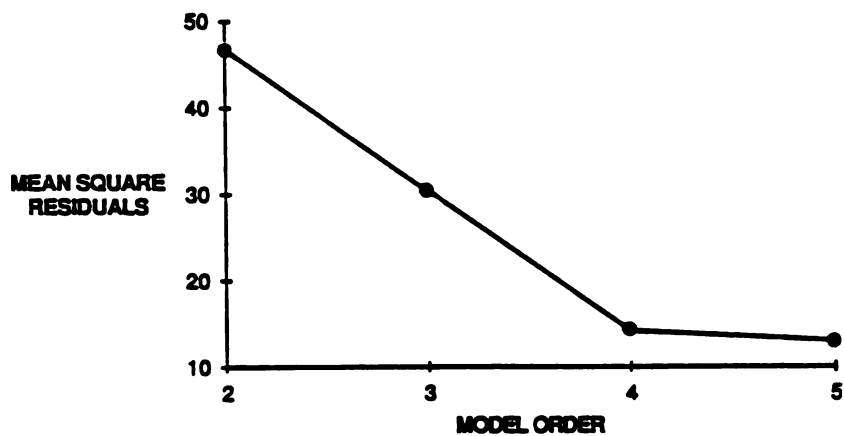


FIGURE 3-23 MEAN SQUARE RESIDUALS FOR G_{11} WITH A TIME DELAY OF 5.

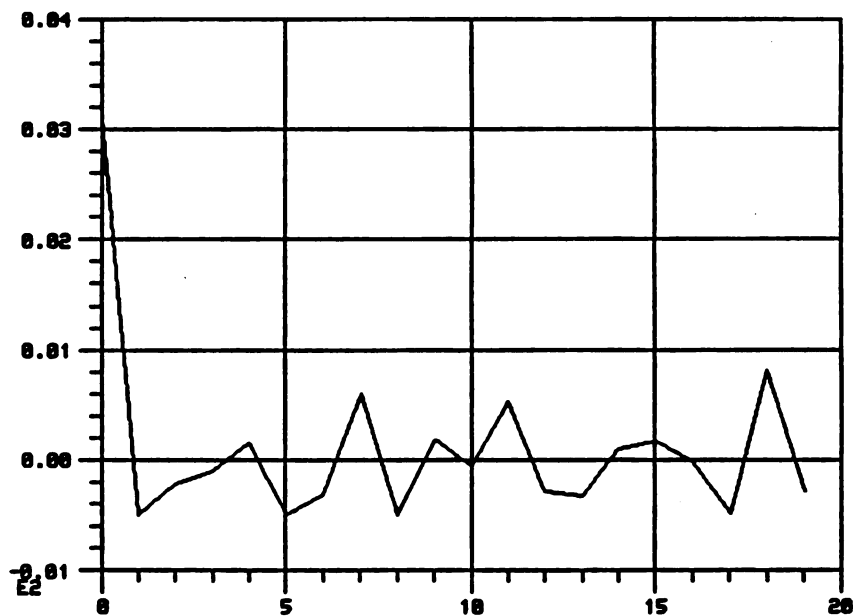


FIGURE 3-24 AUTO CORRELATION OF RESIDUALS OF 4TH ORDER MODEL WITH A DELAY OF 5 FOR G_{11} .

n_2	t
3	105.91
4	11.39
5	1.20

The F-test indicates that for the given risk level a model order of 5 is correct.

However the residuals of a fourth order model with time delay of 5 appear to be white as demonstrated by the sample auto correlation function shown in Figure 3-24.

This model structure was accepted and parameter estimation was performed using recursive least squares on Data Set 1. The estimated model is

$$G_{11}(z) = \frac{(.033z^{-1} - .02z^{-2} + .0024z^{-3} - .051z^{-4})z^{-5}}{1 - .83z^{-1} + .39z^{-2} - .97z^{-3} + .48z^{-4}}$$

A portion of the output of this model driven by the recorded reflux flow is shown in Figure 3-25 and can be compared to the true column response in Figure 3-26.

For transfer function $G_{21}(z)$ Data Set 1 was used. The model order tests were found to be in agreement but some were more definite than others. Applying the delayed polynomial matrix method of the previous section to determine the Kronecker index produced Figure 3-27. The

8 STYRENE

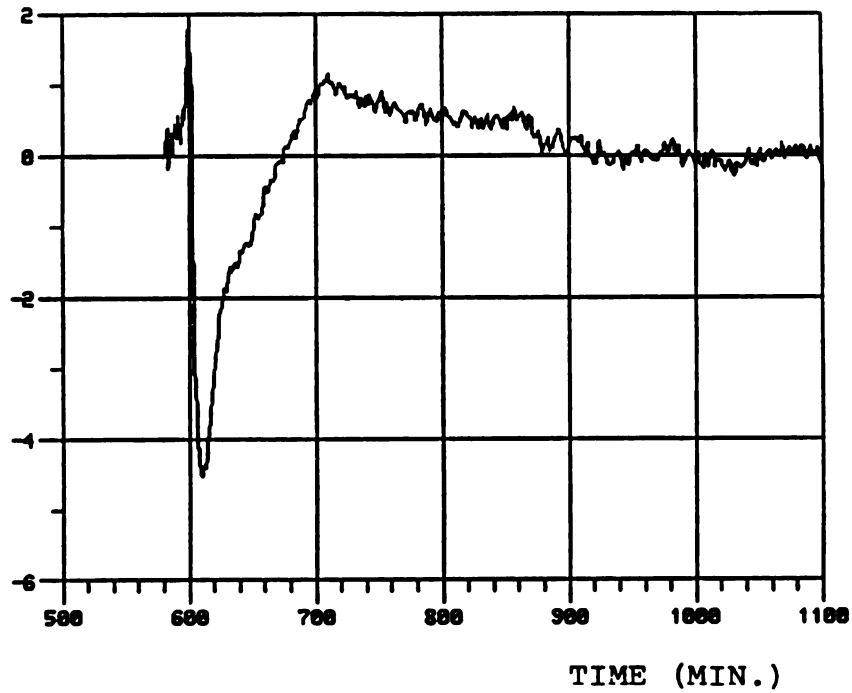


FIGURE 3-25 RESPONSE OF ESTIMATED G_{11}
TO THE RECORDED REFLUX
FLOW OF DATA SET 1.

8 STYRENE

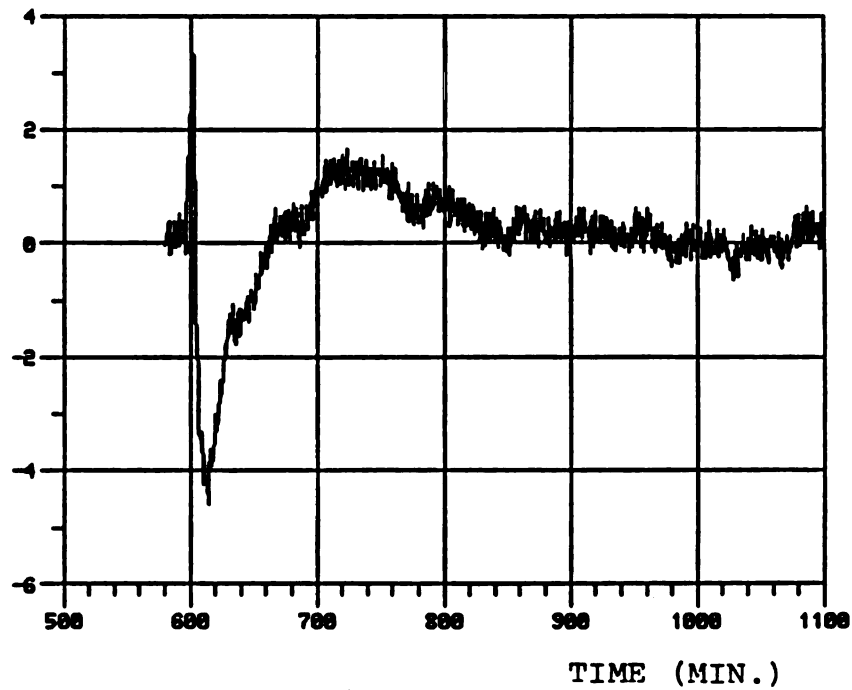
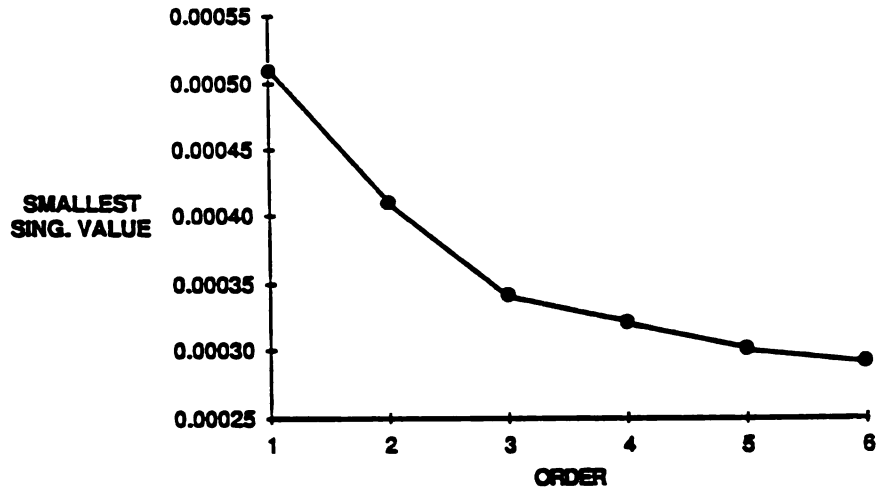
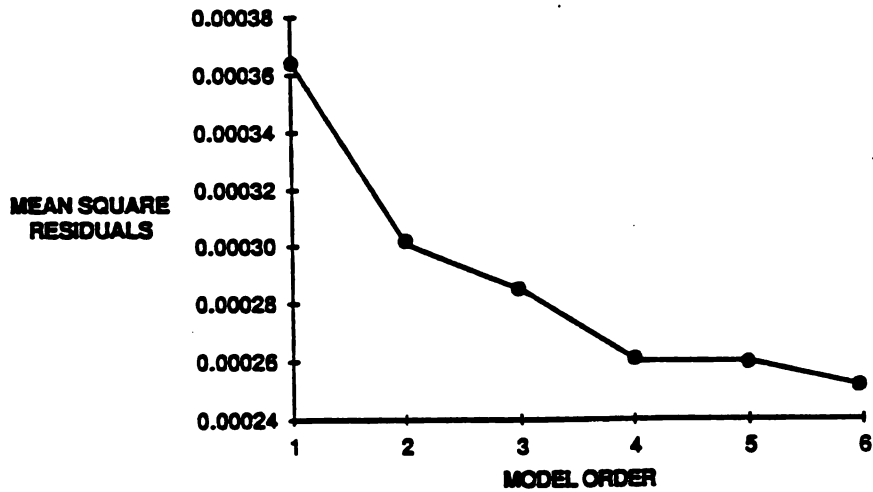


FIGURE 3-26 A PORTION OF THE RECORDED
57TH TRAY CONCENTRATION
FROM DATA SET 1.

G(21) ORDER TEST

FIGURE 3-27 ORDER TEST FOR G_{12} .

G(21) M. S. RESIDUALS

FIGURE 3-28 MEAN SQUARE RESIDUALS FOR G_{12} WITH A TIME DELAY OF ZERO.

evolution of singular values indicates that a third or fourth order model could be appropriate. The mean square residuals, Figure 3-28, clearly show the model order to be 4. The estimated 4th order model with no time delay was

$$G_{21}(z) = \frac{.000033z^{-1} + .00016z^{-2} + .00022z^{-3} + .00015z^{-4}}{1 - .58z^{-1} - .36z^{-2} + .11z^{-3} - .013z^{-4}}$$

The relatively low magnitude of a_4 and b_1 in the model suggests that they might be set identically to zero resulting in a third order model with time delay of 1. This alternative model was estimated. For these competing models $t = 0.279$ and $t^* = 2.39$ for a 10% risk factor. This suggests that a model with order 3 and a time delay of 1 is acceptable.

A model order of 3 with time delay 1 was accepted and least squares estimation lead to the following model

$$G_{21}(z) = \frac{(.00016z^{-1} + .00022z^{-2} + .0015z^{-3})z^{-1}}{1 - .59z^{-1} - .35z^{-2} + 0.94z^{-3}}$$

The auto correlation of the residuals of this model are shown in Figure 3-29 and appear to be white. A portion of the output of this model driven by the recorded reflux flow is shown in Figure 3-30 and can be compared to the true column response in Figure 3-31.

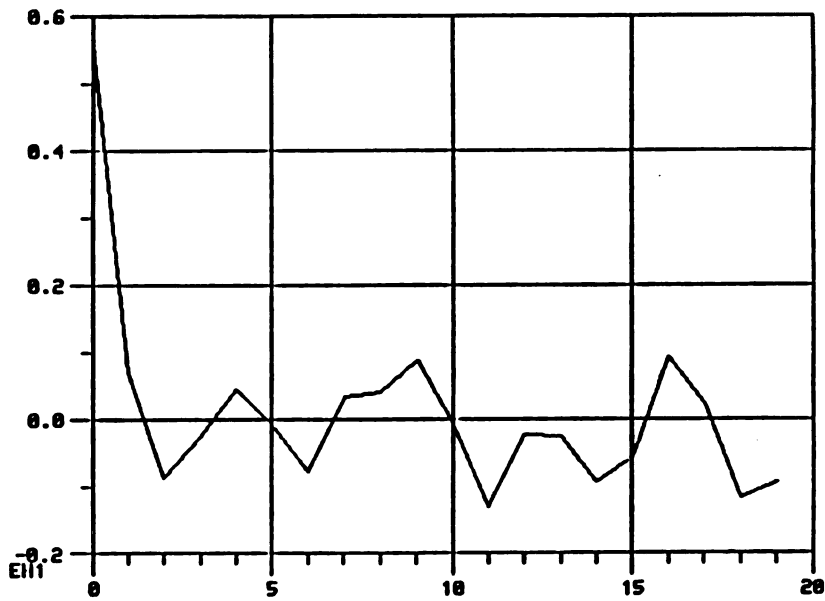


FIGURE 3-29 AUTO CORRELATION OF RESIDUALS
OF A 3rd ORDER MODEL WITH A
DELAY OF 1 FOR $G_{21}(z)$.

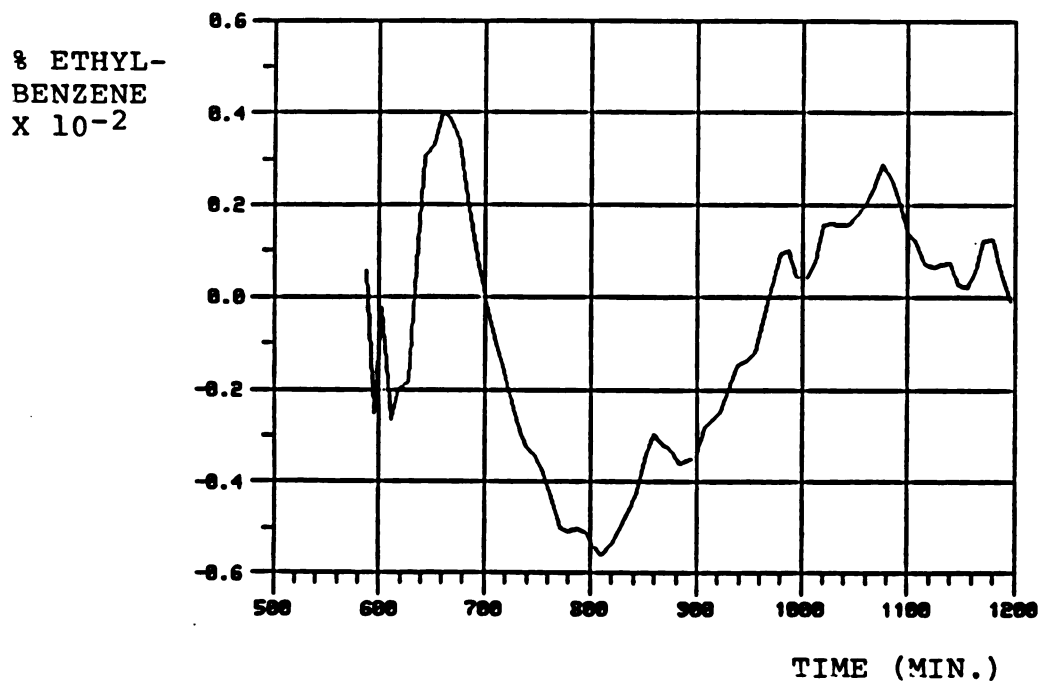


FIGURE 3-30 RESPONSE OF THE ESTIMATED G_{21} TO A PORTION OF THE RECORDED REFLUX FLOW OR DATA SET 1.

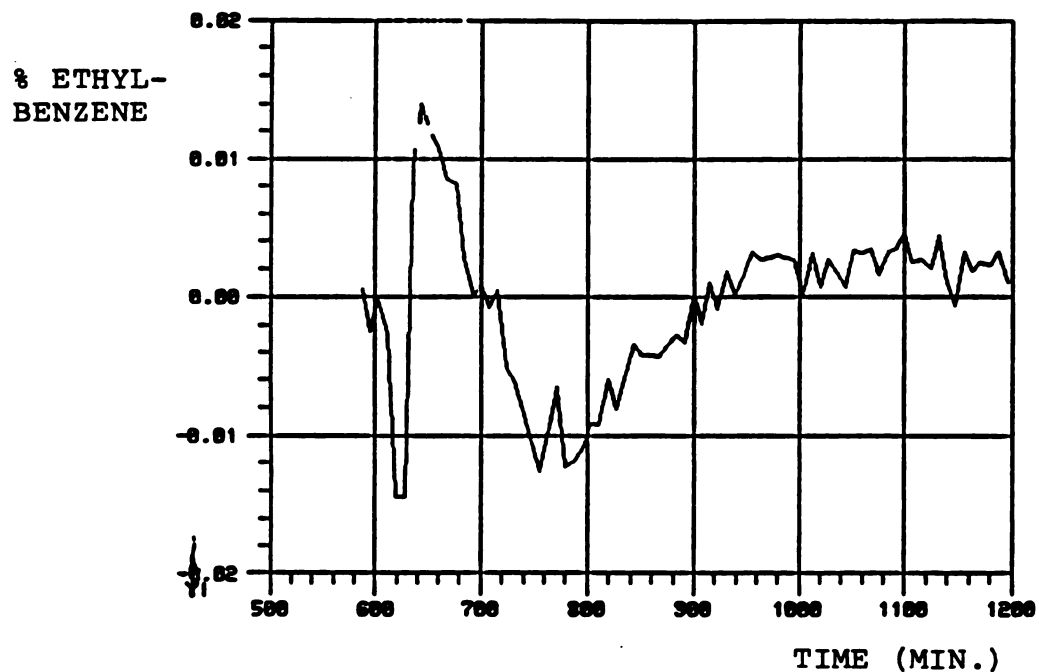


FIGURE 3-31 A PORTION OF THE RECORDED BOTTOMS CONCENTRATION FROM DATA SET 1.

In determining transfer function $G_{22}(z)$ the delayed polynomial matrix method of the previous section was not used because the shape of the response of the bottoms concentration to a step change in steam pressure strongly suggests that at most a second order denominator with perhaps at most one period of time delay would adequately fit this response. The mean square residuals for these competing models were:

1st order, 0 delay	.000076
2nd order, 0 delay	.000072
1st order, 1 delay	.000078
2nd order, 1 delay	.000074

It is clear that for a delay of 1 the model error is increased. For comparing the second order model with no delay to the first order model with no delay the F-test statistic $t = 2.61$ which is lower than the $t^* = 2.83$ for this comparison. Therefore $G_{22}(z)$ was taken to be 1st order with no delay. The resulting model derived by least squares estimation is

$$G_{22}(z) = \frac{-.0026z^{-1}}{1 - .94z^{-1}}$$

A portion of this model driven by the recorded steam pressure is shown in Figure 3-32 and can be compared to the true column response in Figure 3-33.

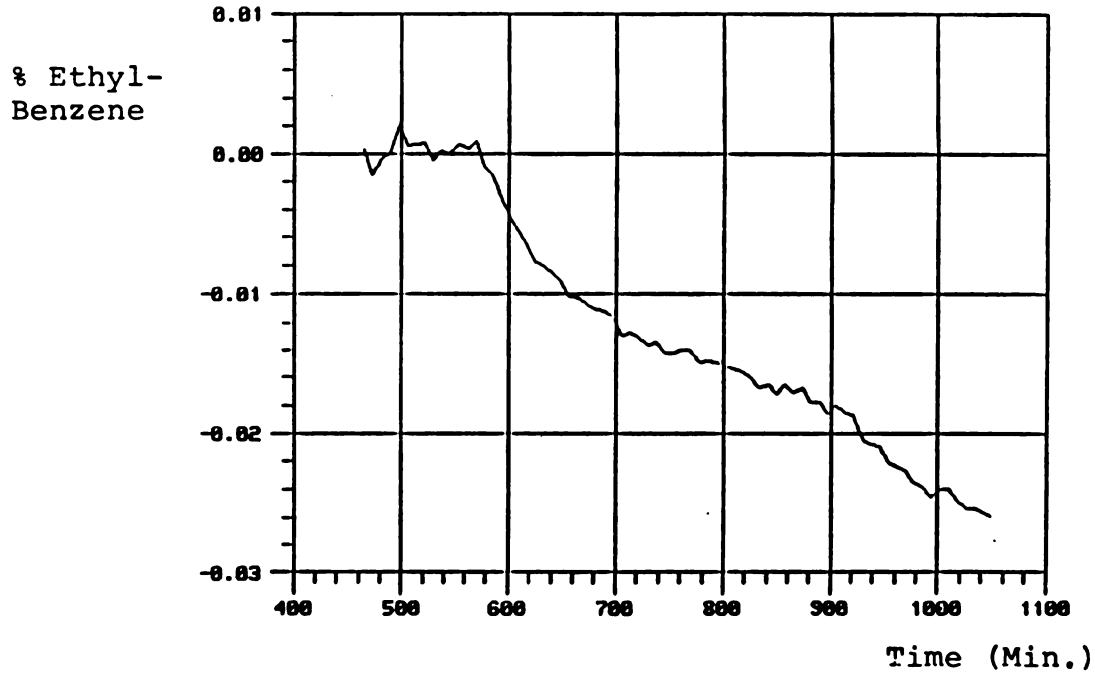


Figure 3-32 Response of estimated C₂₂ to a portion of the recorded steam flow from Data set 2.

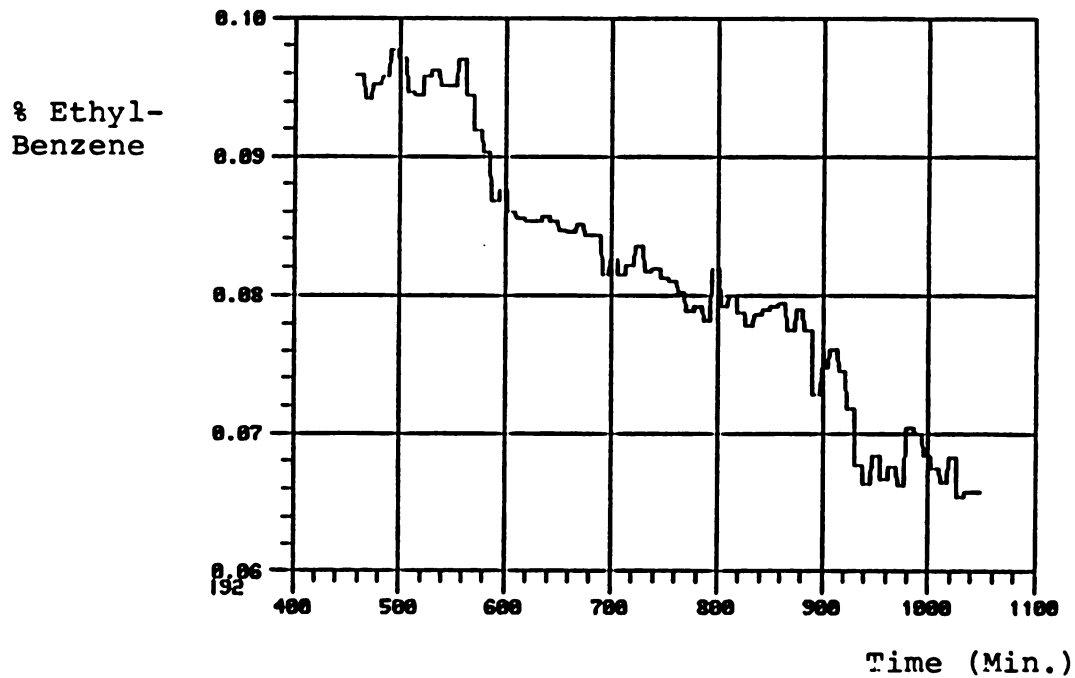


Figure 3-33 A portion of the recorded bottoms concentration from Data set 2.

The construction of transfer function $G_{12}(z)$ proved to be the most difficult due to the data available for model estimation. Data Set 2 was used because of the step changes in steam pressure. However, the drift in the reflux flow could not be discounted because of its strong influence, as evidenced by $G_{11}(z)$. This influence was removed before model estimation by subtracting the output of $G_{11}(z)$ driven by the recorded reflux flow from the record of the 57th tray concentration. The model order tests did not give clear results but it was found that the mean square residuals were minimized for a model order of 3 with time delay of 5. Recursive least squares estimation resulted in the following model

$$G_{12}(z) = \frac{(.11z^{-1})z^{-5}}{1 - .48z^{-1} + .39z^{-2} - .87z^{-3}}$$

3.6.5 Discussion of the Linde Column Model

Several observations may now be stated in regard to the derived model of the Linde Column. The most surprising is the non-minimum phase behavior of the concentration on the 57th tray to a positive change in reflux flow as seen in the inverse response in Data Sets 1 and 3. This behavior is present in $G_{11}(z)$ in the form of the zeroes outside the unit circle. This is the first time such behavior has been reported in the literature. The control implications of this discovery have been

outlined in the introduction and will be discussed in detail in the next chapter.

Data Set 3 was also used to estimate $G_{11}(z)$. Model order tests were fairly consistent with those applied to Data Set 1. Parameter estimation lead to a model which showed a large shift in some of the poles and zeros of transfer function $G_{11}(z)$. The poles and zeros obtained from both data sets are

	POLES	ZEROS
Data Set 1	0.59	1.37
	0.93	-0.38 + j.98
	0.34 + j0.87	
Data Set 3	0.12	1.01
	0.94	-0.55 + j0.81
	0.01 + j0.78	

The reason for these inconsistencies is the fact that Data Set 3 does not have an obvious steady state value for the recording of the 57th tray concentration. Only controlled experiments on the column could resolve this issue. However, it will be seen in the next chapter that a model based controller can be developed which explicitly handles process / model mismatch.

The first order model obtained for $G_{22}(z)$ is consistent with the perception the production operators have concerning the dynamics in this part of the column. They had learned that if the bottoms concentration was too high a large increase in steam pressure would bring it back without oscillations. The two hour time constant obtained for $G_{22}(z)$ is also consistent with the ability of the operators to maintain bottoms concentration specification using manual control on the reboiler steam pressure controller while taking manual samples of the bottom product every 4 hours. Only a system with such a large time constant would make such a manual control scheme possible.

The existence of the coupling terms $G_{12}(z)$ and $G_{21}(z)$ confirms the suspicion of process engineers associated with the Linde Column. These engineers had experienced the effects due to such coupling during start-ups and abnormal operations of the column. The level of coupling represented by $G_{12}(z)$ and $G_{21}(z)$ is also consistent with the ability of two independent PI controllers to maintain control of the column. This will be demonstrated in the next chapter.

3.7 Summary of Chapter Three

This chapter has dealt with the development of a dynamic model of the Linde Column. The research presented in this chapter led to two significant contributions to the literature. A new identification

procedure which includes time delay explicitly was developed through adaptation of current theory on determining the structure and order of a multi-input, multi-output model. In addition to this theoretical contribution, this chapter also describes a form of non-minimum phase behavior in the column which has not been mentioned before in the literature.

The new identification procedure is significant because it greatly reduces the number of parameters necessary to describe multivariable systems with multiple time delays. The reduction in parameters is realized through a new representation of multi-input, multi-output systems called the "delayed polynomial matrix" representation. This new representation explicitly accounts for multiple delays. The procedure first estimates the order of a polynomial matrix model of the system which serves as an upper bound on the number of parameters necessary to describe the system behavior. It then derives the delayed polynomial matrix model in a methodical and straightforward manner. An integral part of the procedure is the use of singular value decomposition as a means of testing for singular matrices. The procedure is well suited for interactive computer use.

CHAPTER FOUR
ADVANCED CONTROL FOR THE LINDE COLUMN

The purpose of this chapter is to investigate the implications that the model of the Linde Column has on control strategy. Of course practical considerations will weigh heavily in the investigation since the Linde Column is a production scale process. No attempt is made to find the best control strategy out of the set of all possible control strategies. Instead, the work described here is focused on a particular alternative model based control strategy suggested by the constraints imposed by the model and practical concerns.

4.1 Current Control Strategy

As described in Chapter Two, the current control strategy of the Linde Column is two independent PI controllers, one controlling bottoms concentration through manipulation of reboiler steam pressure and the other controlling the concentration on the 57th tray through manipulation of the reflux flow. This present scheme has been successful. The column operates in a relatively stable manner and produces a product which meets specifications. However, several dynamic characteristics brought to light in the previous chapter have

detrimental effects on such a control strategy and explain why production engineers have never been truly satisfied with it.

Probably the least interesting characteristics, but certainly one that is seen often in industrial processes, is the apparent sticky valve manipulating the reflux flow. Obviously a sticky valve would have adverse affects on any control strategy. Currently the reflux flow valve does not have a positioner. A positioner should be installed even if nothing else is changed in the control strategy.

A characteristic of more theoretical interest is the interaction between the top and bottom of the column described by $G_{12}(z)$ and $G_{21}(z)$. This interaction reduces the achievable performance for the independent controllers of the current control scheme. The controller response to process disturbances must be made sluggish enough to avoid having the control action in one loop cause an appreciable disturbance in the other loop. A multivariable control strategy could address this problem.

The non-minimum phase behavior at the top of the column noted in Chapter Three via $G_{11}(z)$ is troublesome for the current PI controller used there. A PI controller is not well suited for either time delay or inverse response. A control strategy which takes explicit account of the time delay and inverse response could improve the control of the concentration at the top of the column.

In spite of the disadvantages just outlined, there exists strong practical reasons to use the current control strategy. First of all PI control is well understood by operating personnel. This is important because a control strategy only has a chance to succeed if it is understood and therefore accepted by the people who must live with it on a daily basis. Another advantage PI control has is its smooth operation. It rarely causes abrupt changes in the process input unlike many high performance control algorithms. Probably the most important reason to use PI control is its robustness. This simple control strategy can usually be implemented with little knowledge of the process model. The parameters of the algorithm can be determined experimentally online. Then if the process dynamics change enough to cause a noticeable affect in the controller performance, operating personnel know enough to "detune" the parameter values. Certainly any alternative to the present strategy would have to have these favorable characteristics.

Alternative strategies that would possess the advantages of PI control would be those which maintain the PI controller as an element of the overall scheme. The essence of these approaches is to compensate the PI controller. These schemes remain familiar to the operating personnel while they address problems such as time delay. The Smith Predictor is an example. While these strategies have been reported to work well for the control of distillation columns, a novel approach will be taken in this thesis for reasons that will become clear.

4.2 Literature Survey on Distillation Control

It is useful to review past research on distillation column control before describing the control strategy developed for the Linde Column. This will put the contributions of this thesis in perspective.

Simultaneous control of both product concentrations of a distillation column has received considerable attention in recent years because of the importance of the process. Many different multivariable strategies have been tried either through simulation or application to an operating process. However all these investigations were concerned with the dynamics of pilot scale columns.

For instance, Wood and Berry [8] implemented two different multivariable schemes on an eight tray 9 inch diameter distillation column. They confirmed experimentally what earlier researchers had found through simulations, ratio control (Rijnsdorp [9]) and decoupling compensators (Luyben [10]) were an improvement over the conventional control described in Chapter Two. They conclude that application to industrial columns would show even more improvement.

Dahlqvist [11] investigated the use of self-tuning regulators for control of top and bottoms product compositions. He was more concerned with the details necessary to implement the scheme than the improvement such a scheme might have over conventional control.

Ogunnake and Ray [12] used the model from Wood and Berry to simulate on a digital computer the control obtained from their multi-time delay compensator. The multi-time delay compensator was used with and without decoupling compensation. In both cases the multivariable approach was an improvement over conventional control and they concluded that even better results could be obtained with industrial columns where time delays would even be greater.

Ogunnaike et al [13] then applied Ogunnaike and Ray's multi-delay compensator to a 19 plate 12 inch diameter experimental distillation column. They tested disturbance rejection as well as set point following. They found that the multi-delay compensator out performed conventional control for most tests.

Weischedel and McAvoy [14] studied the application of three different decoupling schemes to three different columns of 13, 17 and 19 trays. Digital simulation was used to test the various control strategies. They concluded that for moderate to high purity product separations decoupling schemes failed to fully decouple the overhead and bottom controllers but the multivariable approaches were a definite improvement over conventional control.

Garcia and Morari [30] applied Internal Model Control to a simulation of the pilot scale column first introduced by Wood and Berry. They too found that a multivariable controller out performed conventional control in simultaneously controlling overhead and bottoms product compositions. Although robust control is one of the attributes

of Internal Model Control Garcia And Morari failed to test this in their simulations.

The research presented in this thesis extends the work of past research on multivariable control of distillation columns by applying one of the multivariable strategies to a model of a full scale column. Several new and useful modifications were made to Internal Model Control to tailor it for the Linde column. The control studies of the Linde column presented in this thesis provide insight into the transition of advanced control to full scale columns.

4.3 Model Based Control, SISO

Internal Model Control (IMC) is one of the few modern, model based control strategies that retains the advantages of PI control and is capable of overcoming its deficiencies. For this reason it was selected as the alternate control strategy for the control studies of this chapter. The basic structure of IMC that was used in this research is shown in Figure 4-1. The structure of IMC and its relation to other control schemes was developed by Garcia and Morari [2]. Their work was based on Brosilow's [31] earlier work on inferential control. It will be shown that this simple structure addresses performance and robustness in a very straight forward manner.

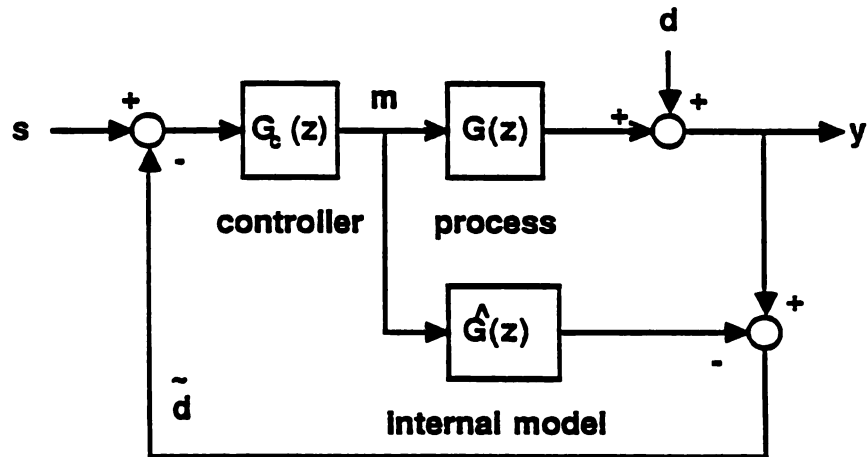


Figure 4-1 Basic Internal Model control structure

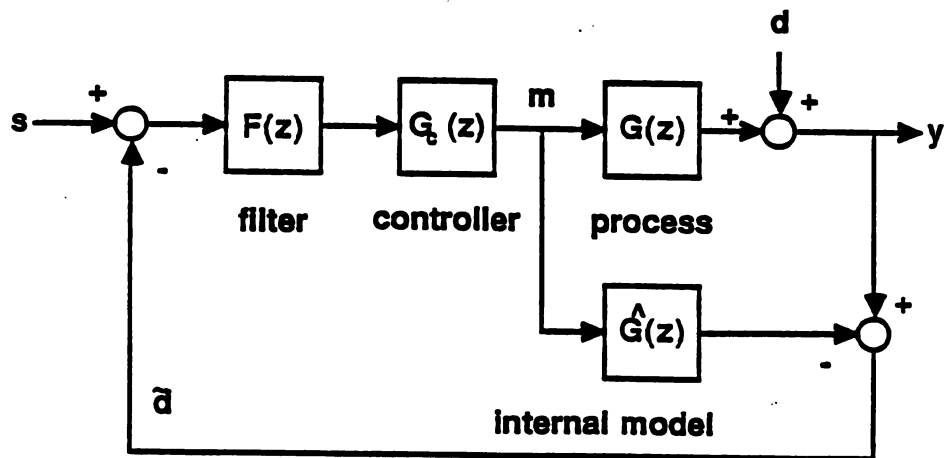


Figure 4-2 Filtered Internal Model control structure

4.3.1 Minimum Phase Processes

The similarity of IMC to conventional feedback control is evident in Figure 4-1. This feature makes it understandable to production personnel. In fact the IMC structure is analogous to the way an experienced operator might control a process. In IMC the control action, u_m , is applied to a model of the process, $\hat{G}(z)$, as well as the process itself, $G(z)$. A prediction of the process output is made by the model and that is compared to the measured process output. In the same way an operator uses his mental model of the process based on his experience. By comparing instrument readings with his expected process response he can identify faulty instruments or large process disturbances and respond accordingly. IMC is actually more intuitively appealing than conventional feedback control.

The biggest reason IMC overcomes the deficiencies of PI control is the special form of its feedback signal $\bar{d}(z)$

$$\bar{d}(z) = (1 + (G(z) - \hat{G}(z))G_c(z))^{-1} d(z) \quad (4.1)$$

Note that for a perfect model,

$$\hat{G}(z) = G(z), \quad (4.2)$$

the feedback signal is the disturbance $d(z)$. This gives automatic time delay compensation. Also note that differences in the model and process are contained in $\hat{d}(z)$. As we shall see this information can be used in a straight forward manner to address robustness.

The other desirable features of IMC can be illustrated by referring to the closed loop equations

$$m(z) = \frac{G_c(z)}{1 + (G_c(z)(G(z) - \hat{G}(z)))} (s(z) - d(z)) \quad (4.3)$$

$$y(z) = \frac{G_c(z)G(z)}{1 + G_c(z)(G(z) - \hat{G}(z))} (s(z) - d(z)) + d(z) \quad (4.4)$$

It is easy to show that for a controller $G_c(z)$ which satisfies

$$G_c(1) = 1 / \hat{G}(1) \quad (4.5)$$

there is automatic integral action leading to zero steady state offset. Since for a constant set point $s(z) = s^*$

$$y_{ss} = \frac{\hat{G}(1)^{-1}G(1)}{1 + \hat{G}(1)^{-1}(G(1) - \hat{G}(1))} (s^* - d) + d = s^*$$

for constant disturbance d . Notice that steady state error is zero even for an imperfect model.

From equation (4.4) it is evident that for a stable minimum phase process perfect control is possible. Let

$$G(z) = \frac{N(z) z^{-1}}{D(z)}$$

Where $N(z)$ and $D(z)$ are polynomials with roots inside the unit circle.

Then if $G_c(z) = \hat{G}^{-1}(z)$ and $\hat{G}(z) = G(z)$

$$y(z) = \frac{\frac{D(z)}{N(z)} \frac{N(z)}{D(z)} z^{-1}}{1 + \frac{D(z)}{N(z)} (G(z) - \hat{G}(z))} (s(z) - d(z)) + d(z)$$

$$= s(z)z^{-1} + (1 - z^{-1})d(z)$$

Notice that the single period of delay is unavoidable since it is inherent in all physical discrete time systems. The case of non-minimum phase systems will be discussed in the next section

Robustness, the ability to control in the event of parameter changes in the process, is addressed by the insertion of a filter in the IMC structure, Figure 4-2. The addition of a filter changes equations (4.3) and (4.4) to

$$m(z) = \frac{F(z)G_c(z)}{1 + F(z)G_c(z)(G(z) - \hat{G}(z))} (s(z) - d(z)) \quad (4.6)$$

$$y(z) = \frac{F(z)G_c(z)G(z)}{1 + F(z)G_c(z)(G(z) - \hat{G}(z))} (s(z) - d(z)) + d(z) \quad (4.7)$$

The filter $F(z)$ can be chosen to ensure stable input and output sequences for a given process-model mismatch. So as the model deviates farther from the true nature of the process, the filter can be modified to slow the controller down to maintain stability.

The filter can also be used to control the closed loop response of the system for a well matched internal model, $\hat{G}(z) = G(z)$, since

$$\frac{y(z)}{s(z)} = F(z)$$

Now if the filter is first order its time constant can be used by operators as a single online tuning parameter to shape the system response or to adjust to changing process dynamics. This is an improvement over PI control since only one parameter needs to be adjusted rather than two.

Other desirable features, such as, control effort limiting and bumpless transfer between manual and automatic, have been described by Parrish and Brosilow [34]. These features together with the ones detailed here make IMC a very appealing control scheme from an industrial point of view. IMC was used in the control studies of this research since it retains the advantages of PI control (zero steady state error, robustness, easy tuning, and conceptually simple) and also offers improved control, especially for processes with time delay or inverse response.

4.3.2 Non-minimum Phase Processes

We have seen in the previous section that for minimum phase processes (stable with no time delay or zeroes outside the unit circle) IMC can produce perfect control based on a controller designed with equations (4.2) and (4.5). When dealing with a non-minimum phase process equation (4.5) cannot be used directly since $G(z)$ is not invertible. In this section several techniques are described to replace equation (4.5)

4.3.2.1 Factorization

One approach to handle a non-invertible process model is to apply the following factorization

$$G(z) = G_-(z)G_+(z) \quad (4.8)$$

where $G_+(z)$ contains all the zeroes outside the unit circle and all the time delays. $G_-(z)$ is then used in equation (4.5) in place of $G(z)$. The factorization (4.8) is not unique. Garcia and Morari [2] offer the following form

$$G_+(z) = z^{-r-1} \prod_{i=1}^p \frac{z - \nu_i}{z - \hat{\nu}_i} \quad (4.9)$$

where r is the time delay of the process and ν_i are the p zeroes of $G(z)$ and $\hat{\nu}_i$ are the images inside the unit circle, i.e.

$$\hat{\nu}_i = \nu_i, \quad |\nu_i| \leq 1$$

$$\hat{\nu}_i = 1 / \nu_i, \quad |\nu_i| > 1$$

Figure 4-19 illustrates this procedure .

The use of the exact model inverse or its factored form of (4.8) for the design of the controller can lead to excessive control action for

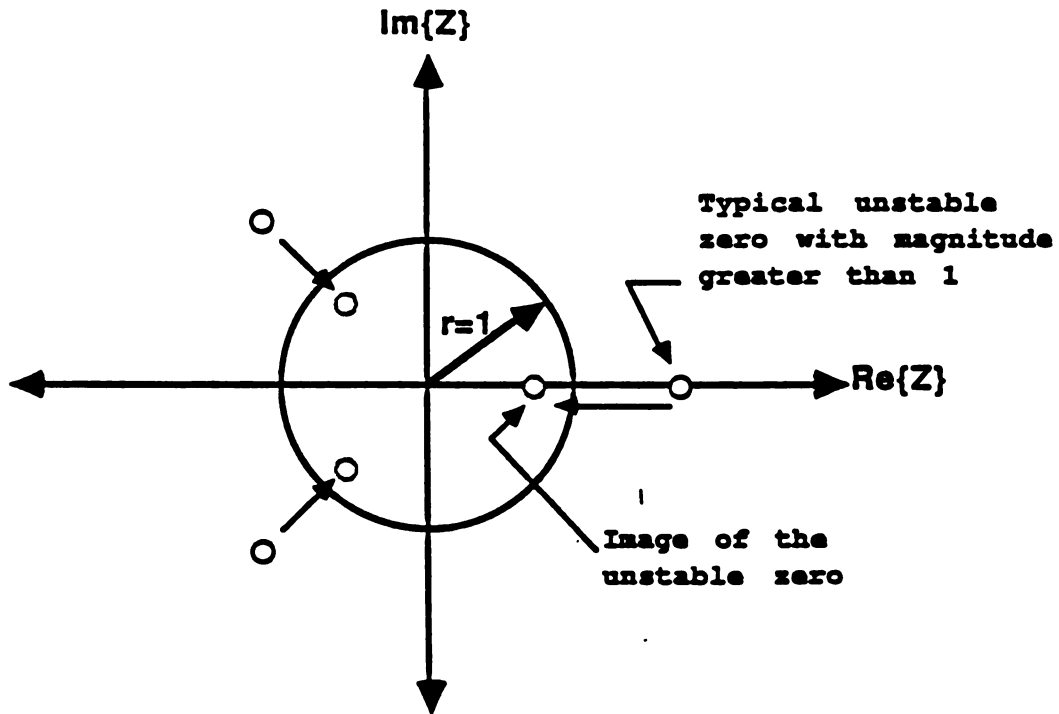


Figure 4-19 Stable images of unstable zeros

minimum or non-minimum phase processes. This is demonstrated for non-minimum phase processes by $G_{11}(z)$ of the Linde Column model,

$$G_{11}(z) = \frac{(0.033z^3 - 0.0199z^2 - 0.00238z - 0.0507) z^{-5}}{z^4 - 0.8267z^3 + 0.3882z^2 - 0.9664z + 0.4814}$$

Using (4.8) and (4.9) to factor $G_{11}(z)$ produces

$$G_+(z) = \frac{z^{-5}(z - 1.3698)(z - 0.3831 \pm j0.9874)}{(z - 0.7300)(z - 0.3417 \pm j0.8808)} \times \frac{(1 + 0.7300)(1 + 0.6835 + 0.8927)}{(1 - 1.3698)(1 + 0.7662 + 1.1218)}$$

$$G_-(z) = \frac{(z - 0.7300)(z - 0.3417 \pm j0.8808)}{z^4 - 0.8267z^3 + 0.3883z^2 - 0.9665z + 0.4143} \times \frac{(1 - 1.3698)(1 + 0.7662 + 1.1218)}{(1 - 0.7300)(1 + 0.6835 + 0.8972)}$$

The resulting controller is

$$G_c(z) = \frac{z^4 - 0.8267z^3 + 0.3883z^2 - 0.9665z + 0.4143}{(z^3 - 0.0465z^2 + 0.3937z - 0.6517)(-0.0506)}$$

Figure 4-3a shows the results of a simulation in which $G_{11}(z)$ was considered as a single input, single output system controlled by an IMC with the filter time constant set equal to zero and a control block

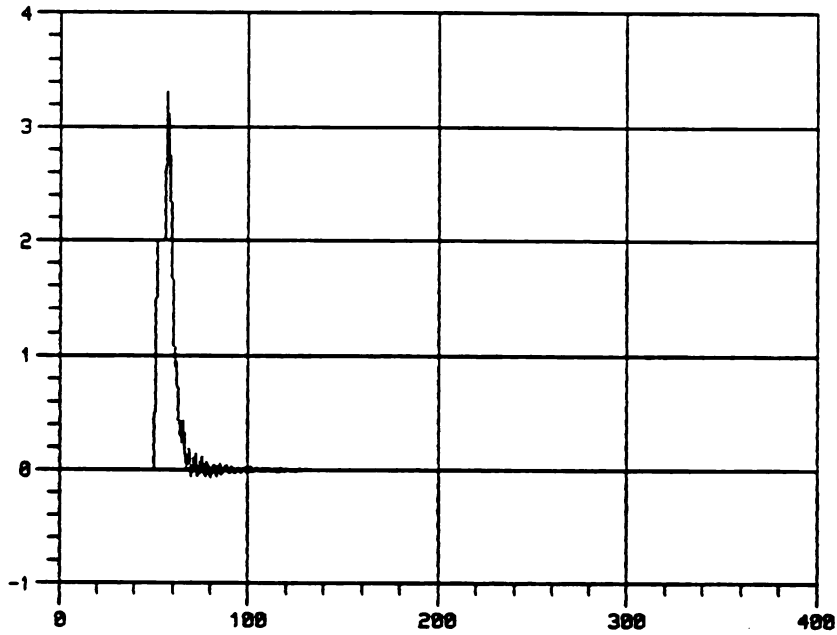


FIGURE 4-3a RESPONSE OF $G_{11}(z)$ TO A STEP
LOAD DISTURBANCE, IMC CONTROL
WITH NO FILTERING.

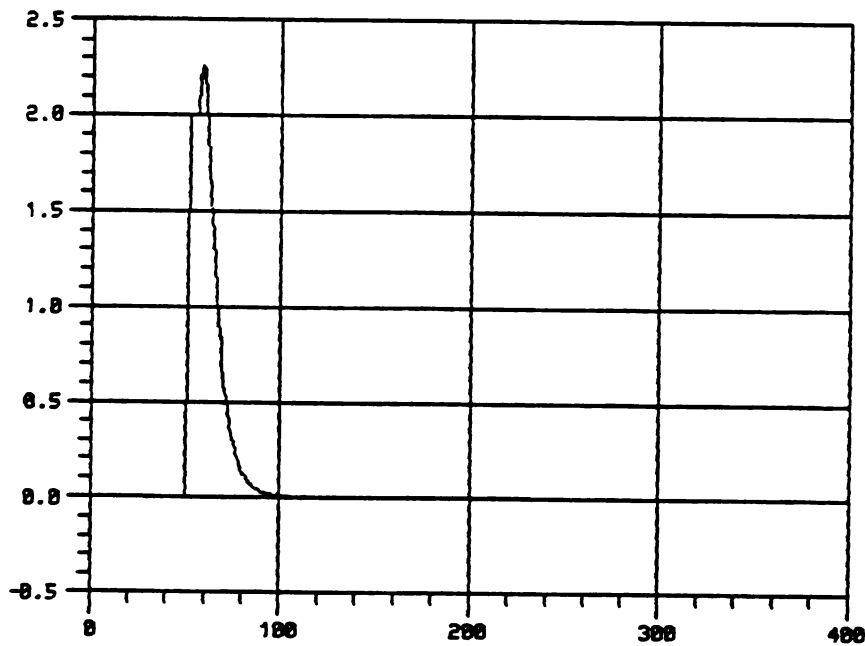


FIGURE 4-3b RESPONSE OF $G_{11}(z)$ TO A STEP
LOAD DISTURBANCE, IMC CONTROL
WITH FILTER TIME CONSTANT = 0.85

given as $G_c(z)$. In this simulation a step load disturbance was introduced at time sample 50. We see that disturbance is compensated for quickly but that there is a large initial spike and oscillations around the set point. Figure 4-3b shows much smoother operation with a large filter time constant of 0.85. As a comparison Figure 4-4 shows the response of the system with the control block set to a constant, i.e. $G_c(z) = 1 / \hat{G}(1)$, and the filter time constant set equal to zero. Notice the smooth operation without the use of the tuning filter.

4.3.2.2 Predictive Controller

Figure 4-4 suggests that a way to avoid a hyperactive controller is to use an approximate inverse of the process other than the one prescribed by (4.9). One possibility is the method presented in [2] in which an approximate inverse is found by solving the following predictive control problem

Consider the impulse response representation of the process

$$G(z) = z^{-r} \sum_{i=1}^{\infty} g_i z^{-i+1}$$

At each discrete time k find the solution to

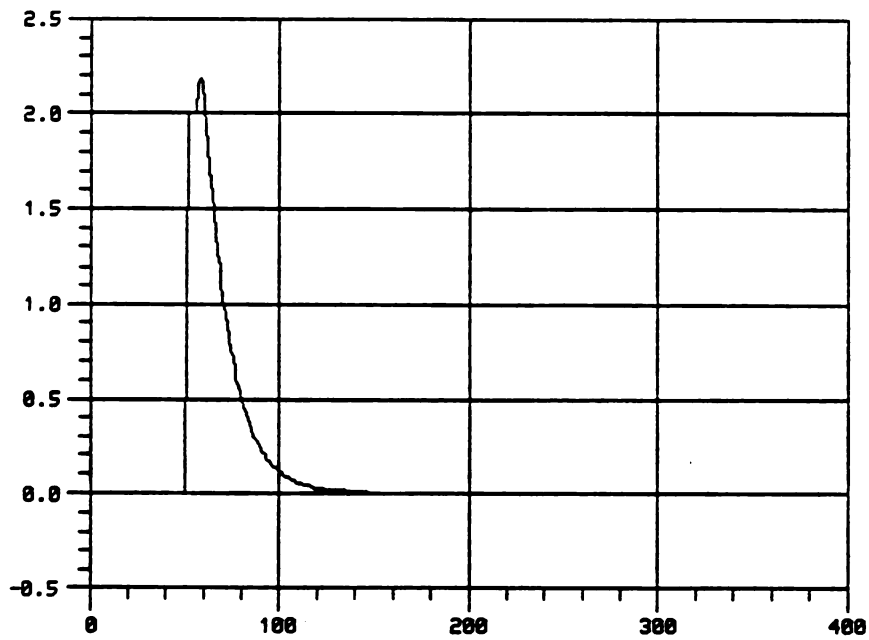


FIGURE 4-4 RESPONSE OF $G_{11}(z)$ TO A STEP
LOAD DISTURBANCE, IMC CONTROL
WITH $G_c(z) = 1/G_{11}(1)$ AND NO
FILTERING.

$$\min \sum_{n=1}^P \gamma_n^2 [y_d(k+r+n) - y(k+r+n|k)]^2 + \beta_n^2 m(k+n-1)^2$$

over the set $\{m(i): i=k, k+1, \dots, k+M-1\}$, subject to the constraints

$$\begin{aligned} y(k+r|k) &= y_m(k+r) + d(k+r|k) \\ &= g_1 m(k-1) + g_2 m(k-2) + \dots + g_N m(k-N) + d(k+r|k) \end{aligned}$$

$$m(k+M-1) = m(k+M) = \dots = m(k+P-1)$$

$$\beta_n^2 = 0, \quad n > M$$

Here $y_d(k+r+n)$ is the future set point, P is the prediction horizon, γ_n^2 are the time varying weights on the output error, β_n^2 are the time varying weights on the input, M is the input suppression parameter which specifies the number of intervals into the future during which $m(k)$ is allowed to vary ($m(k)$ remaining constant afterwards), τ is the system time delay, $y_m(k+r)$ is the output of the internal model, $y(k+r|k)$ is the predicted output, and $d(k+r|k)$ is the predicted disturbance.

This method allows the control engineer considerable flexibility in designing the closed loop response. However, the solution depends on several tuning parameters, P , M , γ_n , β_n , and the solution is accomplished by a least squares approximating problem. In addition, if

on-line tuning is desired a matrix equation must be solved each time a tuning parameter is changed. To avoid the complexity of the predictive control problem, a simpler procedure was developed and used in this research.

4.3.2.3 Reduced Order Controller

The method that follows is based on formulating the controller from an inverse of a reduced order model of the process. This approach is motivated from three observations. (1) The abrupt behavior demonstrated in Figure 4-3a is a manifestation of high frequency components in the control system. Therefore a reduced order model approximating the low frequency dynamics of the process can reduce this high frequency behavior. (2) The real benefit of the IMC structure lies not in the controller but in the internal model. This means that for invertible process models (minimum phase) little performance is sacrificed when lower order models are used for controller design. In fact satisfactory performance is usually obtained even with a proportional controller (i.e. a constant gain equal to the inverse of the model steady state gain) as shown in Figure 4-4. For non-invertible process models (non-minimum phase) the loss of performance can be even less. (3) A reduced order controller would decrease the complexity of the control program. Although it is true that the calculations of the program are usually transparent to the production operators, they are not charged with maintaining the program or updating it for changes in the process. The production engineers who would be responsible for program maintenance

tend to relinquish that responsibility after a rather short time. So it is important to keep the program as simple as possible so that it is understandable for the new engineer.

The concept of reduced order models for controller design is not new. The problem of model order reduction has been addressed in the literature, see Jamshidi [33] for an overview and a good list of references. There are two basic approaches for reducing transfer functions. One deals with manipulations of the transfer function using methods such as continued fraction expansion or Pade' approximation. The other is based the minimization of the difference in the frequency or time responses of the reduced and full models.

The approach taken for $G_{11}(z)$ in this research was of the second type. A reduced order model, $G_r(z)$, with the same time delay as $G_{11}(z)$ was sought which minimized the difference between its time response and that of $G_{11}(z)$. Since there was a level of uncertainty associated with the coefficients of $G_{11}(z)$ due to the noisy data used for estimation, it was natural to use as reduced order models those that were obtained in Chapter Three. This is in contrast to the method proposed by Sinha and colleagues [35] and [36] in which a model is found which approximates the step response of the full model.

Models of four different orders exist for a reduced order model of $G_{11}(z)$: 3rd, 2nd, 1st, and zero or constant. The criteria used to

select the model for controller design was the simulated time response of the closed loop system to the same step load change that was used to generate Figure 4-3. It was found that a first order model resulted in a controller which produced a quick return to set point without overshoot. The 2nd and 3rd order models produced overshoot. The first order model had the added advantage that it did not have a zero outside the unit circle so that it could be inverted directly. The factorization of (4.8) had to be invoked for both high order models to produce stable controllers. For these reasons the following first order controller was selected

$$G_c(z) = \frac{1 - 0.9233z^{-1}}{0.3532} \quad (4.10)$$

For this controller the numerator was adjusted slightly so that its steady state gain was the reciprocal of $\hat{G}_{11}(1)$.

A filter time constant of 0.5 was determined experimentally to produce an acceptable level of controller action. Figure 4-6 shows the response of the system to the same disturbance as Figure 4-3 and 4-4. Notice how the reduced order controller is able to nearly match that of the full order controller, Figure 4-3. Notice also the improvement the selected controller shows over the constant controller, Figure 4-4, and a well tuned PI controller, Figure 4-5.

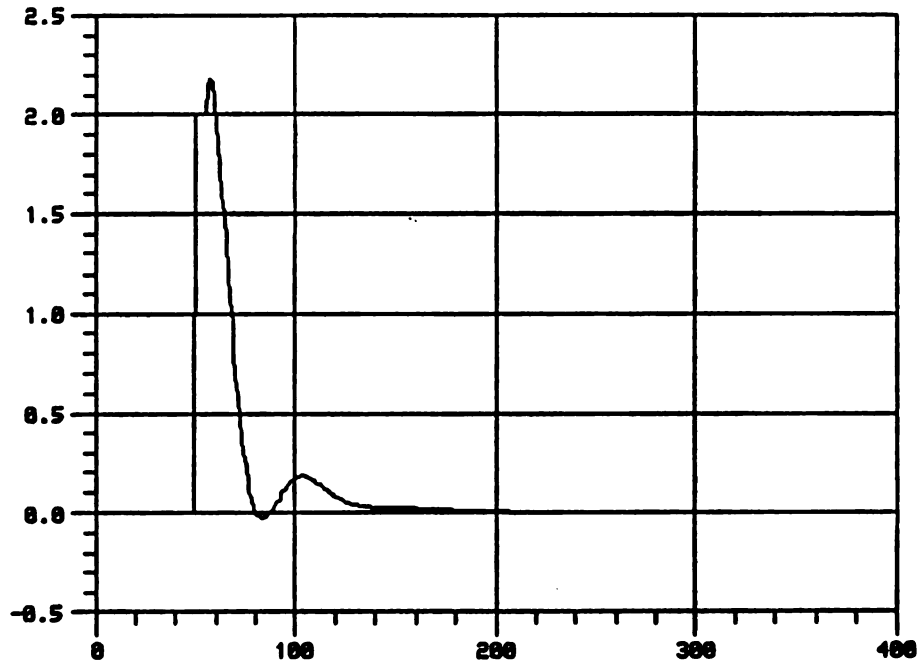


FIGURE 4-5 RESPONSE OF $G_{11}(z)$ TO A STEP LOAD DISTURBANCE, PI CONTROL

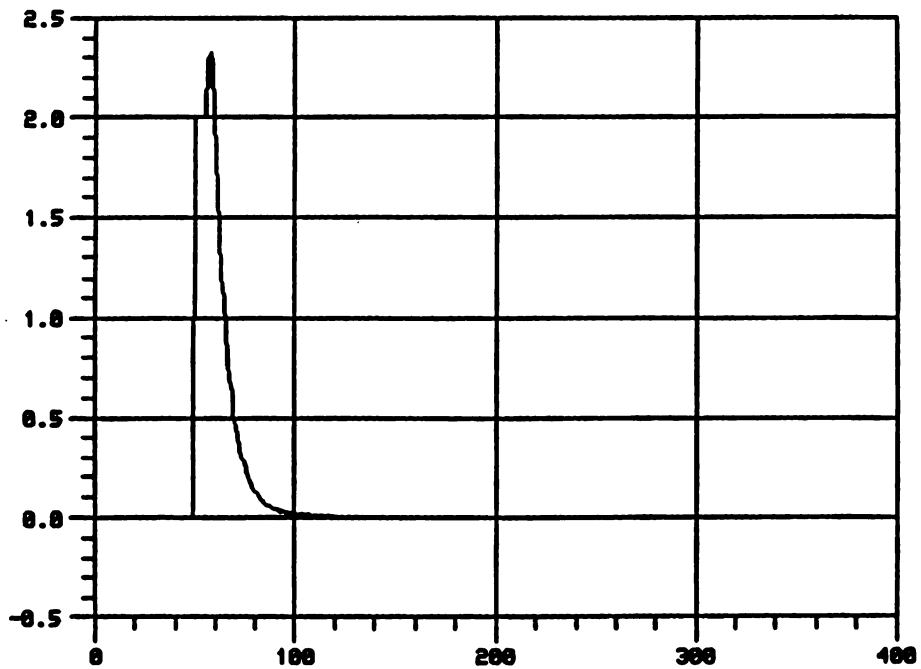


FIGURE 4-6 RESPONSE OF $G_{11}(z)$ TO A STEP LOAD DISTURBANCE, IMC CONTROL

4.4 Model Based Control, MIMO

For a two input, two output system like the Linde Column it is natural to consider the multivariable form of the IMC structure. In this case the internal model $\hat{G}(z)$ becomes a matrix of transfer functions of the form of equation (3-12). Just like the case of a single input, single output system, the controller can be designed as the inverse of the process model and a filter used in series with the controller to address robustness and to shape closed loop response. Garcia and Morari [30] give a detailed design procedure for the multivariable case. However, that structure will not be considered here since it requires uniform sampling of the inputs and outputs. Instead two feedforward controllers each with its own sampling rate will be investigated.

4.4.1 Feedforward Internal Model Control

There are two different structures of feedforward compensated IMC that are applicable to a decoupling problem. The scheme offered by Brosilow [37] is shown in Figure 4-7. An alternative is a modified version of scheme suggested by Garcia and Morari [30] shown in Figure 4-8. As we shall see the design equation for the feedforward compensator $G_{ff}(z)$ is the same for both forms, however the dynamic response is not the same.

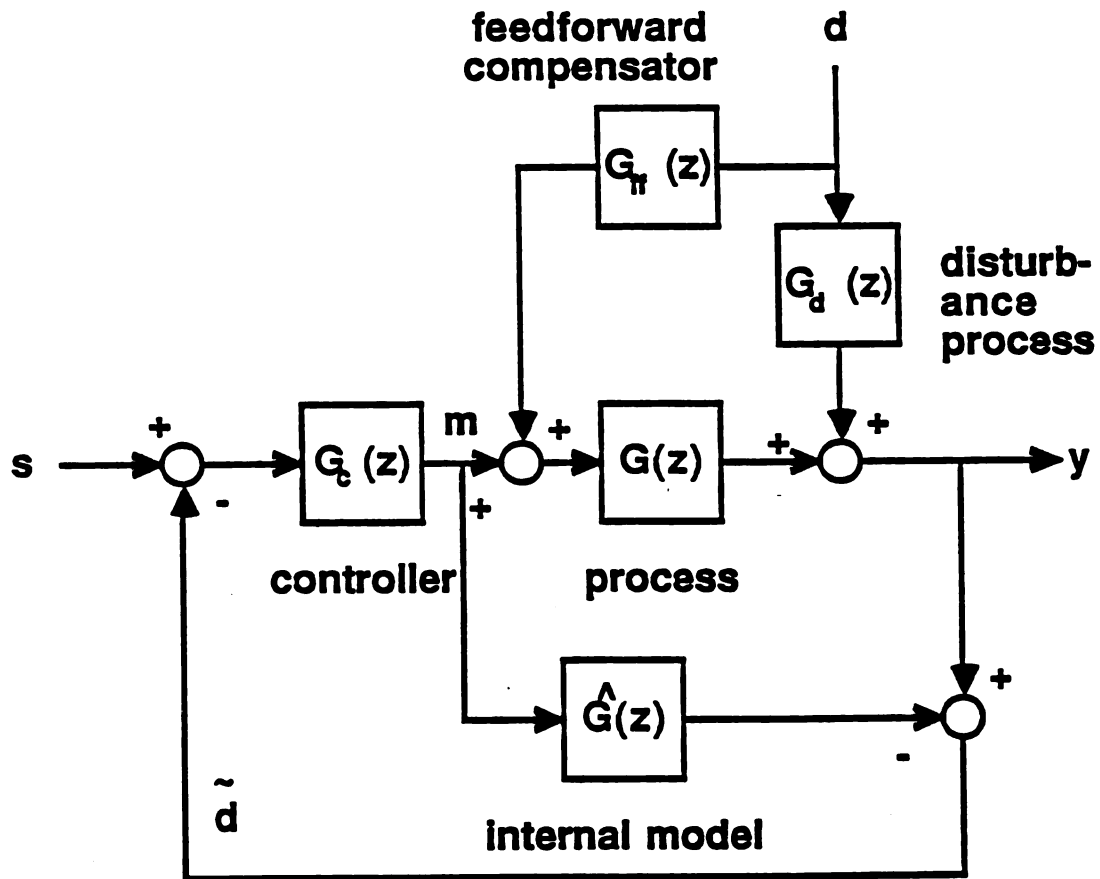


Figure 4-7 Brosilow's Feedforward Internal Model control structure

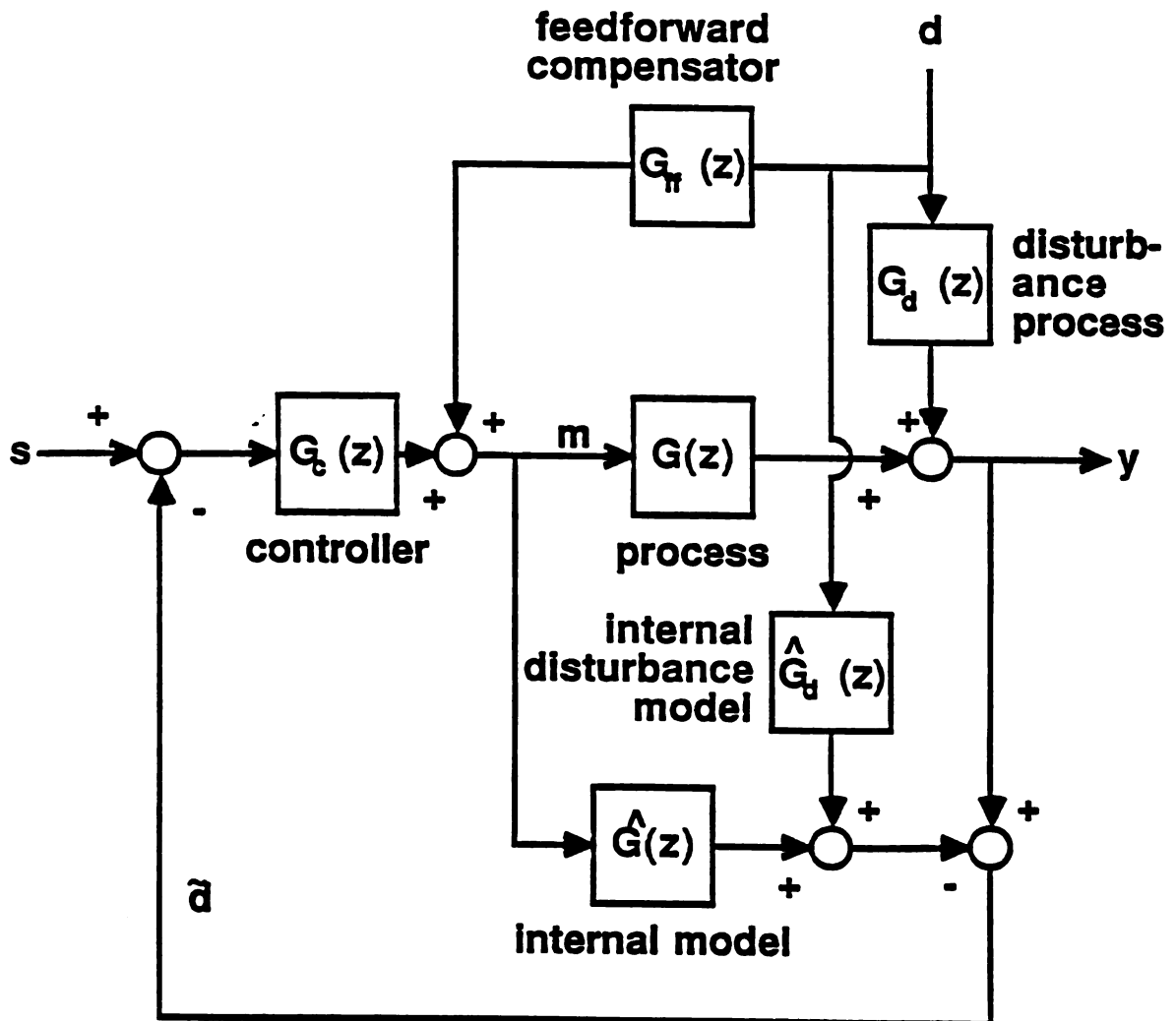


Figure 4-8 Revised Feedforward Internal Model control structure

Consider first the structure of feedforward IMC shown in Figure 4-8. In this scheme the effect of measurable disturbances $G_d(z)d$ are compensated for by $G_{ff}(z)$ so that it may cancel their effect on the process. The disturbance affects are also accounted for by an internal model $\hat{G}_d(z)$. The modification developed in this research was to add the output of $G_{ff}(z)$ to the output of $G_c(z)$ rather than to the input of $G_c(z)$ as presented in [30]. This modification was made so that the calculation of the $G_c(z)$ could be made independently of $G_{ff}(z)$ and thus allow for simplified decoupling of two control loops (simplified decoupling will be explained in the next section). This structure is a unique form of feedforward IMC, and to this author's knowledge has not been presented in the literature. Like other forms of feedforward control it is able to completely cancel the effects of the disturbance in some situations.

Since this form of IMC is new it is necessary to derive the form of the feedforward compensator $G_{ff}(z)$. Straight forward algebra leads to the following closed loop transfer functions

$$m(z) = \frac{G_c(z)}{1 + G_c(z)(G(z) - \hat{G}(z))} [s(z) - d(z)(G_d(z) - \hat{G}_d(z))] + \frac{G_{ff}(z)}{1 + G_c(z)(G(z) - \hat{G}(z))} d(z) \quad (4.11)$$

$$\begin{aligned}
y(z) = & \frac{G_c(z)G(z)}{1 + G_c(z)(G(z) - \hat{G}(z))} [s(z) - d(z)(G_d(z) - \hat{G}_d(z))] \\
& + \frac{G(z)G_{ff}(z)}{1 + G_c(z)(G(z) - \hat{G}(z))} d(z) + d(z)G_d(z) \quad (4.12)
\end{aligned}$$

Now assuming that $\hat{G}(z) = G(z)$ and $\hat{G}_d(z) = G_d(z)$

$$y(z) = G_c(z)G(z)s(z) + (G_d(z) + G(z)G_{ff}(z))d(z)$$

For the disturbance effects to be completely canceled requires

$$G_{ff}(z) = -G_d(z) / G(z)$$

Note that $G(z)$ is not guaranteed to be invertible since it may be non-minimum phase. In this case $G_{ff}(z)$ is designed as

$$G_{ff}(z) = -G_d(z) / G_-(z) \quad (4.13)$$

As we see, the question of model invertibility is also relevant to the design of feedforward compensators for the IMC controller. For non-minimum phase systems an approximate inverse must be found for $G(z)$ in order to apply the design equation (4.13). One can use either the method of [2] or the one described in this thesis. The obvious choice

is to use the same approximation employed in the design of the feedback controller. However, equation (4.13) allows for the cancellation of time delays. Therefore for non-minimum phase processes $G_{ff}(z)$ may be reduced to

$$G_{ff}(z) = -G_d(z)G_-(z)^{-1} z^{-r^*} \quad (4.13a)$$

where $r^* = \min(r_d, r)$ and r is the time delay of $G(z)$ and r_d is the time delay of $G_d(z)$. For such a $G_{ff}(z)$ and with $G_c(z) = 1 / G_-(z)$ the resulting closed loop response is given by

$$y(z) = G_+(z)z^{-r^*}s(z) + d(z)G_d(z)(1 - G_+(z)z^{-r^*}) \quad (4.14)$$

The design equation for the feedforward compensator in Brosilow's scheme can be easily derived starting from the its closed loop equation,

$$y(z) = \frac{G_c(z)G(z)}{1 + G_c(z)(G(z) - \hat{G}(z))} [s(z) - d(z)(G_{ff}(z)G(z) + G_d(z))] + d(z)(G_{ff}(z)G(z) + G_d(z)) \quad (4.15)$$

Now if $\hat{G}(z) = G(z)$ then

$$y(z) = G_c(z)G(z)s(z) + d(z)G_c(z)G(z)(G_{ff}(z)G(z) - G_d(z))$$

$$+ d(z)(G_{ff}(z)G(z) - G_d(z))$$

So as with the previous form of feedforward IMC the disturbance affects are completely canceled if $G_{ff}(z) = -G_d(z) / G(z)$.

As before, $G_{ff}(z) = -G_d(z)G_-(z)^{-1}z^{-\tau^*}$ for non-invertible $G(z)$. This leads to a different closed loop response

$$y(z) = G_+(z)z^{-\tau^*}s(z) - d(z)G_d(z)(1 - G_+(z)z^{-\tau^*})^2 \quad (4.16)$$

It will be shown that these different closed loop responses are noticeable in simulations of the Linde Column.

4.4.2 IMC for the Linde Column

In applying these schemes to the Linde Column, the 57th tray concentration was controlled by manipulating the reflux flow while changes in reboiler steam pressure were considered as measurable disturbances. The bottoms concentration was controlled by manipulating the reboiler steam pressure while changes in the reflux flow were considered as measurable disturbances. This is similar to the distillation control strategy described by Shunta and Luyben [32] in which they used conventional feedback controllers with feedforward compensation. The results described here were achieved by simulating the bottoms controller with a 8 minute sampling interval to coincide

with the sample rate of the bottoms concentration measurement while the other controller had a 1 minute sampling period.

The modification presented in this thesis to feedforward IMC scheme was made to allow for simplified decoupling of the Linde Column controllers. Simplified decoupling was first introduced by Buckley [38] for continuous systems with conventional feedback controllers. A block diagram of this new IMC structure to support simplified decoupling is shown in Figure 4-9. In this diagram the Linde Column is depicted by the transfer functions G_{11} , G_{12} , G_{21} , and G_{22} . The top controller contains the control block G_{CT} whose output is summed with that of the feedforward block G_{FT} to produce the total top control action m_T (reflux flow). This output signal is also sent to the internal model \hat{G}_T . A filter, F_T , is placed ahead of the top control block for tuning purposes. The feedforward signal sent to G_{FT} is the output of the bottom control block G_{CB} . This signal is also sent to the internal feedforward model \hat{G}_{dT} . The output of the feedforward internal model is summed with the output of the standard internal model, \hat{G}_T , and the result is subtracted from the measured top controlled variable (concentration on the 57th tray) to produce the feedback signal for the top controller. The feedback signal is compared to the top set point s_T . The difference in these two signals is the input to the top filter.

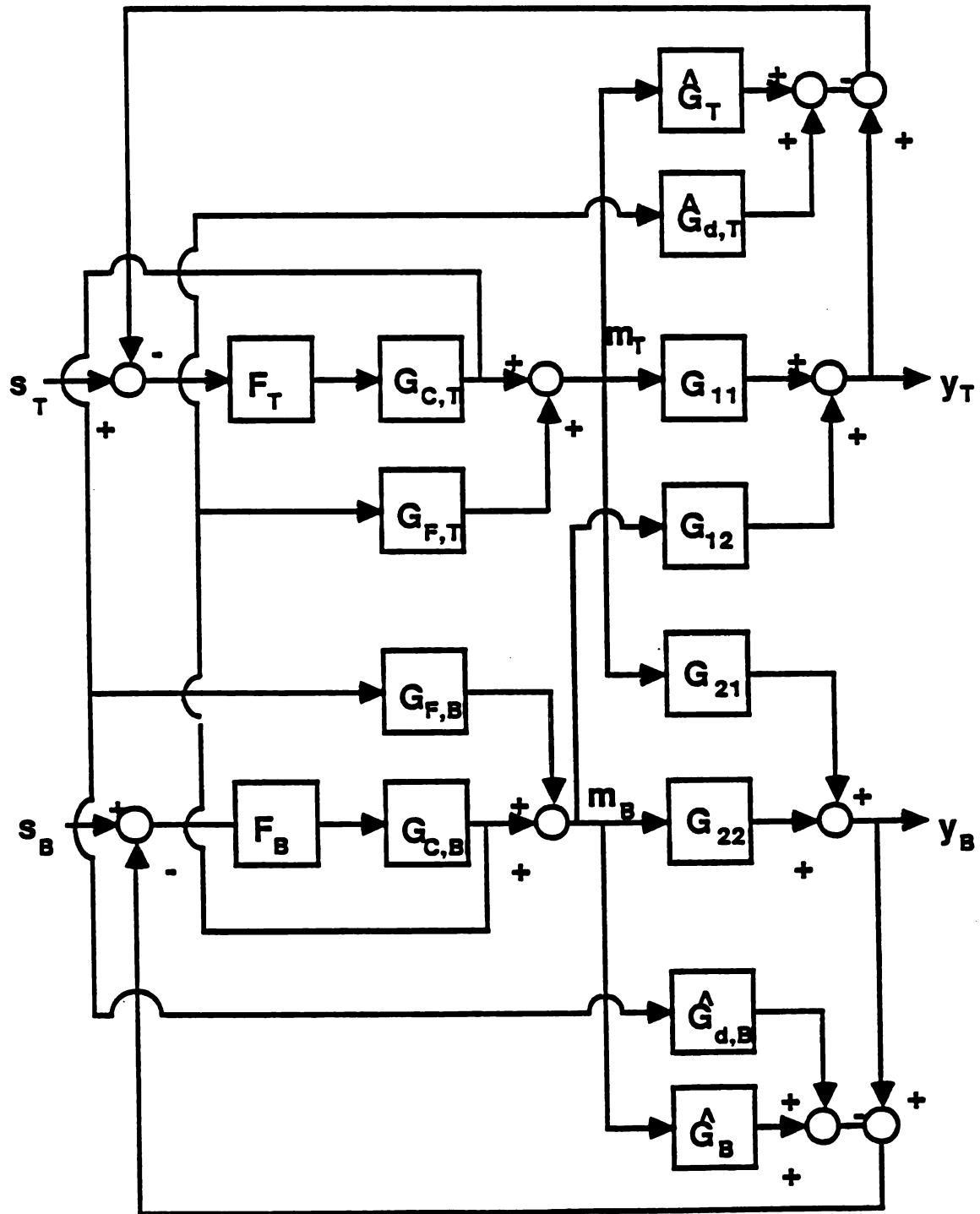


Figure 4-9 Simplified Decoupling with Revised Feedforward IMC

In a like manner, the bottom control action, m_B (reboiler steam pressure), is calculated in the bottom controller using the bottom control block G_{CB} , the bottom feedforward compensator G_{FB} , and the bottom tuning filter F_B . The input to the bottom feedforward compensator is the output of the top control block. The bottom feedback signal is calculated from the bottom internal model \hat{G}_B , the bottom disturbance model \hat{G}_{dB} , and the measured bottom controlled variable (bottoms concentration). The bottom feedback signal is compared to the bottom set point s_B .

This scheme allows the feedback control calculations for both controllers to be made independently and then their results processed and added to each others's to give the overall control signals.

Brosilow's version allows for the same simplified decoupling. A block diagram is shown in Figure 4-10. The difference with Brosilow's version is the lack of an internal disturbance model and the signal applied to the standard internal model. As before, the top controller contains the control block G_{CT} whose output is summed with that of the feedforward block G_{FT} to produce the total top control action m_T (reflux flow). However, only the output of the control block G_{CT} is sent to the internal model \hat{G}_T . A filter, F_T , is placed ahead of the top control block for tuning purposes. The feedforward signal sent to G_{FT} is the

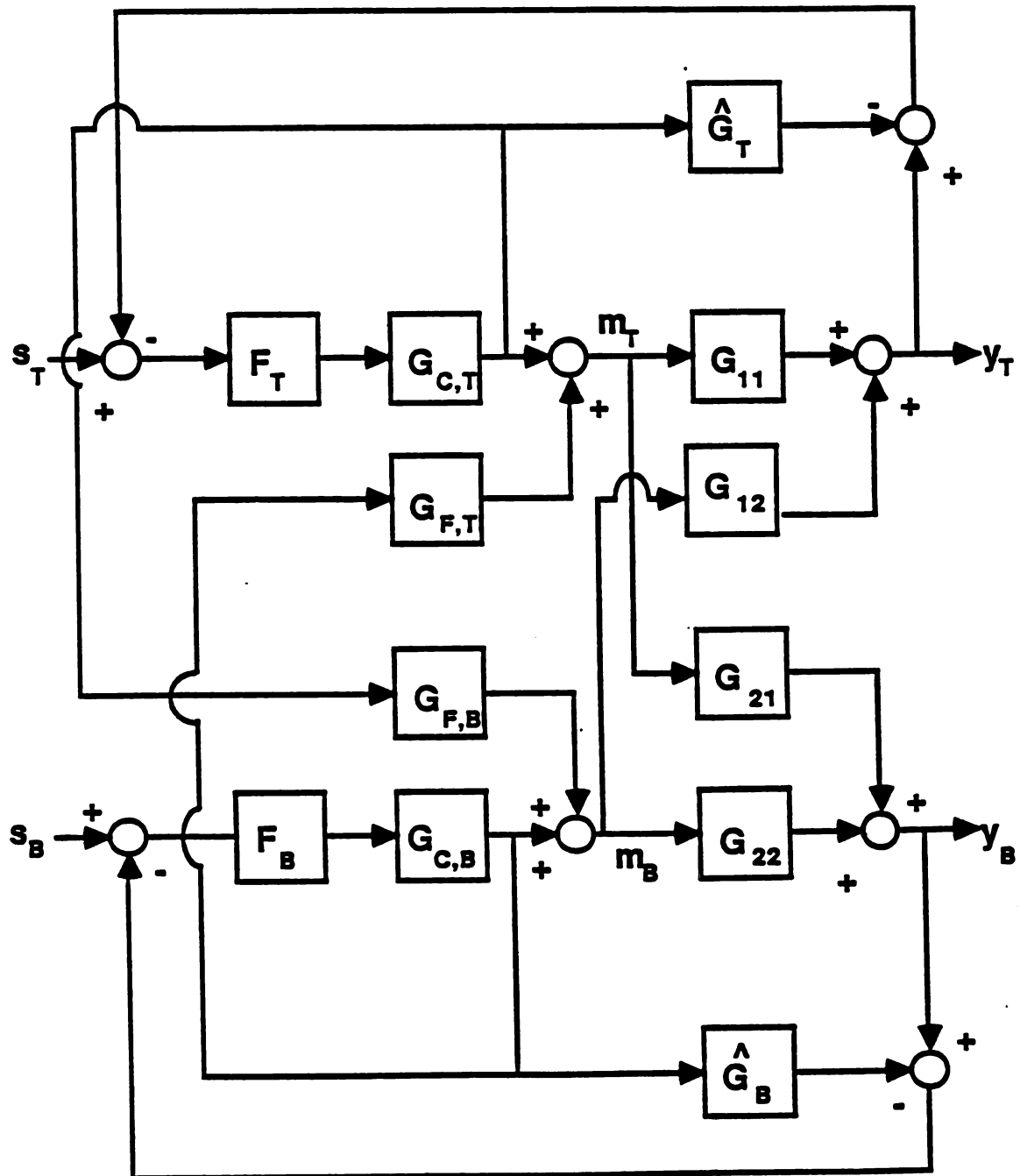


Figure 4-10 Simplified Decoupling with Brosilow's Feedforward IMC

output of the bottom control block G_{CB} . The output of the internal model, \hat{G}_T , is subtracted from the measured top controlled variable (concentration on the 57th tray) to produce the feedback signal for the top controller. The feedback signal is compared to the top set point s_T . The difference in these two signals is the input to the top filter. The bottom controller operates in the same fashion which again allows independent feedback calculations of both controllers. These feedback control signals are again fed forward to the other controller for compensation.

The multirate sampling nature of the two controllers gives rise to a question of how to use, if at all, the values of the feedback calculation of the overheads controller, $m_{CT}(kT)$, which occur in between the sampling instants of the bottoms controller, $8T$, $16T$, ect. In the simulations of the Linde Column it can be observed that much smoother control is achieved if the feedforward portion of the bottoms controller was based on the trailing average, $\overline{m}_{CT}(kT)$ rather than only on $m_{CT}(8T)$, $m_{CT}(16T)$, ect. The trailing average of $m_{CT}(kT)$ can be expressed as

$$\overline{m}_{CT}(kT:N) = \frac{1}{N} \sum_{i=k-N+1}^k m_{CT}(iT) \quad \begin{array}{l} k = 0,1,2,\dots \\ N = 1,2,3,\dots \end{array} \quad (4.17)$$

The effect of the trailing average (when $N = 8$) is to better approximate the assumed 8 minute zero order hold in the reflux flow that is inherent in the pulse transfer function representation of $G_{21}(z)$.

Simplified decoupling as detailed above fails to fully decouple the two control loops for two reasons. (1) $G_{FT}(z)$ cannot be designed as a perfect feedforward compensator because $G_{11}(z)$ is non-invertible. (2) Only the feedback portion of the total control signal from either controller is fed forward to the other controller. Nothing can be done to eliminate the first problem, however the multirate nature of the two controllers allows for nearly eliminating the second problem.

The basic idea behind the following strategy, which will be called critical decoupling, is to take advantage of the fact that the output of the bottoms controller remains constant for seven intervals of the overheads controller because the former has an 8 minute sampling period while the latter has a 1 minute sampling period. In addition, this strategy takes advantage of the trailing average used for the feedforward signal of the bottom controller.

Because the bottom controller is held constant for seven periods of the overhead controller, its total control signal may be used in the feedforward portion of the overheads controller for those seven periods. In fact its total control signal may be fed forward at all times if the bottoms controller calculations are executed before the calculations of the overheads controller.

Likewise, nearly all of the overheads controller output may be used in the trailing average calculation of the feedforward portion of the bottom controller. The trailing average can be based on the previous 7 overheads controller outputs which are obviously known and the current feedback portion of the overheads controller. The trailing average of the overheads controller may now be expressed as

$$m_T(kT:8) = \frac{1}{8} \sum_{i=k-7}^{k-1} m_T(iT) + \frac{1}{8} m_{CT}(kT)$$

This more exact form of decoupling is illustrated for both types of feedforward IMC in Figures 4-11 and 4-12.

4.5 Results and Discussion

The proposed control strategies were tested through simulations of the Linde Column using the model developed in the last chapter. The simulations tested 4 different strategies for rejection of step load disturbances in both the overheads composition and the bottoms composition. The 4 strategies tested were:

- Independent PI.....Strategy 1
- Independent IMC.....Strategy 2
- Simple Decoupled IMC.....Strategy 3
- Critically Decoupled IMC.....Strategy 4

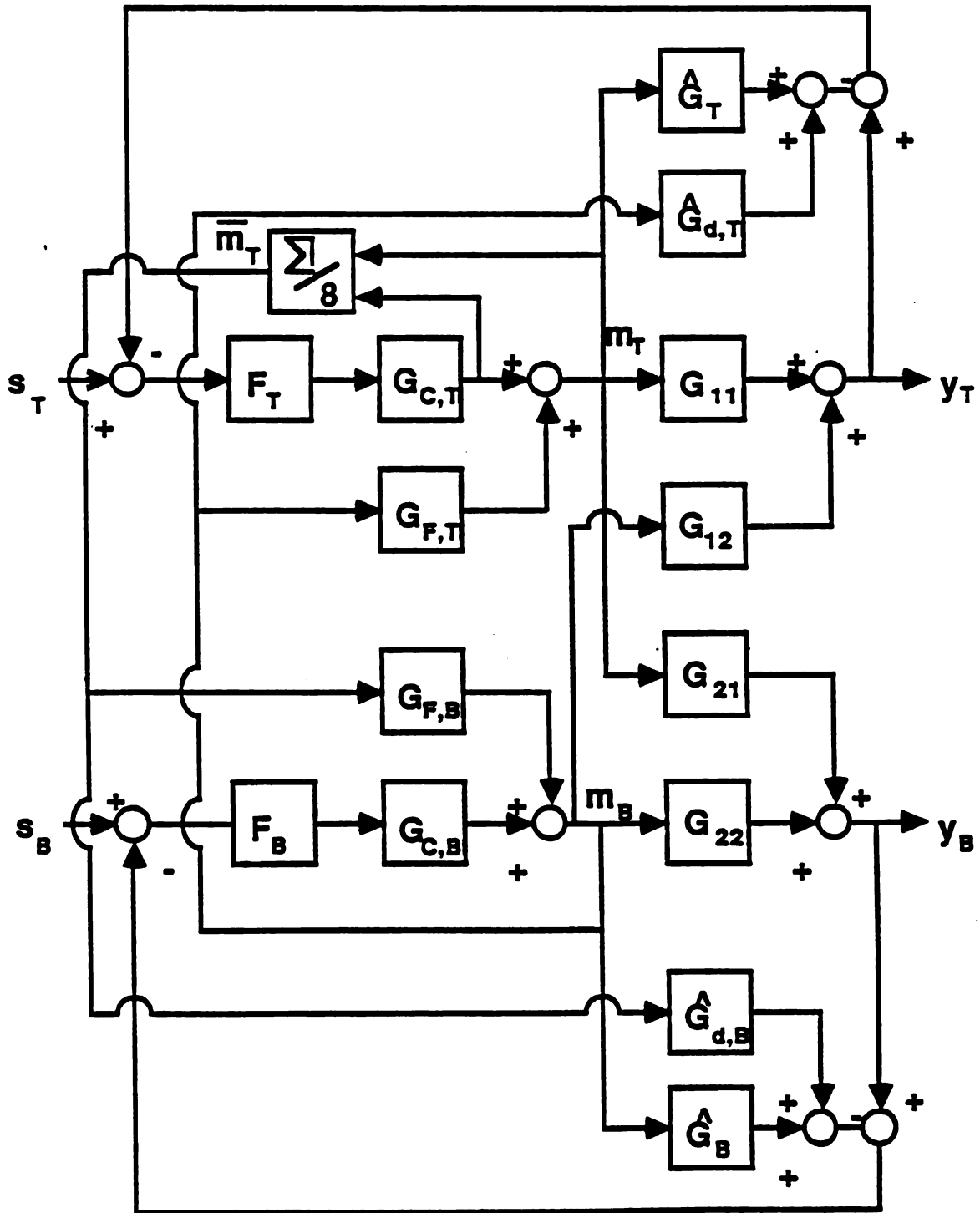


Figure 4-11 Critical Decoupling with Revised Feedforward IMC

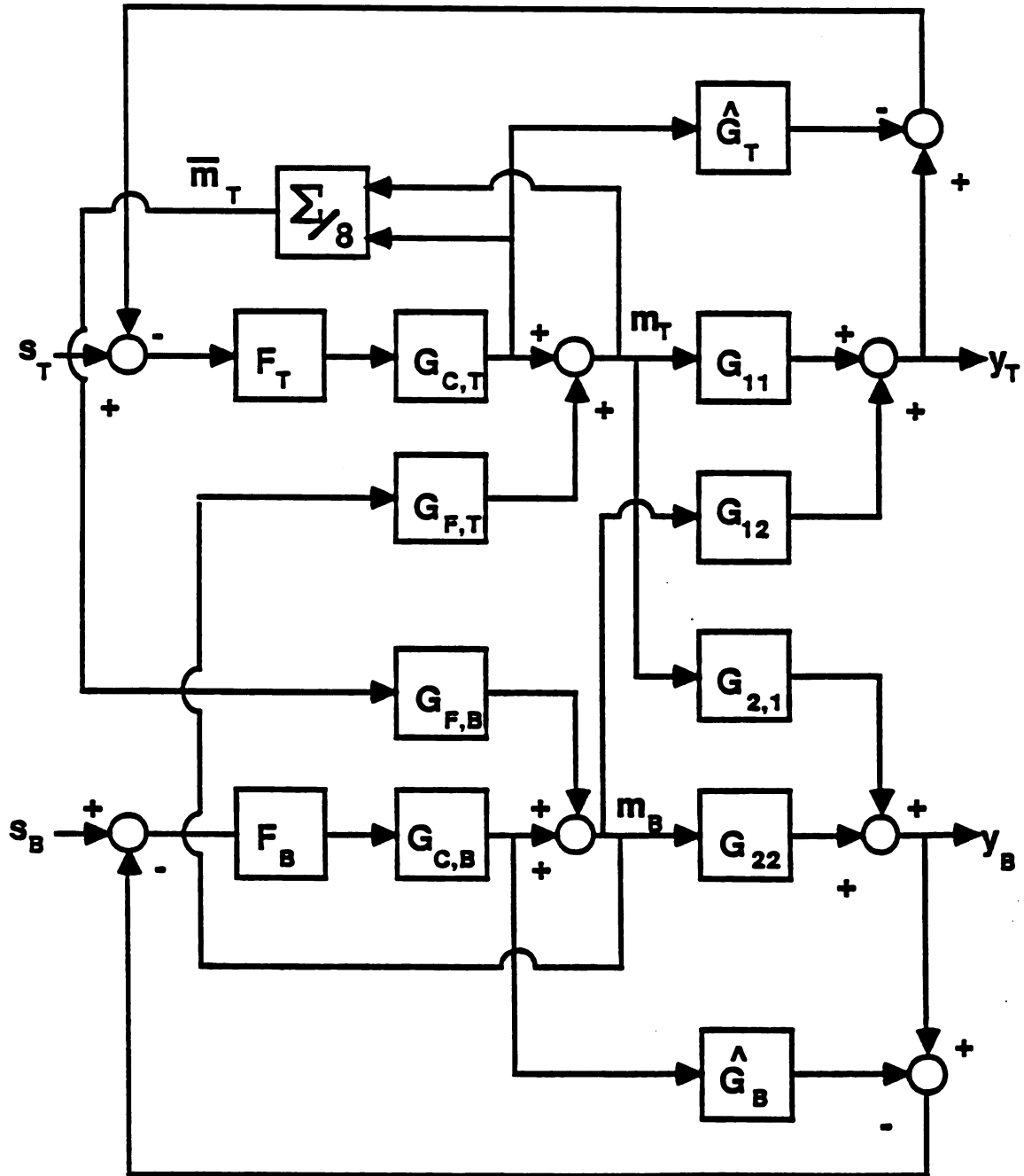


Figure 4-12 Critical Decoupling with Brosilow's Feedforward IMC

Table 4-1 lists the transfer functions for the various components of the IMC strategies. The two PI controllers used are

$$\text{Top: } G_C(z) = \frac{-2.1 + 2.0z^{-1}}{1 - z^{-1}}$$

$$\text{Bottom: } G_C(z) = \frac{-378.7 + 355.0z^{-1}}{1 - z^{-1}}$$

It is interesting to note that because $G_{22}(z)$ is first order with no time delay the PI controller used for bottoms composition control is equivalent to an IMC controller without feedforward compensation. See the Appendix for the proof.

It was found that the Linde Column remained stable under PI control for the disturbances considered. In fact the level of interaction between the two control loops was consistent with the experience of the operating personnel. The response of the 2 independent PI controllers is illustrated in Figures 4-13a and 4-15a for a step load disturbance on the 57th tray, and in Figures 4-14a and 4-16a for a step load disturbance in the bottoms concentration. The interaction between both control loops is quite evident for both types of disturbances. An example of the interaction is seen by the deviation from set point for the bottoms concentration when the load disturbance occurs at the 57th tray in Figure 4-15a.

Table 4-1 IMC Transfer Functions

$$G_{C,T} = \frac{Z - 0.923}{-0.0353Z}$$

$$G_{F,T} = \frac{3.087Z - 2.850}{Z^3 - 0.477Z^2 + 0.388Z - 0.866}$$

$$G_T^A = \frac{0.033Z^3 - 0.020Z^2 + 0.000238Z - 0.0507}{Z^4 - 0.827Z^3 + 0.388Z^2 - 0.967Z + 0.481}$$

$$G_{D,T}^A = \frac{0.10902}{Z^3 - 0.477Z^2 + 0.388Z - 0.866}$$

$$G_{C,B} = \frac{Z - 0.937}{-0.00264Z}$$

$$G_{F,B} = \frac{0.0602Z^3 + 0.0261Z^2 - 0.0221Z - 0.518}{Z^3 - 0.588Z^2 - 0.351Z + 0.938}$$

$$G_B^A = \frac{-0.00264}{Z - 0.937}$$

$$G_{B,D}^A = \frac{0.000159Z^2 + 0.000218Z + 0.000146}{Z^3 - 0.588Z^2 - 0.351Z + 0.938}$$

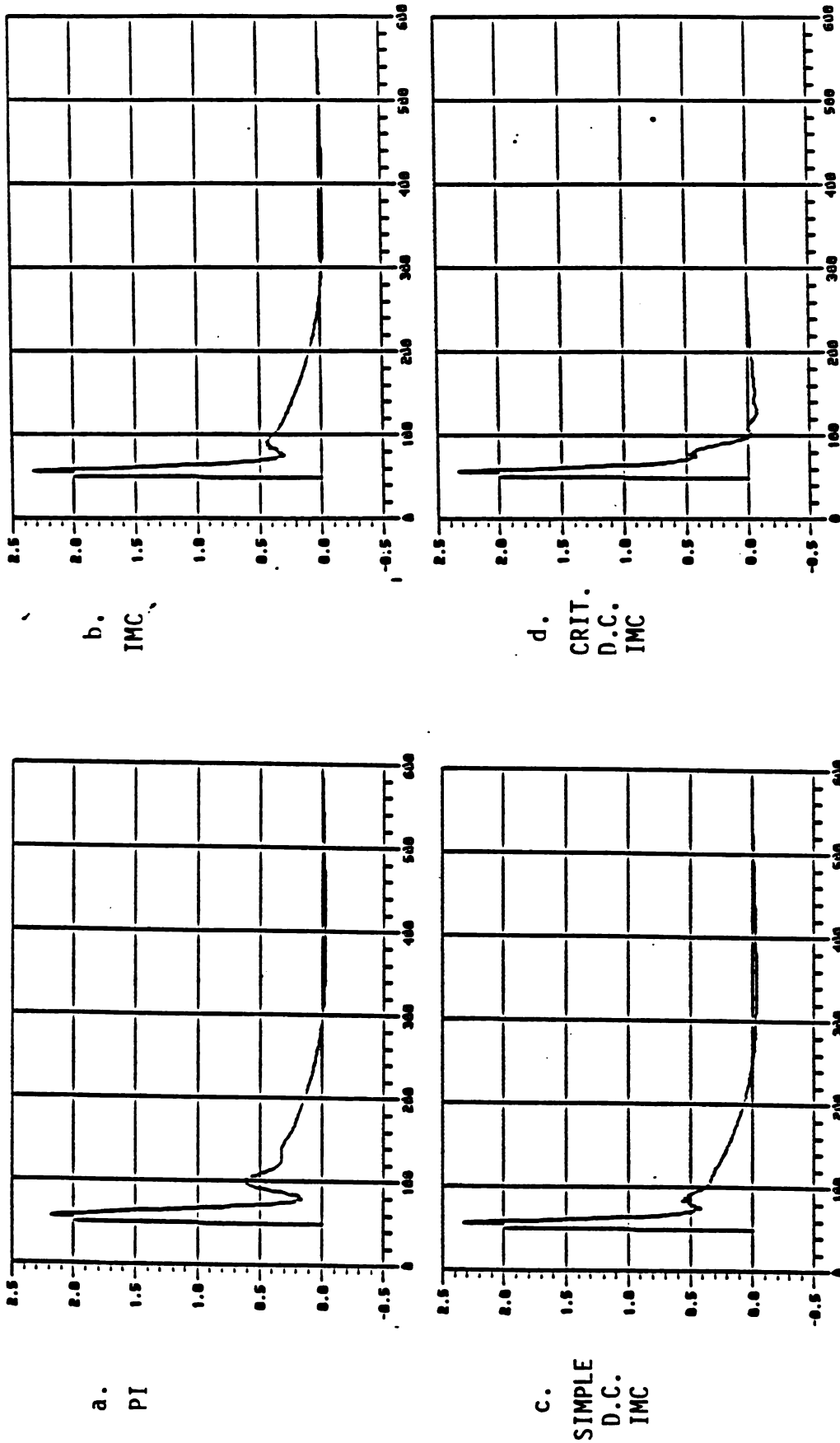


FIGURE 4-13 RESPONSE OF THE 57TH TRAY CONCENTRATION TO A STEP LOAD DISTURBANCE

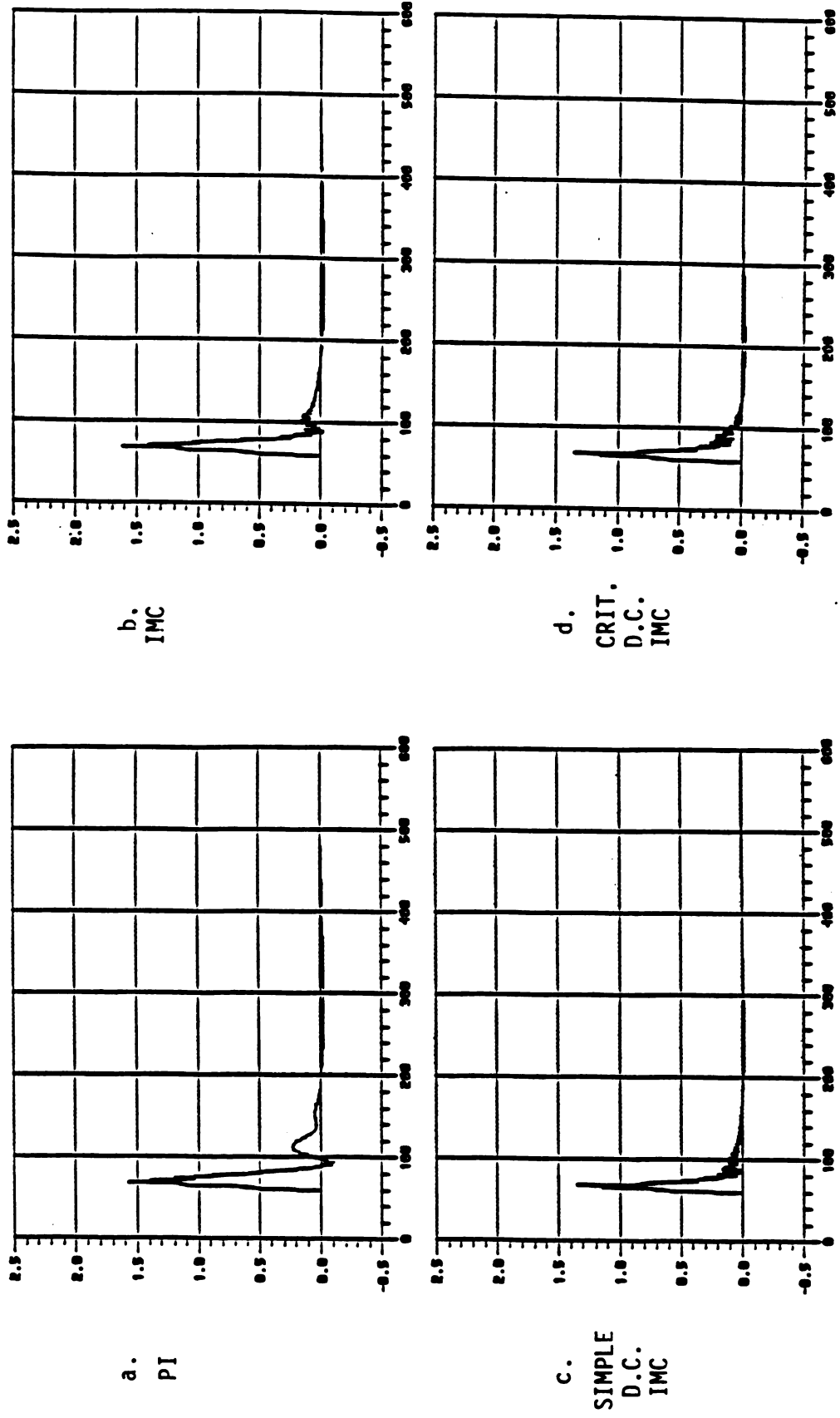
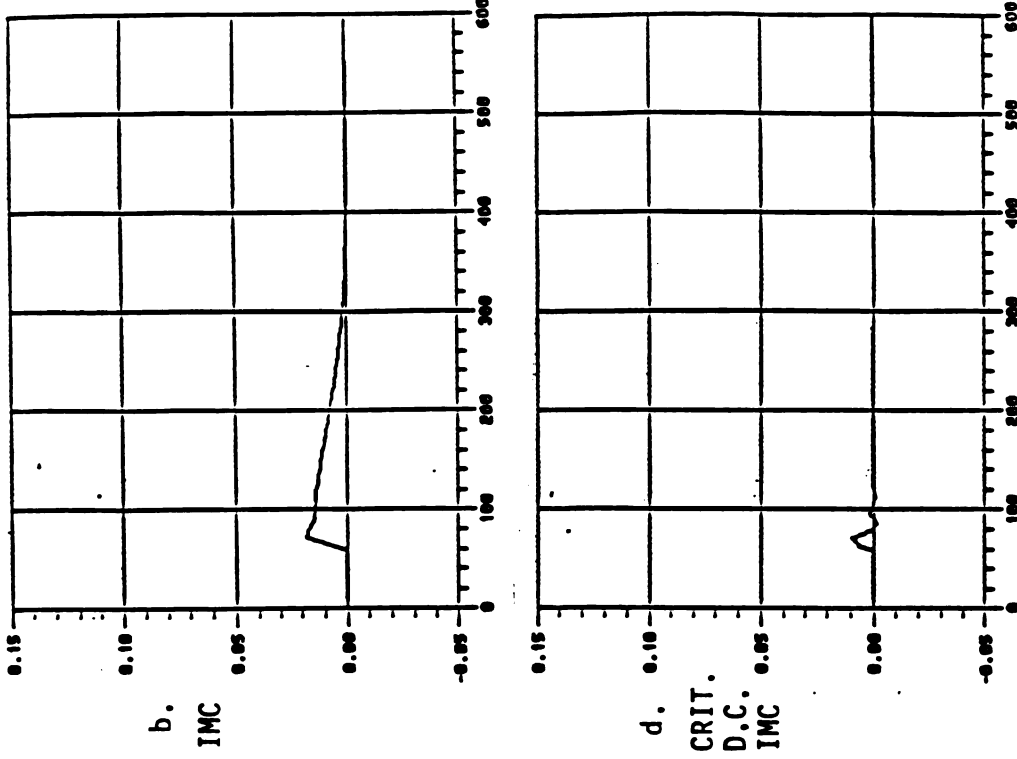


FIGURE 4-14 RESPONSE OF CONCENTRATION ON THE 57th TRAY TO A STEP LOAD DISTURBANCE IN THE BOTTOMS CONCENTRATION



a. PI

b. IMC

c. CRIT.
D.C.
IMC

d. SIMPLE
D.C.
IMC

FIGURE 4-15 RESPONSE OF BOTTOMS CONCENTRATION TO A STEP LOAD DISTURBANCE ON THE 57TH TRAY.

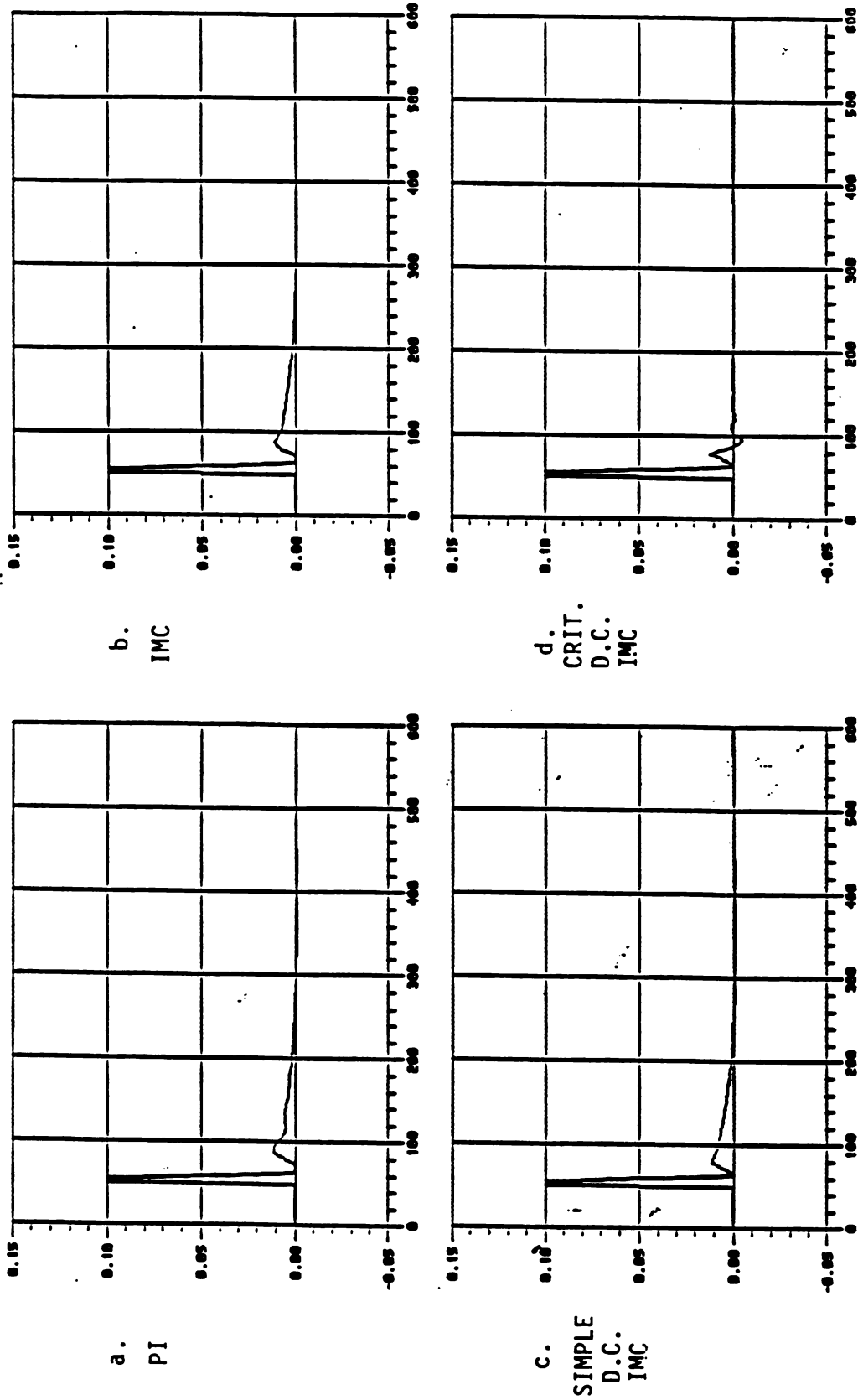


FIGURE 4-16 RESPONSE OF BOTTOMS CONCENTRATION TO A STEP LOAD DISTURBANCE

Control Strategy 2 demonstrated that the major hurdle to improved control is the coupling between the two control loops. Figures 4-13b through 4-16b show the response of control strategy 2. These simulations indicate that a slight improvement is made in the performance of the controller. A comparison of Figure 4-14a with Figure 4-14b shows that the oscillations are reduced and set point is achieved sooner. A comparison of Figure 4-13a and Figure 4-13b leads to the same conclusion. However, no noticeable improvement is seen in the performance of the bottom control loop. Compare Figure 4-15a to Figure 4-15b and 4-16a to Figure 4-16b. This is to be expected since the PI controller on the bottoms composition is equivalent to an IMC controller.

The addition of simplified decoupling in Control Strategy 3 greatly improved the simultaneous control of both product concentrations. The response of Control Strategy 3 is shown in Figures 4-13c through 4-16c for the feedforward IMC introduced in this thesis. Figure 4-17 illustrates the results using Brosilow's version of feedforward IMC. The improvement in performance due to the feedforward compensation is very evident. This is especially true for the controller which is only responding to the interaction between the two controllers. For example, when the bottom controller reacts to the disturbance produced by the overhead controller correcting for a step load change in the 57th tray concentration. This is to be expected since the majority of the overheads control signal is due to the feedback control block. It is precisely this signal that is used by the feedforward compensator in the bottom controller. Figure 4-15c and 4-17c both show dramatic reduction

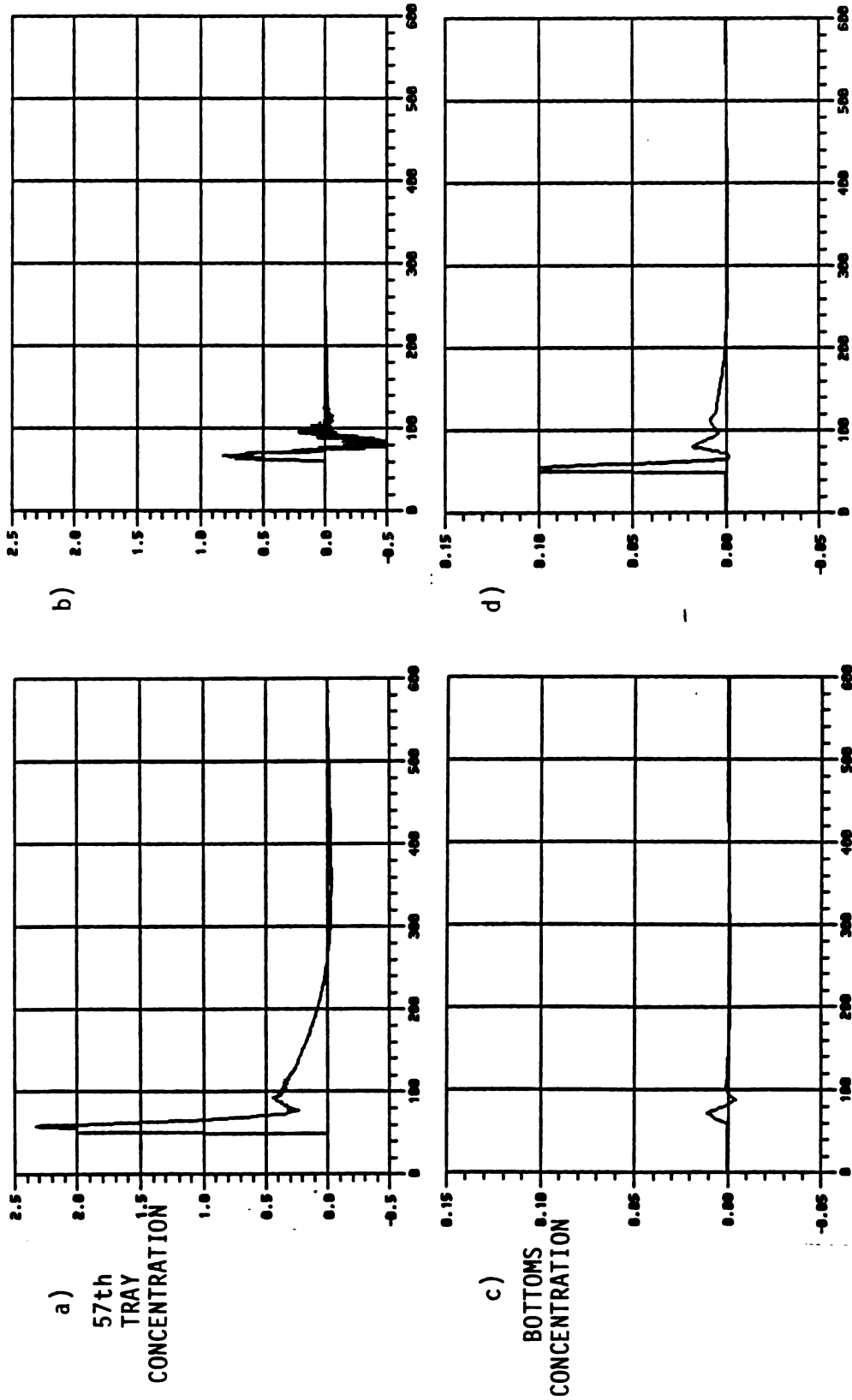


FIGURE 4-17 RESPONSE OF SIMPLY DECOUPLED IMC (BROWILOW'S VERSION) TO A STEP LOAD DISTURBANCE IN: (a,c) 57th TRAY CONCENTRATION, (b,d) BOTTOMS CONCENTRATION

in the deviation from set point for the bottoms concentration compared to classical PI control, Figure 4-15a and independent IMC control, Figure 4-15b. The improvement in the overheads controller is not as dramatic. Compare Figure 4-14b with Figure 4-14c and Figure 4-17b. The lack of improvement is due to the non-minimum phase nature of $G_{11}(z)$.

When the controller which is correcting for the step load disturbance is considered, the response of Control Strategy 3 is nearly identical to that of Control Strategy 1 and Control Strategy 2. For example, compare Figure 4-16c to Figure 4-16a and Figure 4-16b for the bottoms controller. This is to be expected. Under these circumstances the controller in question does not receive much feedforward compensation because the controller at the opposite end of the column is almost totally operating as a feedforward controller. Control Strategy 3 only feeds forward the feed back portion of the other controller.

Control Strategy 4 which makes use of the most information about the column shows the best performance of all the strategies considered. The response of Control Strategy 4 is shown in Figure 4-13d through Figure 4-16d for the revised feedforward IMC and in Figure 4-18 for Brosilow's version. A marked improvement is seen for the case of either controller responding to a step load change at its end of the column. For example, compare the response of the overheads controller to a step load change in the 57th tray concentration, Figure 4-13d, to that of Control Strategy 3, Figure 4-13c. For this case the addition of the feedforward portion of the bottoms controller to the feedforward signal of the over

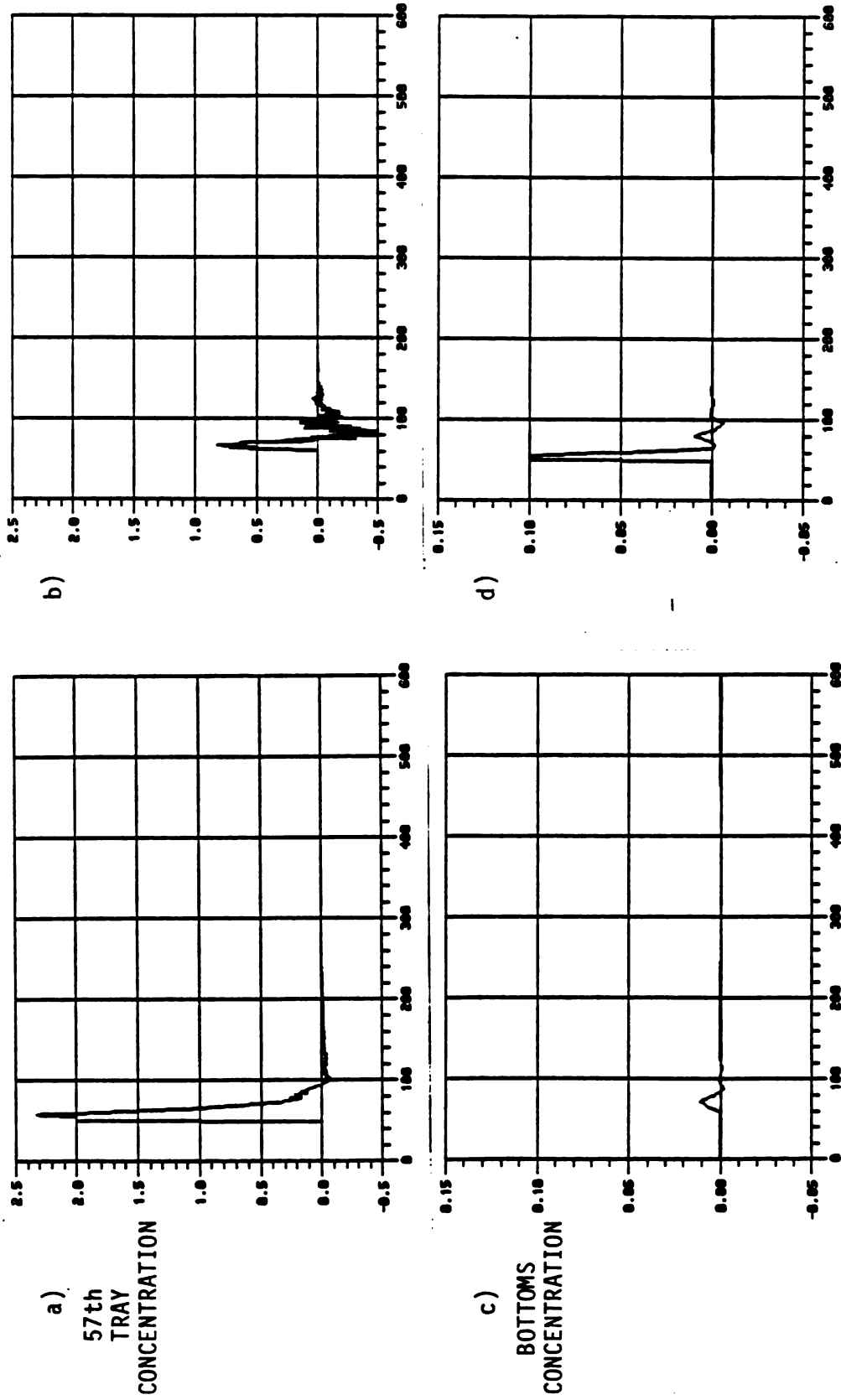


FIGURE 4-18 RESPONSE OF CRITICALLY DECOUPLED IMC (BROSILOW'S VERSION) TO A STEP LOAD DISTURBANCE IN: (a,c) 57th TRAY CONCENTRATION, (b,d) BOTTOMS CONCENTRATION

heads controller has allowed a much quicker return to set point of the 57th tray concentration. This same improvement is seen in the bottoms controller (compare Figure 4-16d to Figure 4-16c). This control strategy has nearly decoupled the two control loops.

4.6 Summary of Chapter Four

This chapter has dealt with the design of a multivariable, model based control system for the Linde Column. The design was influenced by a combination of practical considerations and the dynamic model of the column. Internal Model Control was selected as the alternate control strategy due to the practical benefits of the current PI control strategy. Adapting IMC for the specific characteristics of the Linde Column led to three significant contributions to the literature on the theory of Internal Model Control. These contributions are: 1) a technique of reduced order controller design for non-minimum phase systems, 2) a new feedforward IMC structure, 3) a strategy for multirate, multivariable use of IMC.

The contribution of reduced order controller design is significant because it simplifies the implementation of IMC for non-minimum phase systems. This allows IMC to retain its simplicity for all types of systems. It was found that in the case of the Linde Column there was very little difference in the performance of the simple reduced order controller and the more complicated designs that exist in the

literature. This new approach is very appealing from a practical point of view.

The contribution of the new feedforward IMC structure was significant because it offers an alternative to the existing feedforward structures to allow simplified decoupling of control loops. It was found that this new form of IMC offered improved control of the Linde Column over the existing form.

The contribution of multirate IMC control was significant because it addresses a common problem found in the process industries, namely non-uniform sampling of process variables. This allows IMC to be used for an even greater variety of process control problems. This extension is an example of the contributions that can be made from application oriented research.

Finally the results of this chapter demonstrate that improved control for the Linde Column is possible through an alternative strategy that is appealing to the operating personnel. It is this final contribution that has spawned further work within the Dow Chemical Company.

Chapter Five

SUMMARY AND RECOMMENDATIONS

This thesis has described research regarding the modelling and control of an industrial scale distillation column, named the "Linde Column", located at the Dow Chemical Company's Michigan Division. Justification for this research can be found in two areas. One is the possible economic impact, improved control would have on the operation of the column. The second is the contribution this research makes to bridging the gap between advanced control theory and its practice in the process control industry. The overall objective of this thesis was to determine if advanced control would be beneficial to the Linde column. This objective led to two major themes in the research: 1) develop a dynamic, multivariable model of the column, and 2) propose an alternate control scheme and test it through simulation. The remainder of this chapter will separately summarize the results of both phases of research. Each summary will be followed by suggested future research on particular topics that were addressed. Recommendations on future opportunities for research on a broader scale will then follow.

5.1 Summary of Linde Column Modelling

The research that led to a dynamic model of the Linde column was described in Chapter Three. The model developed is a 2 input, 2 output matrix of discrete time transfer functions. The preliminary problem of estimating the order and time delay of a multi-input, multi-output model was

first addressed. A novel identification procedure was developed to solve this problem. Parameter estimation of the identified model used real operating data. Non-minimum phase behavior was discovered in a part of the column which is not mentioned before in the literature. The new identification procedure and the discovery of non-minimum phase behavior are the two major contributions of Chapter Three.

The novel identification procedure presented in Chapter Three is a significant contribution to the literature on model identification of multivariable systems. This new approach greatly reduces the number of parameters necessary to describe the behavior of multivariable systems with multiple time delays and is based on a new "delayed polynomial matrix" representation of discrete systems. The delayed polynomial matrix representation explicitly accounts for multiple delays in a multivariable system. This is in contrast to the conventional polynomial matrix model which represents time delay by parameters with values equal to zero.

The delayed polynomial matrix method was developed by starting with a generic state space description of a discrete time multivariable

system with multiple input delays. Theorem 3.1 derived the relationship of the state space description to an input/output description with multiple input delays. Lemma 3.1 then demonstrated the relationship of this input/output description to the normal polynomial matrix representation. The delayed polynomial matrix representation was proposed by Remark 3.1 which showed how it reduces the number of parameters in an input/output model of a discrete system. A two phase identification procedure was then outlined. This procedure is based on testing the linear dependence between input and output observations. It first identifies the normal polynomial matrix model from input/output data and then derives the delayed polynomial matrix model.

A computer algorithm for the delayed polynomial matrix method was then described in a way that made it suitable for interactive use. Singular value decomposition was chosen as the numerical tool for testing linear dependence. This is the first time singular value decomposition has been used in an identification method. Two techniques were presented to filter noisy data. Finally, a simulated example demonstrated the ability of this new identification method to perform with up to 20% additive noise on the data.

5.1.1 Results of Linde Column Modelling

Chapter Three then led to developing a model of the Linde column from real operating records of the process. The problem of obtaining good data for model building was first addressed. A review of the data

showed that it contained sufficient information for modelling. However, it also put constraints on the form of the model. The delayed polynomial matrix method of model identification was used where appropriate. It was found to be in close agreement with other identification techniques. Least squares estimation was then used to fit the parameters of the identified model. Discussion of the Linde column model showed that certain aspects of the model were very consistent with the experience of the operating personnel.

This research has produced an important discovery concerning the dynamics of distillation columns in addition to the original contributions to the theory of model identification and controller design. It was found that the concentration on the 57th tray exhibited inverse response to changing reflux flow. This was totally unexpected and has not been mentioned in the chemical engineering literature.

5.1.2 Future Research on Distillation Modelling

The modelling effort of this thesis provided much insight on the dynamics of the Linde column. However, some questions remain unanswered. The differences in the model parameter values obtained from different data sets should be resolved. This can only be done by using data collected during controlled experiments. The present model of the column can be used to determine the amplitude and frequency content of the experimental inputs. The model developed in this thesis is an excellent starting point for future research.

The delayed polynomial matrix method of identification requires further investigation. Alternative noise compensation techniques should be researched. Incorporating the instrumental variable approach to handle correlated noise would enhance the application of the delayed polynomial matrix method. Extending the method to identify a noise model would be another way to compensate for colored noise. Since noisy process data is normal in the process industry, these suggestions would go far toward improving the practical application of this method.

5.2 Summary of Advanced Control for the Linde Column

An alternative control scheme for the Linde column was considered in Chapter Four. The alternate control strategy was selected after a careful examination of the advantages of the current control. Tailoring the new control approach to the model of the Linde column led to several original contributions.

The alternate control strategy selected is a feedforward version of Internal Model Control, IMC. The essence of IMC is the concept that control is applied to a model of the process as well as the process. Assuming the model and the process are well matched, differences in output of the two represent a measure of the process disturbance. Such a scheme offers several appealing features:

1. Time delay compensation is inherent since the controller is only acting upon process disturbances.

2. IMC is understandable to operating personnel because they can identify with the way that the internal model in the IMC strategy predicts the behavior of the process.
3. Robustness is also addressed in the structure of IMC by the addition of a filter ahead of the control calculation. The filter time constant can function as a single tuning constant, thus the operator can respond to unexpected process shifts without resorting to manual control.
4. Easy controller design is another appealing feature of IMC. For well behaved processes, the controller is just the inverse of the process model.

Because IMC addresses these practical issues in a straight forward manner, it was selected over controllers based on more abstract approaches, such as state space or optimal control theory.

Two peculiarities of the column required extensions of existing theory on Internal Model Control. First, one of the two controlled variables, the bottoms concentration, could only be sampled every 8 minutes due to the instrument used. The other controlled variable, the concentration on the 57th tray, which could be sampled as often as wanted, was sampled once a minute to adequately cover its dynamic response. Therefore the multivariable version of IMC could not be directly applied to control the column, because it assumes uniform sampling for all outputs. A multirate feedforward strategy was developed

to address this problem. Secondly, the concentration of the 57th tray exhibited unexpected inverse response with respect to the reflux flow. As a result, the model of this input / output relationship has at least one zero outside the unit circle. A controller designed as the inverse of the model would be unstable. To address this problem, a straight forward approach was developed using a reduced order model of the process. This simpler approach maintains the overall simplicity of IMC for non-minimum phase processes.

Reduced order controller design for non-minimum phase systems is an important contribution of Chapter Four. Compared to the literature, this approach simplifies the practical implementation of IMC for non-minimum phase systems. One solution cited in the literature is to eliminate the unstable zero before inversion [2]. This was tried through simulation. The result was good regulation but the input applied to the process was highly oscillatory and therefore unacceptable. Another solution cited [2] solves a predictive control problem. This solution relies on the formulation of a least squares approximation problem and its solution and involves several tuning parameters. The approach taken in this thesis was to approximate the process by a simple minimum phase system which was then inverted for the controller design. Simulation showed little difference in performance between the reduced order controller and the more complex designs.

Another contribution of Chapter Four was a modification to feedforward IMC to allow for simplified decoupling control. This modification is significant because it offers an alternative feedforward

structure. The closed loop response was mathematically derived to show how it differed from existing feedforward IMC. Simulations showed that it produces improved control for some types of disturbances on the Linde column.

Decoupling control of both product streams on the Linde column was accomplished by applying the new feedforward structure in a multirate fashion. This is a significant contribution because it offers a way to apply multivariable IMC to non-uniform sampling problems. This class of problems is common in the process industry. The multirate extension of IMC is an example of the contributions made by application oriented research.

5.2.1 Results of Advanced Control Simulations

Once the multivariable control strategy was designed, simulations were used to compare it to the conventional control using independent PI controllers at the bottom and the at 57th tray. The simulations tested the response of the controller to step load changes.

The multivariable controller out performed the conventional controllers in the load change simulations. Improved disturbance rejection was achieved in both product streams by the multivariable controller. This is not surprising since the multivariable controller made use of the knowledge of the dynamic coupling and non-minimum phase behavior in the distillation column. This is not to say that PI control

is bad or that it could not be improved. In fact, the model of the column has interesting implications for the current PI control.

5.2.2 Future Control Research

At the very least the present controllers could be tuned using the model developed in this research. The present controllers were tuned manually with the main concern of getting the process to run acceptably but not necessarily optimally. So there is room for improvement here. Of course, techniques exist to compensate PI controllers for deadtime or coupling. These could be used to improve control.

The inverse response on the 57th tray suggests an alternate controlled variable. It was originally reasoned that the control system has an advantage if it controls at the 57th tray since any disturbance detected there must propagate up another 15 trays to affect the output of the column. Therefore, there would be extra time to respond to disturbances. However, the performance of a PI controller is adversely affected by inverse response, so such a controller applied at the 57th tray may not reject disturbances as well as a controller applied at the top of the column where minimum phase behavior can be expected. Control of reflux flow based on distillate concentration using the concentration on the 57th tray as a feedforward term might perform better. Control improvements are available in several different forms because of the knowledge obtained in this research.

The performance demonstrated by decoupling control in the simulations of the Linde Column suggest more research be conducted on the control of moderate to high purity distillation columns by using an interior tray concentration as a control point. Weischedel and McAvoy [14] argued, and then demonstrated with simulations, that decoupling of moderate to high purity columns is not feasible with linear decouplers. The simulations of the Linde Column show that decoupling is feasible if the concentration on an interior tray is controlled. Decoupling is possible for this situation because the separation at an interior tray is low purity. The ability to control a high purity column with this approach does come at a cost; that cost is the non-minimum phase behavior that is present at the interior tray. However, simulations of the Linde Column show that a model based control approach can effectively handle this type of behavior. Future research on a three point control strategy which maintains the concentration in the bottoms product, the overheads product, and an interior tray as an intermediate should prove fruitful for high purity columns.

The control concepts presented in Chapter Four offer new opportunities for further research on IMC control and for the application of IMC to other process operations. Other types of predictive control should be considered to handle non-minimum phase systems. For example, the controller assuming no change in its output, could predict the position of the process beyond the initial inverse response. It could then calculate a change in its output necessary to drive the process to set point over the prediction horizon. The prediction could be based on a first order model with sufficient time

dealy or on a transfer function equivalent to the internal model. The estimate of the process disturbance available in the IMC structure could also be further exploited. Methods to test the whiteness of the disturbance (and therefore not respond) or to predict the disturbance (if it is correlated) would improve the performance of IMC. The trailing average used in the multirate version of IMC could be further investigated. Alternative averages such as a weighted average should be tried. This thesis, like all successful research, raises new questions even as it obtains its objectives.

5.3 Future Research Opportunities

This thesis quite clearly demonstrates that efficient control of industrial processes is a difficult and challenging problem. Global competition is enforcing tighter requirements on yields and production costs. The ability of computer automation to improve yields and reduce production costs, using standard control techniques, has made it a standard entity in every competitive process operation. This thesis illustrated how a closer look at the process can reveal dynamic characteristics which have major implications on process operation. It also demonstrated that a model based control approach could be modified so that it more effectively addresses industrial control problems. The task of the research community is now to demonstrate ways that greater improvements can be realized through more sophisticated use of the computer/automation base that is part of every serious process operation.

Many opportunities exist for research and development of computer based methods which compliment or extend the standard control techniques now in use throughout industry. Some of the promising areas for industrial application will now be mentioned.

Artificial intelligence and expert systems offer solutions to problems that are not easily addressed by standard control programming. In many situations of industrial control, the objective of the controller is not well defined, or the control now implemented by the human operator does not translate well into precise mathematical rules. An expert system based on heuristic rules can provide control strategy for these situations. Monitoring of standard control algorithms and logic is another use of artificial intelligence. The area of process diagnostics has seen a lot of development activity recently. Supervision of feedback controllers by an expert system appears to be a fruitful area for research, especially for adaptive controllers. Research on the use of artificial intelligence to assist human operators during situations of multiple alarms also has a high potential for payoff. In the future, it will be the marriage of artificial intelligence and mathematically based monitoring and control that will prove to be the most effective use of both approaches.

A drawback of expert system programs and standard control programs is that they are application specific. The programs must be developed individually for each production plant. Duplication of similar programs is a partial solution to this problem, but the real answer lies in computer automated program generation. The ideal program generator

would use graphic representation of the process as input and produce a useable control program (which can be further customized) as output. Research in this area would be a real benefit to reducing the cost and time needed to automate production processes.

Greater knowledge of process dynamics and process disturbances is required if automation is to move beyond the standard control techniques. This usually requires a mathematical model of the process for the vast majority of advanced process control techniques. Excellent research opportunities exist in the area of online process modelling and simulation. In the future, process automation systems will have dedicated computer resources for predicting process behavior for control just as in Internal Model Control, but on a much broader scale. The routine application of advanced control is very much dependent on an integrated approach to model building, online process simulation, and updating of process models.

Supporting technologies of advanced process control, namely computers and instrumentation, are as important to its future as its methodologies and algorithms. The complexity of the processing required for advanced process control coupled with the falling prices and increasing power of micro-computers is leading to distributed processing and distributed control. Complete plant wide automation from sales to shipment will require reliable and cost effective computer systems which include: 1) transparent high speed communications, 2) shared computer memory, 3) fault tolerance and 4) application programs which can be designed and tailored by the user. Sensing instruments which have

always been the subject of aggressive research and development will continue to offer fruitful opportunities for research. Instruments which can offer self calibration and self diagnostics, multiple measurements, and digital communications will no doubt be the standard fare in the future. A comprehensive hardware base is necessary for the routine application of advanced process control.

The discussion above has only outlined a few areas of research that are desirable from an industrial point of view. An important area, which was the subject of this research, is the study of current advanced control techniques on industrial applications. Investigations of this kind can be the basis for productive joint ventures between industry and academia. It is industry which can offer challenging control problems and it is academia which can provide fresh approaches where the standard ones have performed unsatisfactorily.

A paradox of computer based control is that one of its greatest assets, flexibility, can also be one of its greatest detriments. This stems from the ease at which ad hoc modifications can be made to standard PID controllers in an attempt to address its shortcomings. This often leads to overly complex control programming which only works marginally at best. The greatest contribution made by this thesis to its industrial sponsor, The Dow Chemical Company, is not the potential improved control of the Linde column, rather it is the investigative approach it used to solve the problem. Already several significant contributions to the profitability of the company have been made by solving control problems by first gaining a deeper understanding of the

process through experimentation and model building; rather than adding more 'fixes' to the existing control scheme. These early successes indicate a positive future for the industrial application of advanced control.

APPENDIX

APPENDIX

The IMC control structure can be converted to conventional feedback form by defining $C(z)$, the feedback controller as

$$C(z) = \frac{G_c(z)}{1 - \hat{G}(z)G_c(z)}$$

where $G_c(z)$ is the control block in the IMC structure and $\hat{G}(z)$ is the internal model.

Now a first order system

$$G(z) = \hat{G}(z) = \frac{bz^{-1}}{1 - az^{-1}}$$

produces

$$C(z) = \frac{\frac{1 - az^{-1}}{b}}{1 - \frac{1 - az^{-1}}{b} \frac{bz^{-1}}{1 - az^{-1}}} = \frac{\frac{1}{b} - \frac{a}{b} z^{-1}}{1 - z^{-1}}$$

which is a discrete form of a proportional / integral controller.

LIST OF REFERENCES

LIST OF REFERENCES

1. McAvoy, T.J., "On the Difference Between Distillation Column Control Problems", presented at the Second Engineering Foundation Conference on Process Control 1981.
2. Garcia, C.E. and Morari M., "Internal Model Control. 1. A Unifying Review and Some New Results", Ind. Eng. Chem. Proc. Des. Dev., 21, 308-323, (1982).
3. Williams, B.J., "Statistical and Theoretical Modelling of a Binary Distillation Column", Conference on Industrial Applications of Dynamic Modelling, Durham, IEE Conference Publication No. 57, (1969)
4. Krishnamoorthy, V. and Edgar, T.F., "Identification and Estimation of Discrete Models for a Distillation Column", University of Texas Research Report No. WP28- 3:50
5. Foulard, C. and Bornard, G., "Identification and System Parameter Estimation of Distillation Processes - A Case Study", Proc. 3rd IFAC Symp. on Identification and System Parameter Estimation, The Hague, (1973)
6. Gauthier, A. and Landau, I.D., "On the Recursive Identification of Multi-Input, Multi-Output Systems", Automatica, 14, 609-614, (1978)
7. Gustavsson, I., "Survey of Applications of Identification in Chemical and Physical Processes", Automatica, 11, 3-24, (1975)
8. Wood, R.K. and Berry, M.W., "Terminal Composition Control of a Binary Distillation Column", Chem. Eng. Sci., 28, 1707-1717, (1973)
9. Rijnsdorf, J.E., "Interaction in Two-Variable Control Systems for Distillation Columns - I", Automatica, 3, 15-28, (1965)
10. Luyben, W.L., "Distillation Decoupling", A.I.Ch.E. Journal, 16, 198-203, (1970)
11. Dahlgvist, S.A., "Control of a Distillation Column Using Self-Tuning Regulators", Canadian Journal of Chem. Eng., 59, 118-127, (1981)

12. Ogunnaike, B.A. and Ray, W.H., "Multivariable Controller Design for Linear Systems Having Multiple Time Delays", A.I.Ch.E. Journal, 25, 1043-1057, (1979)
13. Ogunnaike, B.A., Lemaire, J.P., Morari, M., Ray, W.H., "Advanced Multivariable Control of a Pilot-Plant Distillation Column", A.I.Ch.E. Journal, 29, 632-640, (1983)
14. Wieschedel, K., McAvoy, T.J., "Feasibility of Decoupling in Conventionally Controlled Distillation Columns", Ind. Eng. Chem. Fundam., 19, 379-384, (1980)
15. Freeman, T.G., "Selecting the Best Linear Transfer Function Model", Automatica, 21, 361-370, (1985)
16. Astrom, K.J., "System Identification - A Survey", Automatica, 7, 123-162, (1971)
17. Gustavsson, I., "Comparison of Different Methods for Identification of Industrial Processes", Automatica, 8, 127-142, (1972)
18. Akaike, H., "Statistical Predictor Identification", Ann. Inst. Statist. Math., 22, 203-217, (1970)
19. Akaike, H., "Use of an Information Theoretic Quantity for Statistical Model Identification", Proc. 5th Hawaii Int. Conf. Sys. Sci., 249-250, (1972)
20. Lee, R.C.K., "Optimal Estimation, Identification and Control", M.I.T. Press, 1964
21. Woodside, C.M., "Estimation of the Order of Linear Systems", Automatica, 7, 727-733, (1971)
22. Wellstead, P.E. and Rojas, R.A., "Instrumental Product Moment Model-Order Testing; Extensions and Application", Int. J. Control, 35, 1013-1027, (1982)
23. Buckley, P.S., Luyben, W.L. and Shunta J.P., "Design of Distillation Column Control Systems", Instr. Soc. America, (1985)
24. Budin, M.A., "Minimal Realization of Discrete Linear Systems from Input-Output Observations", I.E.E.E. Trans. Auto. Control, AC-16, 395-401, (1971)
25. Guidorzi, R., "Canonical Structures in the Identification of Multivariable Systems", Automatica, 11, 361-374, (1975)
26. Klema, V.C., and Laub, A.J., "The Singular Value Decomposition: Its Computation and Some Applications", I.E.E.E. Trans. Auto. Control, AC-25, 164-176, (1980)
27. Golub, G.H. and Reinsch, C., "Singular Value Decomposition and Least Squares Solutions", Numer. Math., 14, 403-420, (1970)

28. Smith, B.T., et al., "Matrix Eigensystem Routines - EISPACK Guide", Lecture Notes in Computer Science, 6, 2nd ed., 1976
29. Dongarra, J.J., Moler, C.B., Bunch, J.R. and Stewart, G.W., "LINPACK, Users' Guide", 1979
30. Gacia, C.E. and Morari, M., "Internal Model Control. 2. Design Procedure for Multivariable Systems", Ind. Eng. Chem. Process Des. Dev., 24, 472-484, (1985)
31. Brosilow, C.B., "The Structure and Design of Smith Predictors from the Viewpoint of Inferential Control", Joint Auto. Con. Conf. Proc., Denver, (1979)
32. Shunta, J.P. and Luyben, W.L., "Sampled-Data Noninteracting Control for Distillation Columns", Chem. Eng. Sci., 27, 1325-1335, (1972)
33. Jamshidi, M., "Large-Scale Systems; Modeling and Control", North-Holland, 1985
34. Parrish, J.R. and Brosilow, C.B., "Inferential Control Applications". Automatica, 21, 527-538, (1985)
35. Sinha, N.K. and Pille, W., "A New Method for Reduction of Dynamic Systems", Int. J. Control, 14, 111-118, (1971)
36. Sinha, N.K. and Bereznoi, G.T., "Optimum Approximation of High-Order Systems by Low-Order Models", Int. J. Control, 14, 951-959, (1971)
37. Brosilow, C.B., Inferential Control Seminar Presented at Dow Chemical Company, 1985
38. Buckley, P.S., Chemical Engineering Seminar Presented at Ohio University, 1967

MICHIGAN STATE UNIV. LIBRARIES



31293108011903